WIPPLINGER P E

THE MOLYBDENUM POTENTIAL OF THE SANDSTONE-HOSTED URANIUM OCCURRENCES IN THE BEAUFORT GROUP OF THE SOUTHERN KAROO

MSc UP 1991

Digitised by the Department of Library Services in support of open access to information, University of Pretoria, 2021

UNIVERSITEIT VAN PRETORIA
UNIVERSITY OF PRETORIA
YUNIBESITHI YA PRETORIA

THE MOLYBDENUM POTENTIAL OF THE SANDSTONE-HOSTED URANIUM OCCURRENCES IN THE BEAUFORT GROUP OF THE SOUTHERN KAROO.

by

P.E. Wipplinger

submitted in partial fulfilment of the requirements
for the degree of

MASTER OF SCIENCE

in the Faculty of Science

UNIVERSITY OF PRETORIA

Pretoria

October 1991

Digitised by the Department of Library Services in support of open access to information, University of Pretoria, 2021

Abstract

The sandstone-hosted uranium deposits of the southern Karoo basin in the Republic of South Africa were investigated as a possible source of molybdenum. A summary of global resources, production, co-products (Re and Se) and uses of molybdenum, as well as the geochemical cycle of the metal is given. The investigation comprised mapping and sampling of selected known uranium occurrences in the Karoo. Initial field analysis of samples was done by means of a portable XRF analyzer, followed by laboratory XRF analysis. The calibration of the portable and the laboratory XRF analyzers by means of spikes is described. It is concluded that the portable XRF is a useful field tool in exploration. Ore specimens were examined by means of autoradiography, and reflected and transmitted light microscopy. The statistical analysis of the geochemical results on the basis of field parameters shows that the southeastern palaeostream direction has the highest molybdenum potential expressed in terms of mean Mo concentration, followed by the southwestern direction. The northwestern direction has the highest uranium potential. Of the ten sandstone units investigated the Poortjie Sandstone Member has the highest combined Mo U potential, followed by the Barberskrans Sandstone Member. The rock type with the highest Mo potential is a fissile sandstone. The Mo-potential of a rock increases by about an order of magnitude in terms of the mean Mo concentration if visible organic matter is present. The carbonate-cemented sandstone has a low molybdenum potential. Mineralization associated with laminated sandstone is normally found near the base of sandstone bodies. Accompanying elements with a sympathetic concentration distribution to that of molybdenum are U, V, Co, As and Pb; Zn is indifferent and Cu antipathetic. The elements sympathetic to uranium are Mo, V, Co, As, Zn and Pb, and Cu behaves antipathetic. The evaluation of the results of the Geological Survey's stream-sediment sampling of the Karoo conducted in the late 1970's revealed that only the neutron activation analytical technique for uranium returned anomalies that could be matched with known uranium occurrences. Plant toxicity to livestock as an exploration tool was investigated. Although this gives a good mapping of dolerite-derived copper, the method is unsuitable to U\Mo exploration. An early-diagenetic model based on the movement of oxygenated water through the still unconsolidated sediment is proposed. Where this water passes through pockets where anaerobic conditions prevail due to the presence of decaying plant material, heavy metals borne in solution or as adsorptions are precipitated and ore-bodies may develop. The conclusion is reached that economic exploitation of the uraniferous sandstones for their molybdenum content is unlikely because of the small volume of individual ore-bodies, the irregular distribution of mineralization and grade within them as well as their small thickness and their horizontal attitude which makes extraction of the ore difficult.

Digitised by the Department of Library Services in support of open access to information, University of Pretoria, 2021

Uittreksel

Die uraandraende sandstene in die suidelike Karookom in die Republiek van Suid Afrika is ondersoek as ’n moontlike bron vir molibdeen. ’n Opsomming van wêreldreserwes, produksie, newe-produkte (Re en Se) en gebruike van molibdeen, sowel as die geochemiese siklus van die metaal word bespreek. Die ondersoek behels kartering en bemonstering van ’n seleksie van bekende uraanvoorkomste in die Karoo. ’n Aanvanklike veldanaliese van monsters is met behulp van ’n draagbare XRF-analiseerder uitgevoer, gevolg deur ’n laboratorium XRF-analise. Die kalibrasie van die draagbare en die laboratorium-XRF-analiseerders deur middel van kunsmatige standaarde word beskrywe. Die draagbare XRF-analiseerder word as ’n nuttige stuk eksplorasiegereedskap bevind. Ertsmonsters is deur middel van autoradiografie, en gereflekteerde en deurlate lig mikroskopie ondersoek. Die statistiese analise van geochemiese waardes op grond van veldparameters toon dat die suidoostelike palaeostroom-vloeirigting die hoogste molibdeenpotensiaal het in terme van gemiddelde Mo konsentrasie, gevolg deur die suidwestelike rigting. Die noordwestelike rigting het die hoogste uraanpotensiaal. Van die tien sandsteen-eenhede wat ondersoek is het die Poortjie Sandsteenlid die hoogste Mo\U-potensiaal, gevolg deur die Barberskrans Sandsteenlid. Die gesteentetipe met die hoogste Mo-potensiaal is splytbare sandsteen. Die Mo-potensiaal van ’n rots verhoog met omtrent een grootteorde in terme van die gemiddelde Mo-konsentrasie indien sigbare organiese materiaal daarin teenwoordig is. Die karbonaat-gesementeerde sandstene se molibdeenpotensiaal is laag. Verertsing verbonde aan die splytbare sandsteentipe word gewoonlik naby die basis van ’n sandsteenliggaam gevind. Begeleidende elemente wat ’n simpatieke konsentrasieverspreiding met molibdeen het is U, V, Co, As en Pb; Zn is onsydig en Cu het ’n teenoorgestelde neiging. Elemente simpatiek met uraan is Mo, V, Co, As, Zn en Pb, terwyl die Cu-verspreiding ’n teenoorgestelde neiging het. Die ontleding van die resultate van ’n geochemiese stroombemonsterings projek, wat deur die Geologiese Opname in die laat 1970’s in die Karoo uitgevoer is, toon dat slegs die analitiese metode vir uraan met behulp van neutron aktivering anomalië gee wat in verband met bekende uraanvoorkomste gebring kan word. Vergiftiging van lewende hawe deur plante wat op gemineraliseerde grond groei as eksplorasie-hulpmiddel is ondersoek. Alhoewel daar ’n merkwaardige afbeelding van koper afkomstig van doleriete gevind is, blyk dit dat die metode geen waarde in die U\Mo-eksplorasie het nie. ’n Vroeg-diagenetiese model gebaseer op die beweging van suurstofdraende water deur nog ongekonsolideerde sediment word voorgestel. Indien hierdie water deur lae beweeg wat weens die teenwoordigheid van verrottende organiese materiaal reduserend is, word swaarmetale wat in oplossing of as adsorpsies gedra word neergeslaan en ertsliggame mag vorm. Daar word tot die slotsom gekom dat die ekonomiese ontginning van die uraandraende sandstene vir hul molibdeeninhoud onwaarskynlik is weens die klein volume van die onderskeie ertsliggame, die sporadiese verspreiding van die verertsing en ertsgraad binne hulle sowel as die klein dikte en die horisontale ligging van die erts wat ontginning bemoeilik.

Digitised by the Department of Library Services in support of open access to information, University of Pretoria, 2021

Acknowledgements

The author wishes to express his thanks to the following:

The Chief Director of the Geological Survey for his permission to use the results of this investigation for thesis purposes.

Dr. E. C. I. Hammerbeck and Mr. L. S. Labuschagne, his supervisors, for their continued interest and support in the programme. The latter's interest persisted also after his transfer to the Laboratory, where he was instrumental in the custom XRF calibration and analysis for the project.

Dr. D. I. Cole, his field companion for co-operation, valuable discussions and support during the mapping and sampling stage.

Prof. C. P. Snyman, his promotor for guidance and the technical editing of the manuscript.

His many colleagues from whom he wishes to single out Mr. D. Cloete and Mr. N. Keyser for support to make him computer literate.

The Laboratory staff, Miss. A. Peense and Mrs. M. du Preez for the custom XRF calibration and analysis, Mr. M. Köhler for the preparation of the autoradiographs and Mr. N. D. Mabuela for the printing of the photographs.

His family for enduring the hardship of camp life in the Karoo and bearing with him during the evaluation and writing period.

Digitised by the Department of Library Services in support of open access to information, University of Pretoria, 2021

CONTENTS

Digitised by the Department of Library Services in support of open access to information, University of Pretoria, 2021

Digitised by the Department of Library Services in support of open access to information, University of Pretoria, 2021

1. Introduction

South Africa, like western Europe and Japan, is totally dependent on imports for its molybdenum requirements. According to the 1988 import statistics of the Department of Trade and Industry, South Africa imported 654 000 kg of ferro-molybdenum worth R 9 400 000 during that year. The question therefore arises whether at least part of this demand for the metal could be met locally.

Molybdenum in South Africa is associated with Permo-Triassic sandstone-hosted uranium deposits in the Beaufort Group of the southern Karoo basin, as well as various ore bodies related to acid intrusives. The pluton-related molybdenum deposits were eliminated as potential source of the metal because of low grade and/or volume. The practicability of exploitation of molybdenum from these ore bodies is further complicated by the frequent spatial separation of the molybdenum mineralization from the main commodity, e.g. tin.

Uranium exploration reports from the Karoo basin by private companies (about twenty exploration companies were involved during the mid-seventies) and State organizations (Geological Survey of South Africa, Nuclear Development Corporation of S.A. (Pty) Ltd. and MINTEK) indicated that at least half of the country's resources of molybdenum is related to the sandstone-hosted uranium deposits. Consequently these were selected for the present investigation.

2. Properties and uses of molybdenum

Molybdenum, a silver-white refractory metal with atomic number 42, atomic weight 95,95 and density of 10,2, forms with chromium, tungsten and uranium the sixth group of elements in the periodic table. With an average concentration of about 0.0001% in the earth's crust (Saager 1984) it belongs to the rarer metals. Its melting point of 2 622 ± 40°C is only exceeded by carbon, rhenium, osmium, tantalum and tungsten. Its low coefficient of thermal expansion (the lowest of the pure metals), malleability, ductility, good electrical and thermal conductivity, high strength at elevated temperatures and its resistance to attack by acids (except HNO_3), water dissolved alkalis and liquid metals like Na, Li, Zn, Hg and Bi render it an important commodity in the metallurgical industry (Uzkut 1974). At temperatures over 500°C molybdenum oxidizes to the volatile trioxide, which can be a problem during manufacturing and in certain applications (Saager, 1984).

Molybdenum is used as refractory metal and also is an important alloying metal which is either added on its own or together with Cr, Mn, Ni or W to steel, tool steel, cast iron and other high-technology alloys to improve their tenacity, ductility, magnetic properties and resistance to corrosion. Molybdenum-alloy steel is utilized in the manufacture of cylinder engines, jet engines, turbines, steel pipe-lines and cutting and drilling tools. It is also used in the chemical industry as reagent and catalyst; is a constituent of certain lubricants (the lubricating property of molybdenum disulfide is a function of its lamellar crystal structure and surface chemistry) and is used as a base in the pigment industry (molybdenum orange). Metallic molybdenum is used in the electrical- and electronics industry due to its high melting point. In agriculture molybdenum is an important trace element regulating the metabolism of plants. In livestock excess molybdenum in the diet leads to poisoning, for example cattle suffer from "teart" due to molybdenum accumulations in plants growing on molybdenum-rich neutral to alkaline soils (Goldschmidt, 1954).

The consumption of molybdenum in the various branches of industry as given by Saager (1984) is shown in Table 2.1. The use of molybdenum is largely dispersive and

Table 2.1. Distribution of molybdenum consumption by the various branches of industry (Saager, 1984).

Molybdenum-alloy steel	44%
Stainless steel	23%
Tool steel	9%
Chemicals, lubricants	9%
Cast steel, milling rods	7%
Metallic molybdenum	5%
High technology alloys	2%
Other	1%

Digitised by the Department of Library Services in support of open access to information, University of Pretoria, 2021

with the exception of catalysts little of the commodity is recycled.

Substitution of molybdenum by tungsten in metallurgical applications is possible, but due to the present oversupply of molybdenum on world markets this is unlikely.

Digitised by the Department of Library Services in support of open access to information, University of Pretoria, 2021

3. Global molybdenum resources, production, price and co-products

The world's molybdenum reserves and production capacity are concentrated in four countries. In 1983 world mine output was estimated at 63 000 tonnes of which the United States, Canada and Chile produced 65% and the USSR an estimated 17%. The world reserves are estimated to be 10 million tonnes of which the United States, Chile, Canada and the USSR have 5,3, 2,5, 0,9 and 0,7 million tones respectively. The molybdenum requirements of the western industrialized countries is obtained mainly from the first three countries (Blossom, 1985).

The bulk of the world's molybdenum production is derived from deposits related to granitic plutons. Two types of deposit are distinguished here, the Climax type or molybdenum-porphyries, which are mined primarily for their molybdenite content, and the copper-porphyries, where molybdenite is recovered as a by-product of copper exploitation. The average mineral content in these two types of ore ranges from 0,1 to 0,5 and 0,015 to 0,1 per cent molybdenite respectively (King et al., 1973). In both the copper- and molybdenum-porphyries the mineralization is hosted in stockworks and quartz-rich zones. These stockworks and quartz-rich zones may be hosted within the plutons as well as the surrounding country rock. Deposits of the former type are situated in the western part of the North America and individually have reserves of between 75 and 1 300 million tonnes of ore. Examples are Climax and Henderson in Colorado (USA), Questa (New Mexico) and Endaco and Adanak, both in British Columbia (Canada). The most important porphyry-copper deposits are situated in the Western Cordillera of North and South America. Examples are Bingham Canyon in Utah (USA), Highland Valley in British Columbia (Canada) and Chuquicamata (Chile). Similar deposits are known from Kasachstan and Siberia (both USSR) and Mongolia.

The production from sediment-hosted deposits is small, though some molybdenum is produced from the Kupferschiefer in central Germany (Saager, 1984). Significant molybdenum concentrations are also associated with some of the bedded sandstone uranium deposits in the United States of America (King et al., 1973) and South Africa (Toens et al., 1980). Usually the presence of molybdenum and also arsenic in these deposits is detrimental to uranium recovery especially if an alkaline leach process is used. In this case molybdenum loads on both resin and solvent, thus reducing the loading capacity of the exchanger and may even report as impurity in the uranium product (Le Roux and Toens, 1986). However, if the size of the uranium deposit and its molybdenum concentration are sufficient, molybdenum can be recovered as a valuable byproduct.

In his analysis of molybdenum as a commodity, Saager (1984) explains the sharp price increase in the late seventies from about $2 - $3 to $25 per lb molybdenum trioxide by an under-supply in the metal (32 000t) and a general scenario promoted at that time by the Club of Rome that the Earth's resources of rarer metals were being depleted at an alarming rate. This was followed by sudden drop in prices from 1980 onwards, partly by a settling of the dust caused by this hysteria (as can be seen from the parallel price movement of other commodities) and by a global oversupply of molybdenum (200 000t). The oversupply was brought about by the commencement of production by two large mines, Thompson Creek and Goat Hill (both in the USA), which forced established producers to reduce or even to curtail production. In February 1991 a price of US $ 3,00 per lb of molybdenum trioxide was quoted on world markets (Minerals Bureau, 1991).

Rhenium is an important byproduct of molybdenum exploitation and is commercially recovered as volatile Re_2O_7 from flue dust, formed during the roasting of molybdenite concentrates from porphyry copper-molybdenum ores (first produced in 1942 by Miami Copper Co., USA). It is also concentrated with platinum metals in the anode sludge during electrolytic refining of copper as at Mansfeld, Germany. Current technology permits the economic recovery of rhenium from deposits in which the rhenium content of molybdenite is at least 100 ppm (King, 1973). The rhenium price during 1990 varied from US $ 680 to US $ 750 per pound (van der Vyver, 1991).

Digitised by the Department of Library Services in support of open access to information, University of Pretoria, 2021

4. The geochemistry of molybdenum

In nature molybdenum is found mainly in its IV and VI valent forms; the former is typical of magmatic, metamorphic and other endogene environments, whereas the latter is dominant under exogene conditions. In endogene environments the presence of sulphur, for which Mo^{+4} has a stronger affinity than iron, always leads to the precipitation of molybdenite (the mineral usually exploited for its Mo content), or its amorphous equivalent jordisite, before most other sulphides are precipitated. Molybdenum is therefore found in this environment only as traces in other sulphides and in silicates. In molybdenite Mo is only substituted by rhenium, but S may be replaced by Se and Te and it is indeed the sulphide that has the highest potential for the substitution of sulphur by Se (Goldschmidt and Storck, 1939, quoted by Uzkut, 1974). The following sub-chapters are based on the geochemistry of molybdenum as described by Uzkut (1974).

4.1. The geochemical behaviour of molybdenum in the endogene environment

In the igneous composition spectrum, with increasing SiO_2 and alkali contents from dunite to granite, the mean Mo concentration of the ultrabasic rocks (dunite, peridotite and pyroxinite) is low (between 0,4 and 0,6 ppm) and then rises from gabbro (0,8 ppm) to granite (2,4 ppm) (Fig 4.1). A similar, though not so steep, increase in the Mo content with increasing differentiation is found in the more acidic extrusive rocks. The extrusive equivalents, with the exception of rhyolite, have higher Mo contents than their intrusive equivalents. The more acid magmatic rocks and especially the extrusive varieties (which have a higher specific grain surface area and are therefore more leachable on weathering) act as a molybdenum source for the exogene environment.

The behaviour of molybdenum during crystallization of granitic melts is controlled by the following factors:

i. **Initial Mo concentration** in the melt.

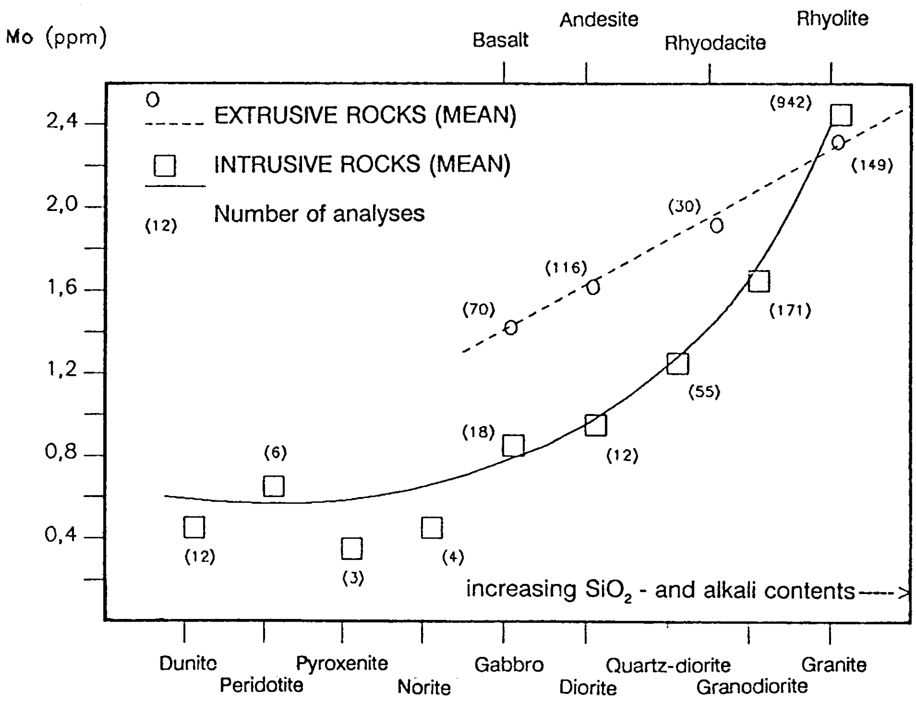

Fig. 4.1. The molybdenum content of the differentiation spectrum of intrusive and extrusive igneous rocks (after Uzkut, 1974).

ii. A high **water content** of the melt which reduces the melting point of the magma and makes it more fluid, thus improving the mobility of components within the melt, so that the formation of coarse crystals is promoted.

iii. With an **alkali content** in the melt of more than 4,5% Na+K, molybdenum will become progressively enriched in the liquid phase. Above this value, which in melts represents the iso-electric point of the amphoteric molybdenum, the ionic species $[MoO_3]^{2-}$ is stable. This species cannot be accommodated in the solid phases and thus becomes progressively enriched in the liquid phase. Below this value $[MoO_4]^{4-}$ is stable and can be accommodated by plagioclase in the early crystallizing phase (Gevorkyan, 1968) and thus becomes dispersed.

iv. High **contents of Fe and Ti** in the melt have a negative influence on the concentration of molybdenum in the residual melt, as these are the principal elements which can be ionically substituted by molybdenum in solid phases like amphibole, pyroxene, biotite, titanite, ilmenite, magnetite and hematite.

v. The presence of other **volatile contents** in the melt, e.g. HCl lowers the crystallization temperature of alkali feldspar in granitic melts, resulting in progressively more alkaline residual melts; a HCl concentration of more than 2,5% also inhibits the crystallization of biotite, in which molybdenum may substitute for iron, thus enhancing the chances of molybdenum to concentrate in the residual melt; on the other hand the presence of sulphur in the melt may lead to the crystallization of molybdenite during the main stage of crystallization.

The pegmatitic domain with its generally lower contents of Ti, Fe, Na, Ca and its higher content of K, compared to granite, provides ideal conditions for Mo enrichment. Incompatible elements like Zr, Be, B, rare earths, W, Mo and Sn are concentrated in accessory minerals in pegmatites, and molybdenite is economically exploited from some pegmatites.

After crystallization of the siliceous phases of a pegmatitic melt (mainly in the form of Na-K-feldspars, quartz and muscovite) the pneumatolytic stage of magmatic differentiation is reached in which the volatile constituents of the melt (mainly halogenides, water, H_2S and CO_2) predominate. Initially this environment is acidic due to the presence of HF and H_2S. Molybdenum in this milieu at temperatures above 373°C (the critical point of water) is mobile in the form of gaseous halogenides and can be precipitated through the following chemo-physical changes and ore deposits may result:

i. A **drop in temperature** below 373°C results in hydrolization of Mo halogenides to form MoO_3.

ii. A **decrease in pressure** of the system due to fluids rising into higher levels of the earth's crust results in the escape of the more volatile HCl and HF (which are responsible for a very acidic milieu), so that the pH increases and the solubility of molybdenum decreases.

iii. The **precipitation of chlorine- and fluorine-bearing minerals** (e.g. topaz, mica, apatite and fluorite) will also lead to an increase in pH and a decrease in the solubility of molybdenum.

In the hydrothermal domain (i.e. temperatures below 373°C) liquid water is the dominant phase. The solutions are usually of an alkaline nature and heavy metals exist as sulphur-complexes. Molybdenum is present as thio-molybdate ($MoOS_3^{2-}$). It is precipitated from solution through a drop in the alkali-ion concentration as a result of the crystallization of alkali feldspar and zeolite. This lowering of the pH also leads to the co-precipitation of quartz. A molybdenite-alkali feldspar-quartz paragenesis is typical for the hydrothermal domain. This precipitation process is triggered by a decrease in temperature.

4.2. The geochemical behaviour of molybdenum in the exogene environment

The exogene environment is the domain in which atmospheric oxygen and the presence of water (as the medium in which all the chemical and physico-chemical processes take place) play a decisive role in the behaviour of elements. The variation in pH and Eh of different natural environments is discussed by Garrels and Christ (1965) as follows: Only surface water with good circulation is oxidizing and confined waters lose their oxygen rapidly. Confinement may be due to fixation in rock, soil pores or the prevention of overturn in open waters. Baas Becking et al. (1960) examined pH-Eh data available in the literature. They established a field on the pH-Eh diagram which encloses all kinds of natural waters (Fig 4.2).

Organic-free waters lose their oxidizing character by reaction with reducing agents such as silicates and carbonates containing ferrous iron (for example biotite, chlorite, amphibole, pyroxene, siderite and ankerite) and sulphides. A further result of the hydrolysis of the silicates is a rise in pH, so that the environment becomes more

Digitised by the Department of Library Services in support of open access to information, University of Pretoria, 2021

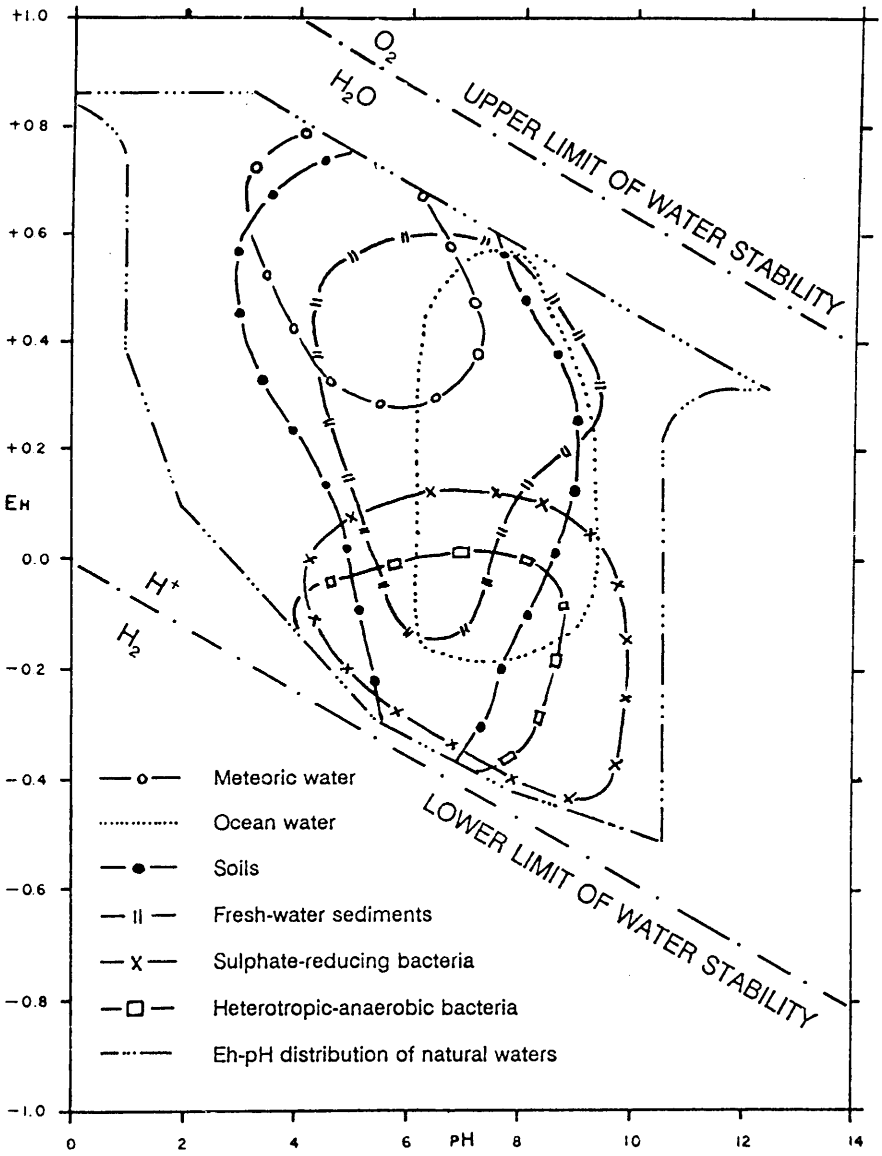

Fig. 4.2. Distribution of Eh-pH values for natural waters and fields enclosing various aqueous environments relevant to this study (after Baas Becking et al. 1960).

alkaline at the same time.

In organic-rich environments biochemical reactions quickly remove oxygen, resulting in the production of CO_2 and H_2S. Deoxygenation bactèria play an important role and the pH is lowered as CO_2 and H_2S are generated. Some bacteria are able to produce hydrogen, and oxidation potentials may even sink to close to the water stability limit.

In the exogene environment molybdenum is one of the most mobile and soluble elements, mainly in the form of the molybdate anion which forms water-soluble MoO_4^{2-}-complexes over the whole pH-range, even in that portion of the alkaline field where most other heavy metals are immobile. Molybdenite (the dominant and virtually sole Mo mineral in the earth's crust), however, is virtually insoluble in water and must be oxidized to become mobile. Acid magmatic rocks (as a result of their enhanced molybdenum content) are the dominant suppliers of molybdenum to the exogene environment. The main reagents that liberate molybdenum from these rocks are O_2 and CO_2 introduced by rain water. The ideal conditions for oxidation of molybdenite are a pH=7, Mo activity=10^{-4} and Eh=100mV - conditions not generally prevalent in nature. The oxidation process is strongly influenced by the presence of other ions in solution and by micro-organisms, which may suppress or expedite mobilization of molybdenum. Once mobilized the molybdenum is either retained in the soil or flushed out by rain water and added to the ground water.

Of the seventeen Mo minerals which are known in the exogene environment only two, wulfenite $PbMoO_4$ and powellite $CaMoO_4$, are of limited economic importance. Powellite fluoresces bright yellow under ultraviolet light, a property useful in exploration (Gleason 1972). Molybdenum is transported readily by sub-surface water along joints and fractures and may be precipitated as powellite at considerable distances from its starting point.

Molybdenite breaks down according to the following two equations:

$$MoS_2 + 12H_2O = MoO_4^{2-} + 2SO_4^{2-} + 24H^+ + 18e^-$$

$$MoS_2 + 4H_2O = MoO_4^{2-} + 2S^0 + 8H^+ + 6e^-$$

These equations respectively represent a sulphate-sulphide reaction, which is irreversible under normal conditions (25°C, 1 atm), and a reversible sulphide-sulphur reaction.

The only way that molybdenum reaches the exogene environment unaltered is in the form of inclusions and ionic substitutions in resistant detrital minerals (for example in zircon, titanite, and ilmenite). Molybdenum in this form is dispersed rather than concentrated during sedimentary processes.

Under surface conditions various readily soluble Mo complexes are formed. In the alkaline domain thio-molydates (indicated by MoO_4^{2-} in the pH-Eh diagram, Fig 4.3) predominate. These in turn may form soluble mixed complexes with sulphate and chlorine ions. In an acid environment the role of these anions diminishes and poly-molybdate complexes (indicated by $HMoO_4^-$ in the pH-Eh diagram) prevail.

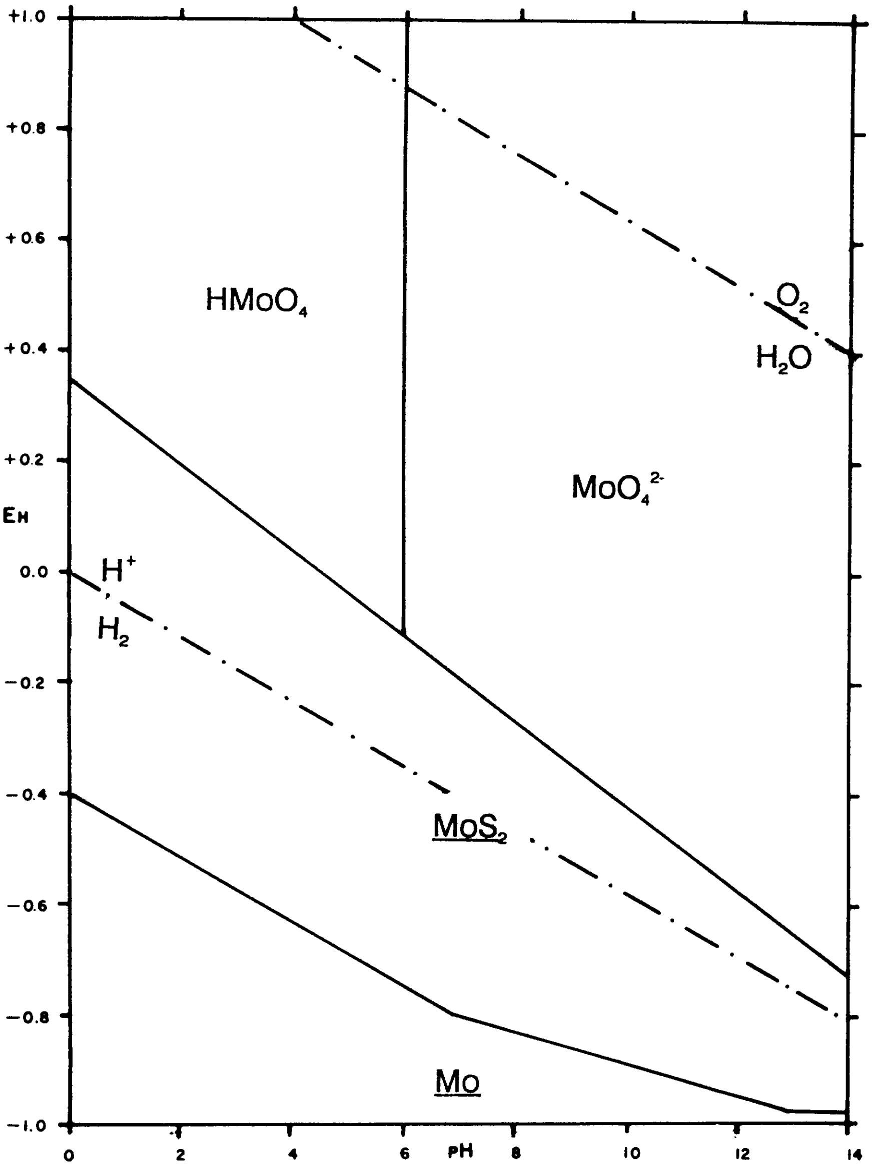

Fig. 4.3. Eh-pH diagram for the system Mo-S-H_2O for $a_{Mo}=10^{-4}$ at 25°C and atmospheric pressure after Tischendorf et al. (1968).

As source for molybdenum precipitation in the exogene environment only molybdate-anion complexes and molybdate-anion-mixed complexes come into question as they represent the only stable soluble forms of molybdenum in this environment. The four possible types of molybdenum precipitation are discussed:

i. **Precipitation as molybdenum sulphide**: The presence of sulphide sulphur in the exogene domain is rare and near the surface exists only under very special conditions. The removal of molybdenum as the sulphide from solution is mainly controlled by changes in the oxidation-reduction potential and is rather insensitive to variations in pH. Sulphate-reducing bacteria do expedite the precipitation of molybdenum as sulphide. In nature these conditions are only satisfied during ground water circulation in a continental environment, especially during the formation of lignite. Only from ground water under very reducing conditions can molybdenum sulphide be precipitated. This may result in molybdenum ore deposits. In the oxidation zone of sulphide deposits jordisite may form.

In a marine environment no molybdenum sulphide precipitation takes place as the pH and Eh values of sea water are too high. Sulphur is here present in the form of sulphate. Even under euxinic conditions, where the Eh values are low enough for sulphate to be reduced to H_2S, molybdenum sulphide is not precipitated as the concentration of dissolved molybdenum in sea water is too low.

ii. **Precipitation as molybdates**: As molybdenum is soluble in the form of molybdate-anion complexes over the whole pH-range, its precipitation is controlled by the presence of cations with which molybdenum forms insoluble molybdenum minerals. The most important of these are Pb^{2+} (wulfenite), Ca^{2+} (powellite), Co^{2+} (pateraite), Bi^{3+} (koechlinite), Cu^{2+} (lindgrenite) and UO_2 (umohoite, iriginite). These minerals form mainly in acid to neutral environments related to the oxidation zone of sulphide bodies, where most of the accompanying elements are soluble.

The stability of the Ca^{2+}-cation is Eh-independent, but dependent on pH and the partial pressure of CO_2. It is soluble in acid environments. MoO_4^{2-}-bearing solutions will in the presence of Ca^{2+}-ions precipitate powellite as soon as the pH rises to about neutral. Ca^{2+} is an important dissolved species in river water and will precipitate any dissolved molybdenum as powellite. This is added to the bed-load and is thus dispersed. The result is that river water contains only traces (of the order of 1 ppb) of dissolved molybdenum.

iii. **Co-precipitation and ionic exchange processes**: The molybdate anion is very effectively co-precipitated by colloidal iron-, aluminium- and manganese oxides and hydroxides as well as by clay minerals. This fixation of molybdenum is pH-dependent and most effective under acid conditions in the pH-range 3,5 to 4 where the total dissolved molybdenum can be extracted. The high molybdenum content (of the order of 350 ppm) found in iron-manganese nodules on the ocean floor (compared to the 10 ppb in normal ocean water) is ascribed to its concentration from sea water by this process (this represents an enrichment factor of the order of 35 000). In the normal pH-range 7,1 to 8,5 of sea water iron- and manganese oxides can remove 10 to 50% and 40 to 70% of dissolved molybdenum respectively through co-precipitation. Colloidal oxides and hydroxides of especially iron, but also manganese and aluminium, are also the main molybdenum accumulators in soils. In this case the molybdenum precipitation is due to electrostatic forces, ie. the negatively charged molybdate anion is attracted by the positively charged colloid of the relevant hydroxide.

iv. **Adsorption of molybdenum on organic material and clay minerals**: Organic material removes molybdenum from the environment in two ways, namely by living organisms (metabolically) and by decaying organic material (adsorption).

Molybdenum is an important and indispensable trace element in living plants where it metabolically controls the nitrogen intake and further bio-synthesis in the plant. Plants in certain environments, mainly acid, sandy soils and iron-rich

Digitised by the Department of Library Services in support of open access to information, University of Pretoria, 2021

soils suffer from a molybdenum unavailability which can be remedied in agriculture by the addition of sodium molybdate. These soils are not necessarily poorer in molybdenum than other soils, but the content of soluble molybdenum which can be assimilated by plants is low. Excessive amounts (more than 5 ppm Mo in dry plant matter) of molybdenum in pastures may result in the poisoning of livestock.

Living plants can accumulate substantial amounts of molybdenum, up to 225 ppm in dry plant matter and up to 0,3% in plant ash. The concentration of molybdenum is dependent on the availability of the element in the soil. The average Mo-content of dry plant material is given in the literature quoted by Uzkut (1974) as 0,2 ppm and that of plant ash as 0,1%. The molybdenum content in the original vegetation is the basis for commonly observed molybdenum enrichment in coal. Both a molybdenum excess and a deficiency in soil result in abnormal plant growth. In the fields of geobotanical and biogeochemical prospecting use is made of the appearance of plants and of their contained molybdenum respectively. The metal accumulation is more dependent on the molybdenum content of the soil than on the plant species. The technique is therefore, not based on the identification of specific indicator plants, although it is conceivable that certain plant species may have a higher tolerance for molybdenum poisoning than others.

Apart from the metabolic accumulation of molybdenum in living plants, the metal may be further concentrated by its extraction from oxidized ground water by decaying vegetable matter. The molybdenum content of coal increases with decreasing ash content, indicating its intimate association with the organic matter. In their work on coal from central Asia Kuznetsova and Saukov (1961) show that molybdenum (and rhenium) are contained in the form of metal-organic compounds, formed by the reaction with active groups of humic acids, and also as dispersed microscopic sulphide inclusions (probably in the form of colloidal rhenium-bearing jordisite) together with iron sulphide.

Peat bogs and swamps in brackish continental waters are concentrators of molybdenum. The pelites and limestones that form in this environment often are suitable source materials from which molybdenum can be mobilized by oxygenated ground water to be re-precipitated in favourable settings characterized by physical and chemical gradients amenable for concentration (for example pockets rich in organic matter and in H_2S). The potential of gravels, grits, sands and cherts as source beds tends to be very low.

In sapropelic sediments (both fossil and recent) molybdenum enrichment can be correlated with the organic carbon content. These sediments are argillaceous deposits containing between 5 and 15 percent organic carbon (mainly in the form of bituminous material) and 3 to 20% pyrite (mean 8,2%), and are enriched in trace elements. The pyrite is typically framboidal. The most important trace elements associated with the organic fraction are Ag, **Mo**, Zn, Ni, Cr, V, and to a lesser extent Co, Pb, the rare earth elements, Y, Se, U, and Te. These sediments, which include the so-called black shales and oil shales, form under euxenic conditions in deep basins in the open sea and also in restricted basins (both deep and shallow) usually, but not necessarily, in a marine environment. The detrital particles (from rivers feeding into the basin and atmospheric fall-out) and the organic material (in the form of dead phyto-plankton) descend from a surficial, oxygenated water layer through anaerobic H_2S-rich deeper water layers to accumulate on the basin floor. The anaerobic conditions result from a lack of circulation so that the layers in the stratified water body do not mix. The organic material in the sediments on the basin floor is transformed anaerobically. Sulphate in the sea water in this environment is reduced by sulphate-reducing bacteria to sulphide, which in turn reacts with iron compounds contained in the pore water to form FeS and FeS_2.

In the case of the Black Sea (a modern sapropelic depositional environment with an average molybdenum concentration of between 10 and 100 ppm in the sediment) the molybdenum content of the oxygenated surficial water and of the anaerobic deeper water layers is respectively 70 % and 90 % lower than that of normal sea water. Consequently precipitation of molybdenum sulphide is

Digitised by the Department of Library Services in support of open access to information, University of Pretoria, 2021

impossible under these concentrations. In the sediment pH-values of about 9 prevail which exclude clay minerals as a possible co-precipitant. The absence of oxygen in the anaerobic zone excludes Fe-oxides as co-precipitants. The iron precipitates as sulphide (and may well remove some of the molybdenum). A close association of molybdenum with the organic fraction of the sediment shows that organic matter is the main adsorbant of molybdenum. A reduction of the molybdate anion to V-valent molybdenum, which can be better adsorbed by organic matter, is probably involved.

Normal sediments generally have a low molybdenum content, which, however, increases with an increasing clay content. Here the colloidal state of the clay particles controls their ability to adsorb molybdenum.

4.3 The geochemical behaviour of molybdenum during diagenesis, metamorphism and anatexis.

Through burial a sediment or rock is subjected to increased pressure and temperature. The weight of the sediment or rock overlying the material in question, results in hydrostatic pressure on that material. This hydrostatic pressure is proportional to the depth of burial. The increase in temperature with depth is the result of heat flowing from the interior of the earth to its surface and is a function of the thermal gradient and conductivity of the rock below.

Diagenesis is the first stage of transformation of a fresh sediment into rock. The definition (Winkler, 1976) of the pressure-temperature field in which diagenetic processes take place comprises the full pressure spectrum and the temperature field below 220 ± 20°C. The various facets of diagenesis of sediments are described by Larsen and Chilingar (1979) as follows:

I. the formation of new minerals through i. oxidation in a very restricted domain close to the surface of the sedimentary body; ii. consumption of free oxygen by organisms and iii. reduction of hydroxides of Fe^{3+}, Mn^{4+}, V, Cr, etc and sulphates through anaerobic bacteria.

II. the redistribution of material in the sediment resulting in concretions and cementation.

III. consolidation of the sediment (lithification) through reduction of porosity, both as a result of repacking and of a process of solution-recrystallization.

IV. dehydration of hydrous minerals and recrystallization.

Compaction of the sediment together with dewatering by reduction of porosity is a continuous process during burial. This is especially the case in clay deposits where the porosity decreases from an initial 60 - 85% to 35 - 45% at depths of about 200 metres and to only 6 - 10% at a depth of 2 000 metres.

Natural fluids in rock near the surface consist largely of water derived from the hydrosphere. These waters are expelled from the sediment continuously during burial and diagenesis. They are described by Fyfe et al. (1978) as saline, with Cl^- the dominant anion together with varying amounts of HCO_3^- and SO_4^{2-} and sometimes even dominating. Na^+ is the dominant cation, with Ca^{2+} more abundant than in ocean water and in some instances even present in higher concentration than Na^+. The total dissolved mineral content in the water increases with temperature and depth. Dewatering of clay deposits during diagenesis releases water (compare the above percentages) which has to escape upwards and usually manifests itself on surface in the form of springs. This vast quantity of normally salty water has, as a result of the volume involved, the ability to move mobile elements, even those with very low solubilities. The dissolved material may become concentrated or dispersed on its path to the surface.

With depth in the earth's crust the role of the pore fluids diminishes and the major portion is held in the mineral structure as well as mono-molecular films of water in cracks and along grain boundaries. Metamorphism is essentially an iso-chemical process (Winkler, 1976). According to Fyfe et al. (1978) a normal sediment after diagenetic porosity reduction contains something like 5% of chemically bound water.

Through metamorphism as a result of burial to 30 km and heating to 600°C by the normal temperature gradient, this bound water will reduce to the order of 1 - 2%. This hot and salty hydrous water is expelled upwards and the volume involved cannot be disregarded, and again a transport medium exists that can remove incompatible elements from the rock being metamorphosed. Fyfe et al. (1978) propose that these metamorphic fluids may be released along cracks formed by hydraulic fracturing. They see the many veins found in metamorphic rocks as evidence for this. These veins, which range from microscopic to many metres across, are frequently filled with quartz, calcite etc.. As with expelled diagenetic pore fluids the resulting waters are alkaline.

Molybdenum in the form of independent minerals and adsorbed on to other minerals is susceptible to removal by these diagenetic and metamorphic fluids, while molybdenum in detrital minerals will only become mobile after anatexis. Uzkut (1974), therefore, comes to the conclusion that metamorphic rocks should be relatively depleted in molybdenum. Figures to substantiate this are scarce. It is questionable how far the molybdenum, which has entered the hydrous phase, actually travels before being re-precipitated. The impression is gained that under normal conditions this process is dispersive. Only when a carbon-rich rock is metamorphosed dry, is molybdenum not removed from the rock, but preserved as molybdenite in association with graphite.

The subducting plate model supported by various authors (i.e. Hamilton, 1989; Mason, in press and Fyfe et al., 1978) is an example where hydrous fluids (probably already enriched in incompatible elements) are focussed in a self-perpetuating drive towards the surface of the earth by lowering the melting point of the overlying mantle rocks. The fluids are derived from the metamorphism of the rocks in a subducting slab consisting of hydrated oceanic lavas and possibly some material derived from the clastic wedge on the continental margin (Fig. 4.4). The most important minerals supplying hydrous fluids by transformation are muscovite, biotite, and hornblende. The magmas produced by the melting of the mantle are felsic and form the intrusions related to the copper- and molybdenum porphyry ore-bodies, for example those found along the western continental margin of North and South America.

Digitised by the Department of Library Services in support of open access to information, University of Pretoria, 2021

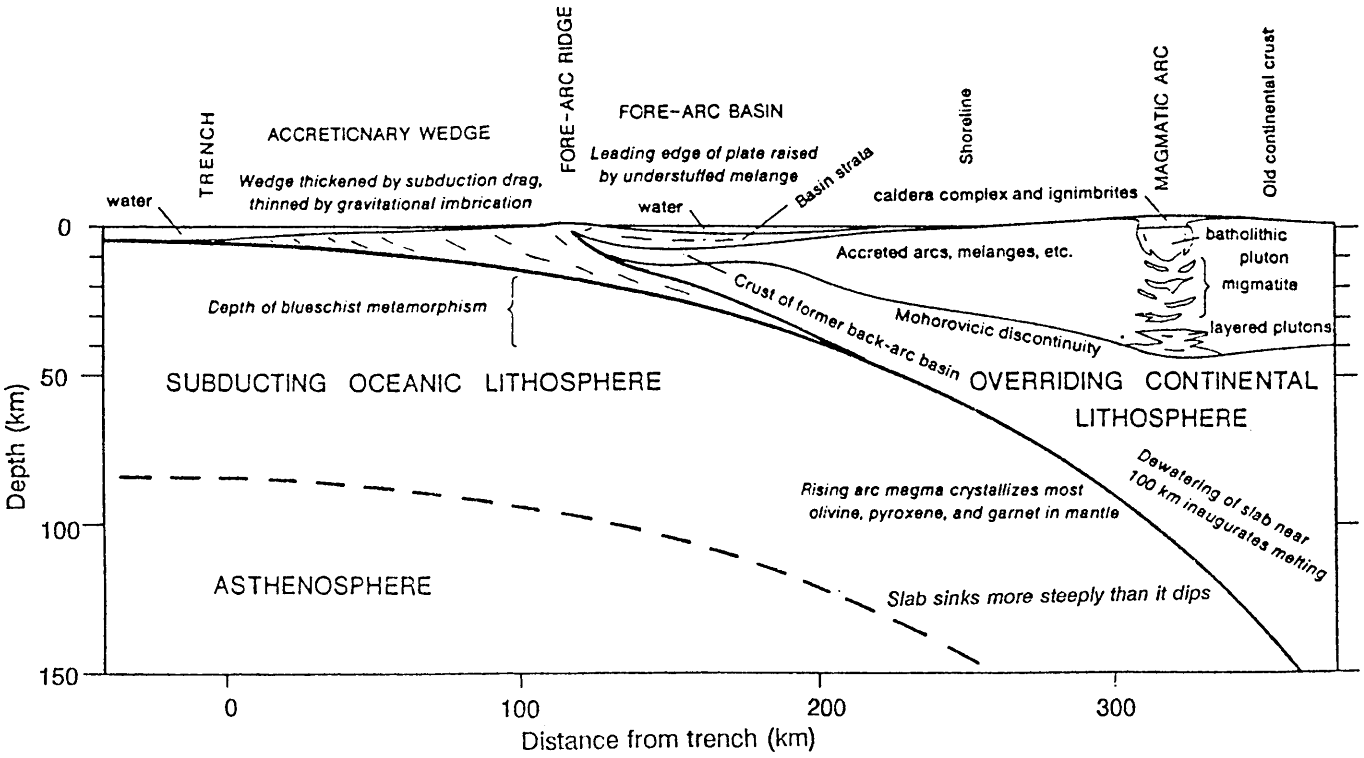

Fig. 4.4. Section across a continental-margin subduction system (after Hamilton, 1989), illustrating the domain of metamorphic de-watering of the subducting oceanic plate and related melting of the mantle, giving rise to a magmatic arc.

4.4. Rhenium and the geochemistry of molybdenum

The metallic element rhenium was first isolated by Ida and Walter Nodack in 1925, so filling the blank space of element number 75 on the periodic table. Rhenium (which has been termed a "new wonder metal") and its alloys have excellent heat- and corrosion-resistant properties, and are used in electric contact points, corrosion-resistant alloys, filaments and in high-temperature thermometry. It is the only element that can substitute for Mo in molybdenite and ranks with gold and the elements of the platinum group as of the scarcest stable elements in the universe. Nodack and Nodack (1931, quoted in Tischendorf et al., 1968) gave this concentration as 0,0036 g/t.

Already in 1931 Nodack and Nodack reported on the enrichment of rhenium in certain molybdenites (Re concentrations in molybdenite range between 1 ppm and 1,88 %). The enrichment of rhenium in molybdenite is explained by similar ionic radii - $r(Mo^{4+}) = 0{,}70$ Å and $r(Re^{4+}) = 0{,}72$ Å - and a probable ionic substitution series MoS_2-ReS_2. The Re end-member of this series has so far, however, not been found in nature. From their Eh-pH diagram (Fig. 4.5) Tischendorf et al. (1968) deduce that the ReS_2 stability reaches higher into the oxidising domain than that of MoS_2. They therefore expect that molybdenites that have formed in more oxidising environments should contain higher Re concentrations than those formed under more reducing conditions. Indeed, they predict that the Re end-member, should it exist, would form in the Eh domain where MoS_2 is not yet stable. They substantiate this by the higher Re concentration observed in some copper sulphides (chalcopyrite, chalcocite and bornite) formed under relatively strong oxidising conditions in Cu-Mo deposits. During the crystallization of these copper-sulphides (also the Cu-Re sulphide, dzhezkazganite) molybdenite is obviously unstable. In contrast to the Eh control on the Mo-Re distribution, this distribution is pH independent.

The geochemical behaviour of molybdenum and rhenium during the oxidation of molybdenite differs enough to result in a separation of the two elements in the exogene environment (Fig. 4.5.). ReS_2 the form in which rhenium is accommodated in molybdenite, is oxidized to rhenates at slightly higher Eh values than MoS_2. Rhenium in the presence of sulphur is still soluble as Re^- under reducing conditions (pH dependent Eh values of between -300 to -700 mV), conditions resulting in the precipitation of molybdenum as molybdenum sulphide. This difference in chemical behaviour is used by Uzkut (1974) to explain why the rhenium content of sedimentary molybdenite and secondary molybdenum minerals is much lower than that of molybdenite derived from igneous rocks. This conclusion is, however, not completely correct, as the pH-Eh field involved is situated outside that occupied by natural waters (compare with Fig. 4.2). Petersen et al. (1959) describe rhenium in concentrations of 0,005 to 0,1 % associated with the palaeostream channel-hosted uranium-molybdenum deposit known as the Sun Valley Mine in northern Arizona. They found rhenium to be in a water-extractable form, probably associated with ilsemannite, the weathering product of jordisite. These findings indicate that sedimentary molybdenites cannot be

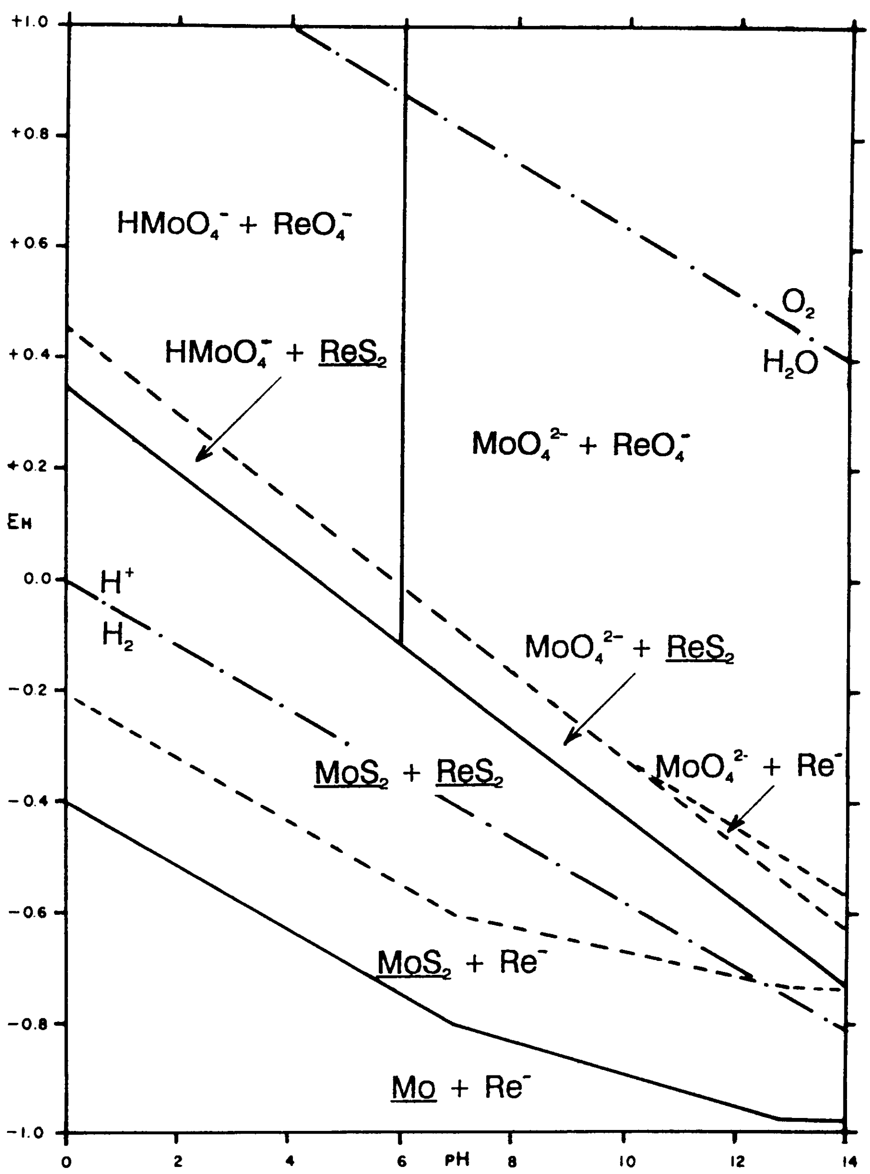

Fig. 4.5. Eh-pH diagram for the system Mo-S-H_2O and Re-S-H_2O for $a_{Mo} = 10^{-4}$ and $a_{Re} = 10^{-7}$ at 25°C and atmospheric pressure after Tischendorf et al. (1968).

summarily eliminated as a possible source of rhenium. Due to the lack of suitable calibration standards the molybdenites of the Karoo were not be examined for their rhenium content. This problem, however, should be pursued further if molybdenum is to be exploited from the Karoo.

Digitised by the Department of Library Services in support of open access to information, University of Pretoria, 2021

5. Karoo molybdenum investigation

From the records of all known South African molybdenum occurrences (Cole et al., 1991; Crocker et al., 1977; Martini, 1980; Herzberg, 1970; Stephan, 1976 and Stephan, 1977; Toens et al., 1980) the sandstone-hosted uranium occurrences of the Beaufort Group in the southern Karoo basin appear to be the most favourable exploration target, as they have better molybdenum grades, a close association between molybdenum and uranium and larger volumes than other occurrences.

Uranium was first discovered in the vicinity of Beaufort West prior to 1952 (Bruet, 1952), but the discovery was not followed up. Between 1965 and 1973 SOEKOR intersected radioactive beds during their drilling programme, but this fact was only made public in 1973. In their investigation of rocks of geological similarity to those hosting uranium in the United States, the Union Carbide Exploration Corporation discovered uraniferous sandstone outcrops in the Beaufort West area in 1970 by means of a car-borne radiometric survey. This programme covered most of the outcrop area of the Karoo Sequence in the Southern Karoo and the discovery triggered a major exploration boom in the Karoo. To date about 1 000 uranium discoveries have been made, 570 of which are in an area of about 95 000 km^2 between 20°30’ and 25°40’ east and 31°00’ and 33°10’ south. The present study is confined to this area (Fig. 5.1.). The uranium occurrences and their sedimentology have been described by various authors (Moon, 1974; Stear, 1980; Kübler, 1977; Le Roux, 1985; Pretorius, 1977 and 1985), but little attention has been given to the associated molybdenum.

In the early stages of the project it became clear that only a selection of these occurrences could be visited due to financial and time constraints. An initial feasibility study revealed that in certain cases weeks could be spent on mapping and sampling a single occurrence without reaching data saturation. However, by reserving about two days per occurrence a reasonable understanding could be gained of its nature. The number of occurrences for investigation was also reduced from 570 to 49 by means of a rating scale (Table 5.1). Localities selected and examined are listed in Table 5.2, and the more important lithostratigraphic units relevant to this study are summarized in Figure 5.2.

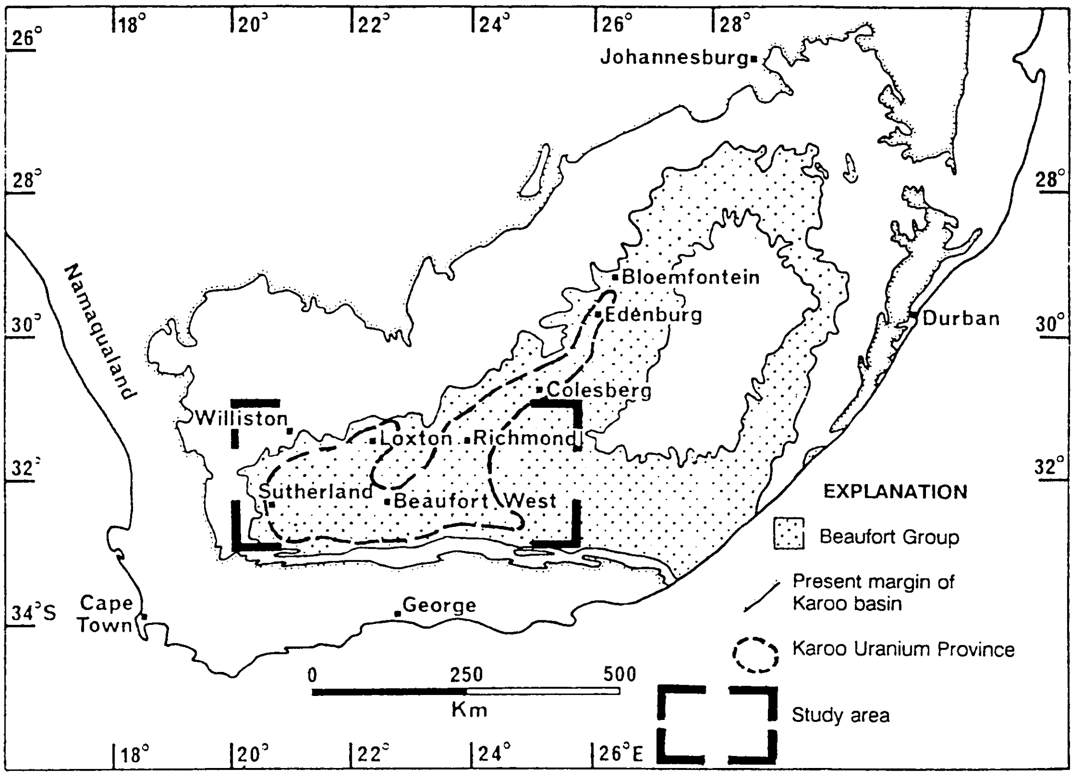

Fig. 5.1. Locality map indicating the study area in the southern Karoo.

Table 5.1. Ratings used to reduce the number of occurrences prior to commencement of field work.

Parameter	Rating
1. Available exploration data by private and State organizations	0-5
2. Molybdenum information based on exploration results	0-2
3. Amenability of outcrop to detailed mapping and sampling	1-3
4. Clustering of deposits on a sub-regional scale	1-5
5. Reported ore grade	0-3
6. Reported radiometric signature	0-2

	2-20

If little or no molybdenum is present the net rating is given as zero.

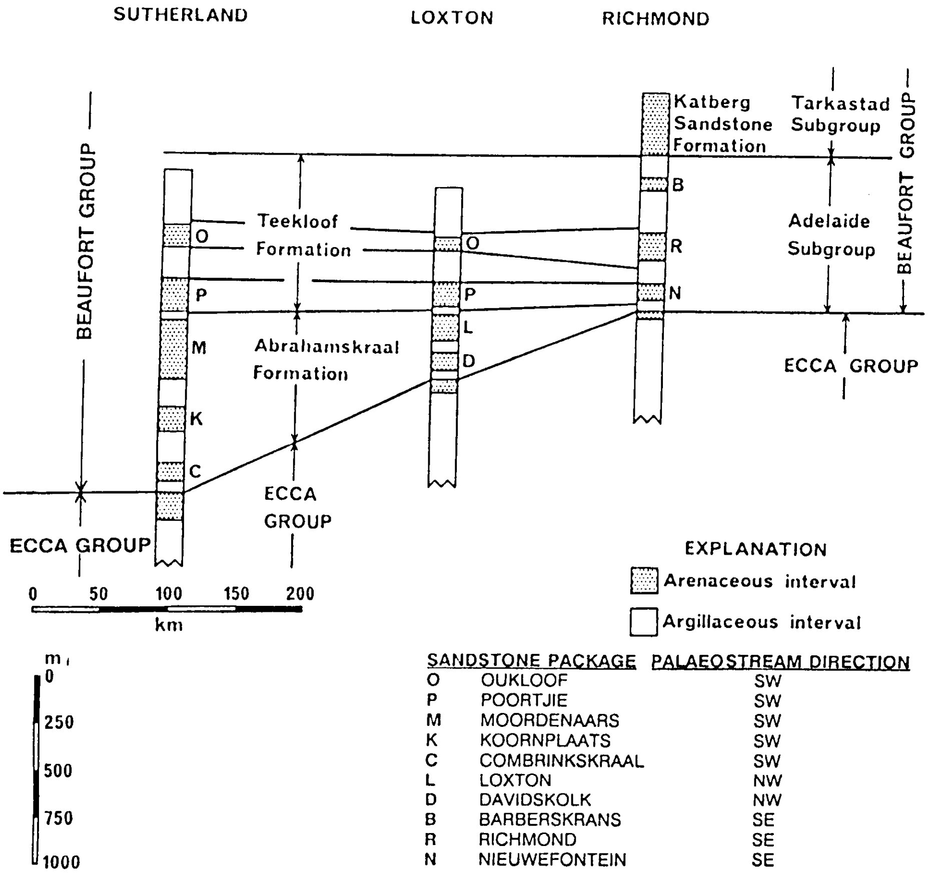

SANDSTONE PACKAGE		PALAEOSTREAM DIRECTION
O	OUKLOOF	SW
P	POORTJIE	SW
M	MOORDENAARS	SW
K	KOORNPLAATS	SW
C	COMBRINKSKRAAL	SW
L	LOXTON	NW
D	DAVIDSKOLK	NW
B	BARBERSKRANS	SE
R	RICHMOND	SE
N	NIEUWEFONTEIN	SE

Fig 5.2. Lithostratigraphic units relevant to the molybdenum investigation.

The field investigation comprised the following:

i. detailed ground radiometric and compass surveys of the mineralized sandstone outcrops;

ii. determination of the stratigraphic position of the occurrence;

iii. the collection of ca. 20 samples per occurrence;

iv. the determination of the elevation of each sample relative to the base of the arenite body;

v. identification of sedimentary textures, structures and facies;

vi. determination of grain size and rock type and

vii. the measurement of palaeostream directions.

Drilling results from previous exploration ventures were used where possible to delineate the sub-surface extent of the ore bodies. Unfortunately molybdenum analyses

Digitised by the Department of Library Services in support of open access to information, University of Pretoria, 2021

Table 5.2. Uranium occurrences investigated in the field.

LOCALITY Farm name and number	1: 50 000 map No.	SANDSTONE MEMBER
Vogelfontein 436	3221BA	Oukloof
Leeuwe Kloof 402	3221BB	Oukloof
Krugels Claim 459	3221BB	Oukloof
Goede Verwagting 462	3221AD	Oukloof
Driefontein 464	3221AD	Oukloof
Blomfontein 406	3221BB	Poortjie
Damsfontein 397	3221BB	Poortjie
Driefontein 464	3221AD	Poortjie
Koekemoer 482	3221AD	Poortjie
De Goede Hoop 463	3221AD	Poortjie
Ezelfontein 433	3221AB	Poortjie
Vinkekuil 144	3221CA	Poortjie
Klippekraal 145	3221CA	Poortjie
Banks Gaten 250	3221AC	Poortjie
Rondom 247	3221AD	Poortjie
Matjes Kloof 235	3221BC	Poortjie
Karee Poort 80	3223AD	Poortjie
Haane Kuil 335	3223CA	Poortjie
Brakfontein 329	3222DA	Poortjie
Riet Vallei 452	3221BB	Poortjie
Quaggasfontein 357	3121CD	Poortjie
Brandewyns Gat 214	3222AA	Poortjie
Kaffersfontein 328	3222DA	Poortjie
Rystkuil 351	3222DB	Poortjie
Vlekfontein 90	3123CB	Poortjie
Taai Bosch Fontein 137	3122BC	Poortjie
Mealieberg 45	3220DB	Moordenaars
Beerenvalley 150	3220DB	Moordenaars
Elandsfontein 128	3220DA	Moordenaars
Bullekraal 251	3221AD	Moordenaars
Die Bad 286	3221DB	Moordenaars
Vindragersfontein 280	3221DA	Moordenaars
Van Der Byls Kraal 265	3221DA	Moordenaars
Hendrikskraal 298	3221AC	Moordenaars
Riet Kuil 307	3222AC	Moordenaars
La-de-da 178	3222AD	Moordenaars
Bushmans Kop 302	3222AD	Moordenaars
Veldmans River 9	3222CC	Moordenaars
Cyferfontein 115	3322BA	Moordenaars
Vischgat 223	3121DB	Loxton
Blydevooruitzicht 299	3121CB	Davidskolk
Kokers Graafs Vlakte 221	3122AC	Davidskolk
Onbekend 141	3124BD	Barberskrans
Nmark 119	3225AB	Barberskrans
Kraanvogel Valley 120	3124CB	Barberskrans
Augustus Kraal 129	3124CA	Barberskrans
Richmond Townlands	3123BD	Richmond
Knapdaar 45	3123BC	Nuwefontein
Schraal en Bitter Vlakte 61	3024CC	Wortelfontein

Digitised by the Department of Library Services in support of open access to information, University of Pretoria, 2021

were available for only a small minority of these boreholes. Borehole positions were used as control points for mapping purposes where these could be identified positively in the field. The detailed compass mapping of the uranium-molybdenum occurrences and the area immediately surrounding them was plotted in sketch style on a scale of 1:2 000 to enable later identification of sample sites should the need arise.

5.1. Sampling

Individual samples of radiometrically anomalous host rocks and those in their immediate surroundings vary from grab samples to channel samples. With the exception of a few samples collected from the dumps of the open pit on Riet Kuil and the underground test mine on Rystkuil (situated 44 km west and 44 km southeast of Beaufort West respectively), all are from the surface and although care was taken to collect fresh material as far as possible, the samples represent rock weathered to various degrees. However, the presence of unoxidised sulphides in the majority of polished sections studied indicates that the object of sample freshness was largely achieved.

Individual samples had a mass of about 2 kg. Sample selection was based on the appearance of the rock and the scintillometer signal. The former criterion ensured that rocks formed under favourable conditions, but from a uranium-deficient provenance, were also investigated. Thus host rocks with a possible molybdenum potential, but without a distinct radiometric signature, were also included in this study.

5.2. Field instrumentation and analysis

For initial field delineation of the uraniferous bodies use was made of Chemtron and Exploranium scintillometers operated by the researchers and field assistants.

The Outokumpu X-Met 840 portable XRF analyzer acquired for the project to semi-quantitatively delineate molybdenum-bearing rocks in the field was selected owing to

Digitised by the Department of Library Services in support of open access to information, University of Pretoria, 2021

its built-in safety attributes, ease of operation, robustness and light weight. With the aid of this radio-isotope-based battery/mains-powered instrument analyses are obtained from the surface of powdered or liquid samples. The X-ray fluorescence spectrum obtained through isotope irradiation of the sample is recorded on 250 energy channels by means of a proportional counter and assays are automatically calculated by means of the built-in micro-processor. The output is alpha-numeric on the display panel or on hard copy through a coupled printer.

It is possible to analyze for the elements with atomic number between Al and U by making use of four different radio-isotopes. The ^{109}Cd isotope gives optimum detection limits for both molybdenum on the K_α- and for uranium on the L_α line (Fig 5.3, ASOMA Instruments) and was therefore selected for the project despite its short useful life of about three years (half life of 1.3 years) in preference to the ^{241}Am isotope (half life of 433 years).

The instrument has eight calibration modules and each can be used for the analysis of up to six elements. Thus theoretically 48 elements can be determined per measurement by switching from one module to the other. The measuring time per reading can be varied from one second to 32 000 seconds with practical measuring periods between 60 and 300 seconds.

Field preparation of samples consisted of crushing of about 4 g of material by means of a custom-made diamond mortar and screening to -0,15 mm. The remainder of the sample was either rejected or sent to the Geological Survey laboratory in Pretoria for complete and accurate analysis. All anomalous samples as well as a selection of samples which returned low field analyses were submitted for laboratory analysis. Analysis during the field stage of the project varied from actual field procedures on the outcrop with a power supply from rechargeable batteries to camp-bound procedures in which the day's samples were analyzed by means of a power supply from 220 V mains or a 0,5 kW generator. As the crushing of the samples turned out to be the most time-consuming link in the analytical chain, which resulted in a slow-down of field mapping, most analyses were done in the camp at night and over weekends.

Digitised by the Department of Library Services in support of open access to information, University of Pretoria, 2021

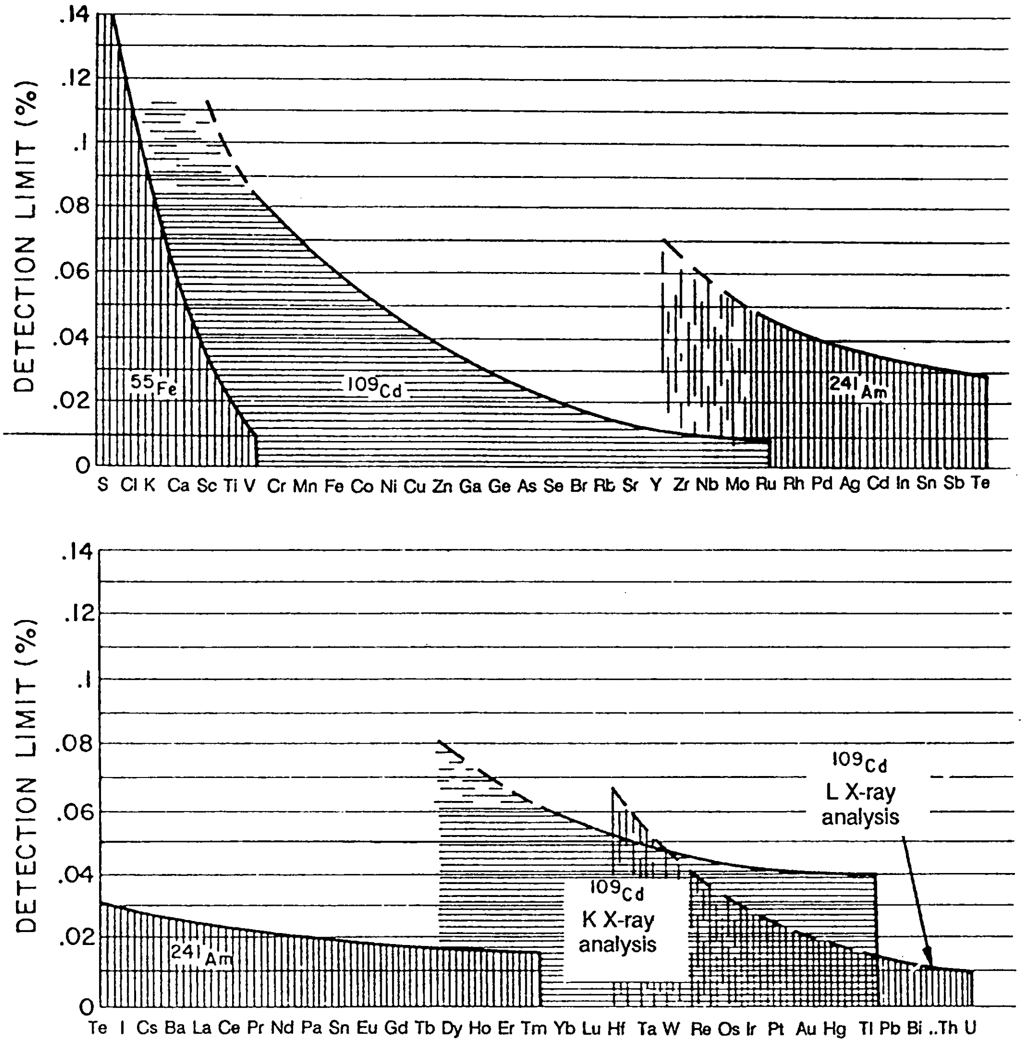

Fig. 5.3. Theoretical detection limits by means of various radio isotopes in XRF analysis. (The bottom diagram is an extension of the top one)

Time and money are saved by using a portable XRF analyzer as field exploration tool since costly revisits are eliminated, because promising trends can be followed up either straight-away, or while the researcher is still in the area and the observations are still fresh in his mind. The total number of samples submitted to the laboratory is also reduced. The field analyses, though not as accurate as those of the laboratory, also act as a control of any possible systematic errors in the laboratory.

Digitised by the Department of Library Services in support of open access to information, University of Pretoria, 2021

5.3. Calibration of portable XRF spectrometer

To calibrate the Outokumpu X-MET 840 XRF analyzer separate spike sequences with concentrations 10, 20, 50, 100, 200, ..., 10 000 ppm were prepared for the elements of interest. Barren Karoo rock was selected from borehole core and after it had been crushed, was used as matrix for the spikes.

Initially the instrument was calibrated for each element on a separate module. The correlation between X-MET and laboratory analyses turned out to be poor. The reason for this is that no allowance was made in the calibration process for inter-element spectral interference. In the next calibration exercise it was hoped to solve this problem by reading all spikes on the same module, but the correlation did not improve.

To find the reason for the unsatisfactory results, the XRF spectra were plotted for all analyzing channels for individual spikes and some analyzed sample powders. Comparison of the positions of the spectral lines of the elements of interest revealed that serious inter-element interference is present, for example the $U_{L\beta}$ and the $Zr_{K\beta}$ lines interfere with the $Mo_{K\alpha}$ line, resulting in inflated Mo values (Fig. 5.4). In the case of a molybdenum-free uranium spike (2000 ppm U) a value of 136 ppm Mo was obtained. Similar interference problems exist (not shown in Fig. 5.4) between the $U_{L\alpha}$ line and the $Sr_{K\alpha}$ and $Rb_{K\alpha}$ lines, as well as between the $Zr_{K\alpha}$ and the $Sr_{K\beta}$ lines.

In the third calibration test a variation of the method developed by Rhodes and Rautala (1983) was employed, in which use is made of mixed spikes. These are prepared to agree with the nine concentration permutations (Fig 5.5) that are possible for two interfering elements. In this case the mono-element spike sequences of interfering elements were read together into one module with a selection of field samples (fulfilling the permutation criterion) previously analyzed by the laboratory. This calibration set consists of spikes of the elements U, Mo, Rb, Sr and Zr together with samples of mixed-element composition. In Figure 5.6 a comparison between laboratory and X-Met analyses of the third calibration test for molybdenum and uranium is shown. This comparison, though not based on exactly identical material (only a small portion of each sample was crushed and used for field analysis, with the remainder of the sample

Digitised by the Department of Library Services in support of open access to information, University of Pretoria, 2021

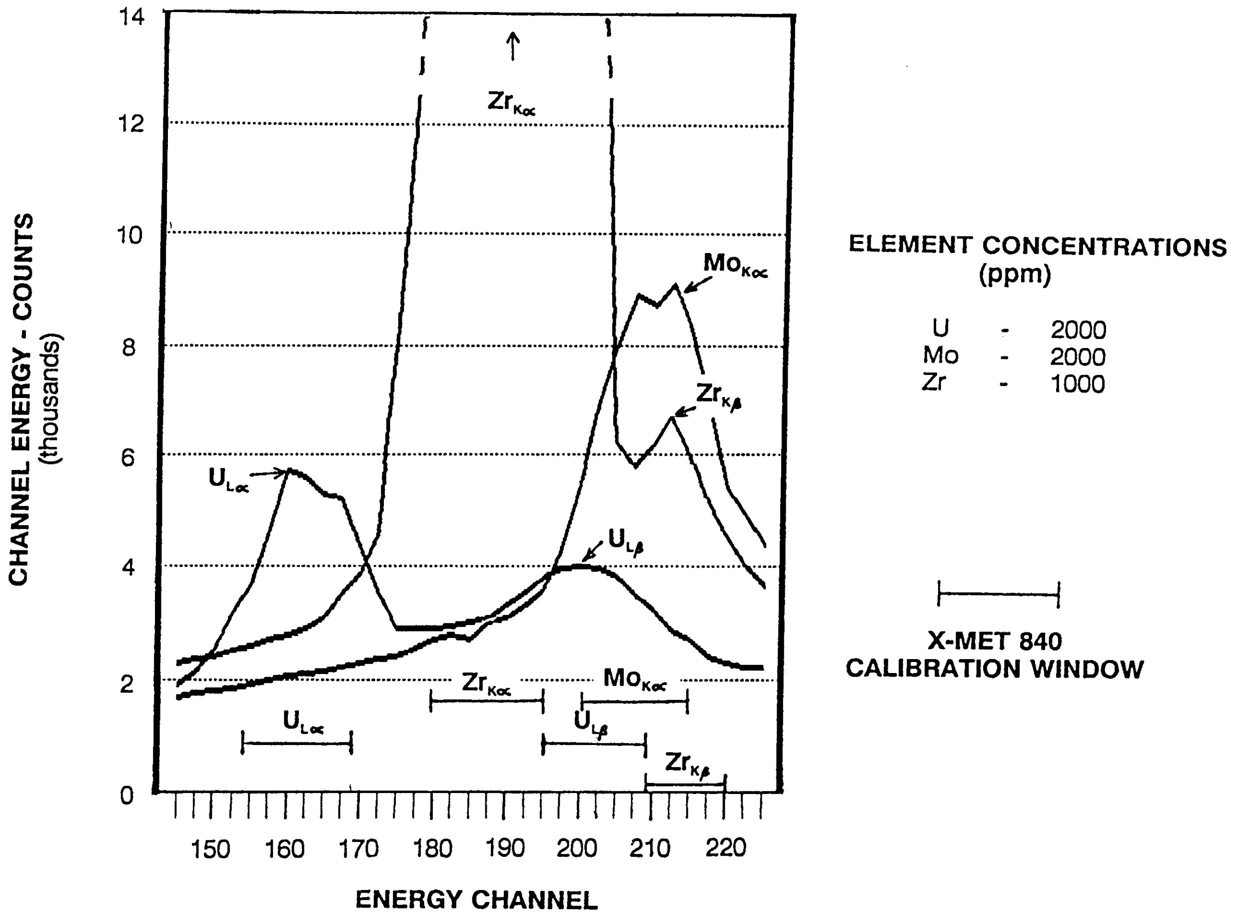

Fig. 5.4. Interference of the $U_{L\beta}$ and $Zr_{K\beta}$ fluorescent lines with the $Mo_{K\alpha}$ line.

low$_1$-low$_2$	**low$_1$-med$_2$**	**low$_1$-high$_2$**
med$_1$-low$_2$	**med$_1$-med$_2$**	**med$_1$-high$_2$**
high$_1$-low$_2$	**high$_1$-med$_2$**	**high$_1$-high$_2$**

Fig. 5.5. Concentration permutations possible for two interfering elements.

being used in the laboratory) shows that with this calibration the X-MET 840 returns analyses of a semi-quantitative nature which are of sufficient quality to guide the researcher in the field.

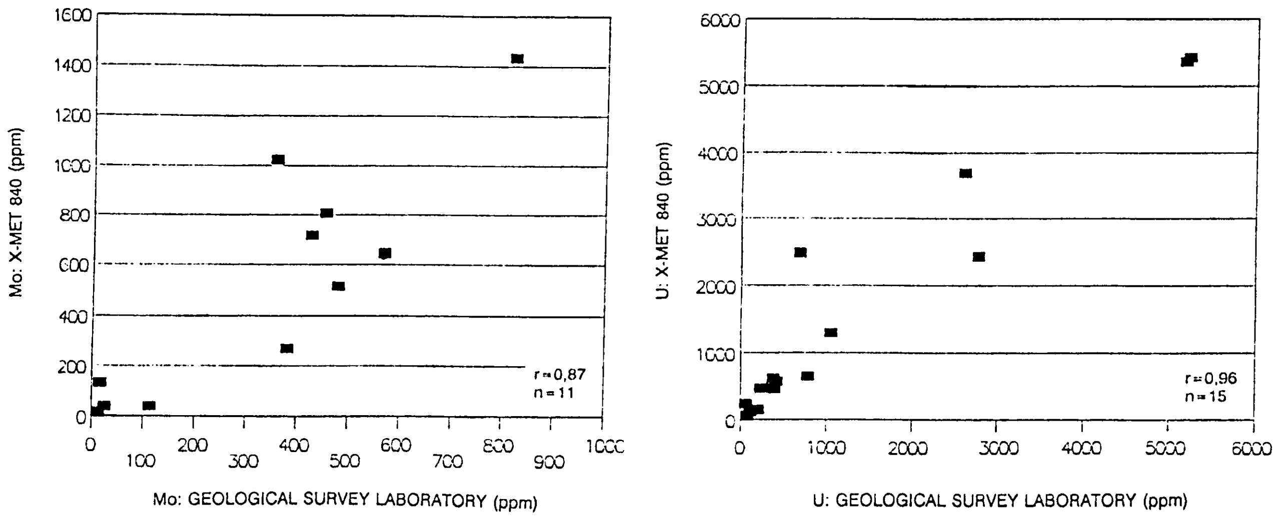

Fig 5.6. Comparison of laboratory- with X-MET analyses (third calibration)

5.4. Detailed laboratory analysis

The laboratory investigation comprised XRF analysis and petrography of the selected samples.

5.4.1. Laboratory XRF analysis

In the case of XRF analysis various analytical paths were followed and compared, and eventually an instrument was specially calibrated for the project.

The laboratory analysis was initially done by means of the Phillips 1600 XRF spectrometer at the Geological Survey. The calibration of this instrument is intended for the routine trace element analyses of the South African geochemical project and is based on international standards. These standards, however, only cover the lower range of values normally encountered during geochemical exploration, but not the higher values characteristic of economic and sub-economic mineral deposits. The higher values obtained in the initial stages of the project, were therefore inaccurate due to the uncontrolled extension of the calibration line. Analyses for uranium, molybdenum

Digitised by the Department of Library Services in support of open access to information, University of Pretoria, 2021

and elements which interfere with their spectral lines (Rb, Sr, Zr, Th and Pb) were therefore done on a Phillips 1400 XRF spectrometer which was specially calibrated for these elements by means of spiked calibration standards and of samples of known composition initially used for the calibration of the X-MET 840. The molybdenum and uranium values so obtained were compared with those of a reputable independent laboratory by means of a duplicate representative sample set (Fig. 5.7.). The values obtained after the calibration of the Phillips 1400 XRF spectrometer form the basis of the statistical analysis.

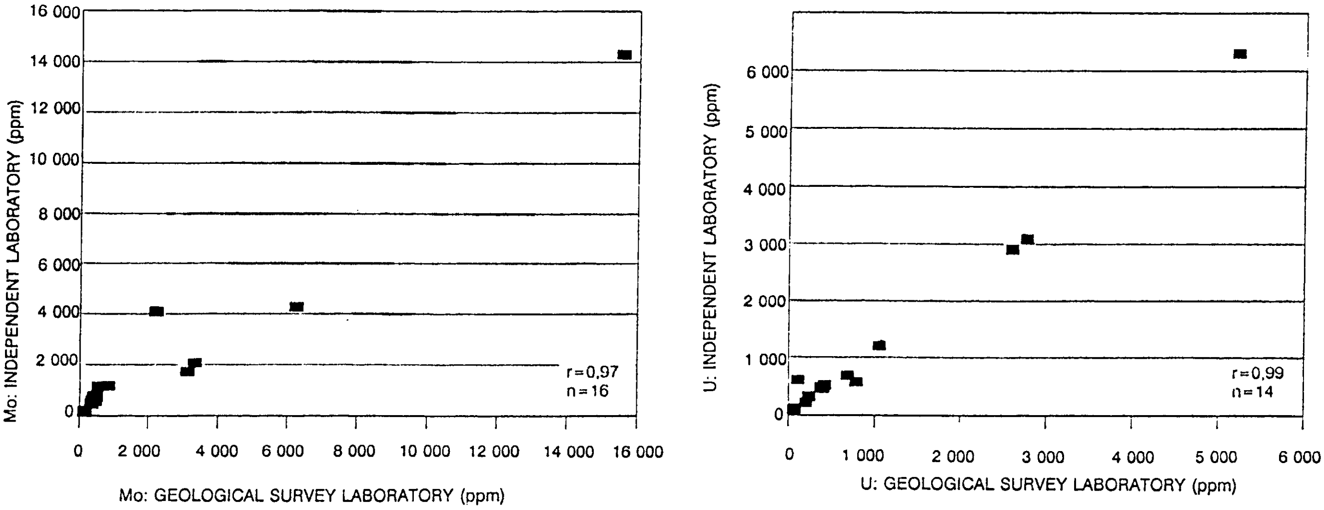

Fig. 5.7. Comparison of the special calibration on the Phillips 1400 XRF spectrometer with analyses by a reputable independent laboratory.

5.4.2. Petrography

A suite of 68 field samples was selected for microscopic examination. On account of their high radioactivity, twenty seven of these were further subjected to autoradiography in the photographic laboratory of the Geological Survey to identify positions favoured by uranium.

Digitised by the Department of Library Services in support of open access to information, University of Pretoria, 2021

5.4.2.1. Autoradiography

Ever since the discovery of radioactivity photographic emulsions have been used to locate alpha particle emitters in geological specimens and various other materials. This was followed by radioluxography, in which light emissions from activated phosphorus zinc sulphide coatings on the specimen surface were recorded photographically. Both methods have the shortcoming that light-sensitive material is involved.

With the advent of solid-state nuclear track detectors during the seventies darkroom facilities could be replaced by relatively inexpensive autoradiographic techniques which can even be employed under field conditions.

Flexible sheets of cellulose nitrate are exposed to the radioactive material to be examined. This method has found a wide range of applications such as nuclear reactor rate measurement, autoradiography of irradiated specimens and the detection of the presence of radon in mines and in soil. The method is based on the structural damage caused by the heavy, charged particle along its path through the film. The damaged region is chemically more reactive and can be etched preferentially, giving rise to conical tracks readily observable under the optical microscope. The advantage of this method is that it requires no special equipment, as for instance a nuclear reactor in the case of fission track studies (Brynard, 1983), or laboratory and darkroom facilities (Basham and Easterbrook, 1977 and Basham, 1981).

In this case the smooth surfaces of the polished pieces were placed on sheets of Kodak Detecteur CN85 on a glass pane. The contact was established and maintained by a layer of foam rubber on the back of the samples, which was in turn covered with a second pane. This sandwich was then compressed to eliminate any movement. The polished surface of the samples was subsequently photographed through the cover glass and transparent detector film to enable the matching of a particular radioactive spot on the specimen with its radiation image. The exposure time of the cellulose nitrate sheets to the samples was three weeks. The sheets were then etched for six hours and thirty minutes in a 10% NaOH solution and then rinsed for 90 minutes under running water.

Digitised by the Department of Library Services in support of open access to information, University of Pretoria, 2021

By means of the autoradiographs sources of radioactivity could be located quickly and effectively prior to their identification by mineralogical methods. The high resolution and superb optical properties of autoradiographs facilitate macroscopic and microscopic (even under higher magnification) comparison by the superimposition of the alpha track image on the specimen.

On a macroscopic scale the autoradiographs reveal that the uranium is disseminated in the sandstone, but that bedding-planes have a strong influence on the local concentration of the radioactive minerals (Fig. 5.8). The permeability of the unconsolidated sediment was probably greater parallel to the bedding and the uranium minerals consequently precipitated along these passages. The mineralization visible on some cracks in the rock are interpreted as having formed during the present cycle of weathering through mobilization and re-precipitation of uranium. On a microscopic scale the specimen can be searched on the autoradiograph overlay for specific mineral grains which can be studied optically after removal of the autoradiograph (Fig. 5.9. a.

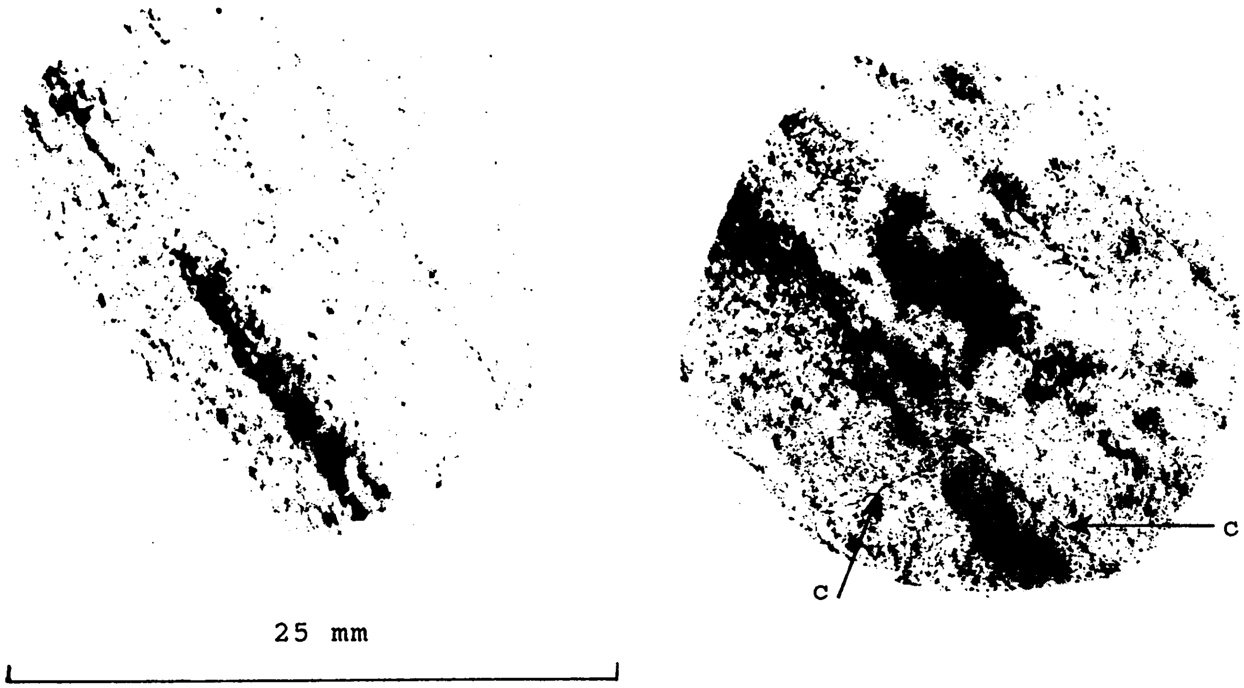

Fig. 5.8. Autoradiographs of polished blocks showing the control of bedding planes on the distribution of uraniferous minerals. The right-hand image also shows a hair-line crack (c) filled with a uranium mineral.

Digitised by the Department of Library Services in support of open access to information, University of Pretoria, 2021

and b.) Individual larger specks of radioactive material located in this way were found to be uraniferous phytoclasts (Fig. 5.9. b.).

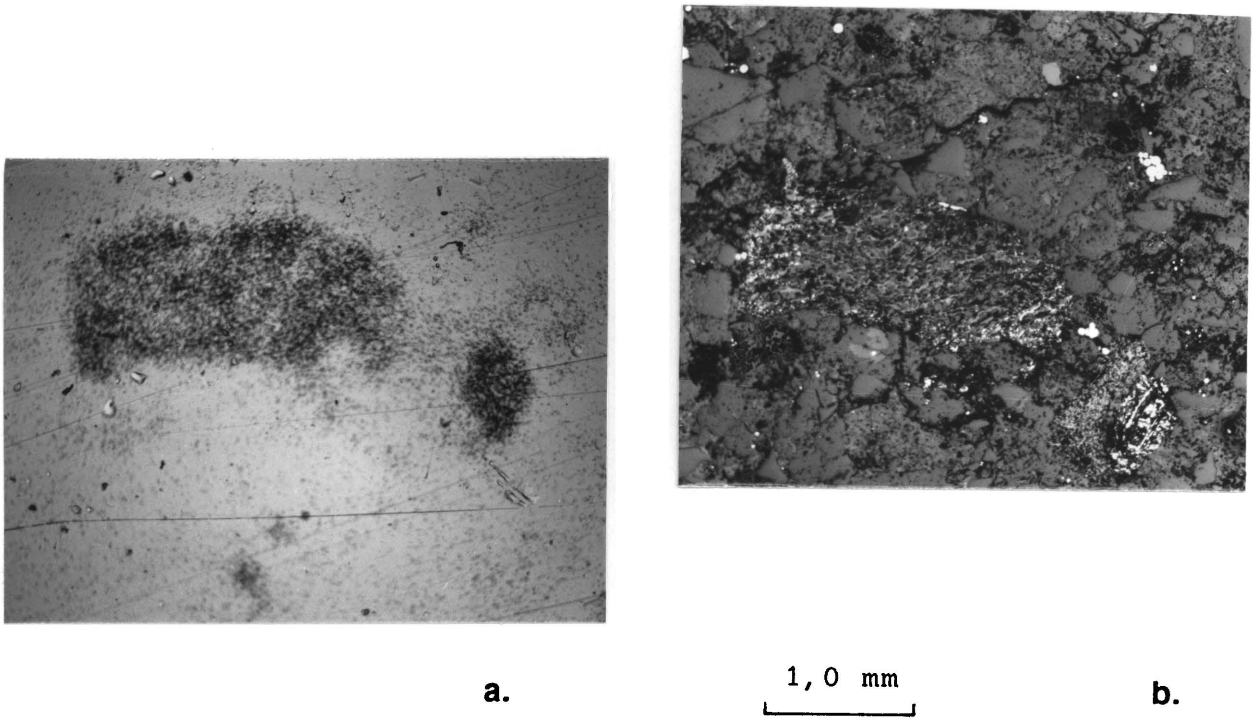

Fig. 5.9. a. Autoradiograph as overlay on a polished specimen indicating the position of a radioactive source as seen through the microscope. **b.** Radioactive material after removal of the overlay. (both reflected light)

5.4.2.2. Microscopy

The suite of samples selected for microscopic investigation was studied mainly by means of the ore microscope, but some transmitted-light microscopy was also used.

The uranium-molybdenum-bearing sandstones are fine grained and consist of sub-angular fragments of quartz, feldspar and rock. Microscopically the laminated and the carbonate-cemented ore types can be distinguished from each other by examination of the fabric. The former is characterized by a clast-supported fabric (Fig. 5.10. a.) whilst that of the latter is matrix supported (Fig. 5.10. b.). This matrix of the carbonate-cemented type consists of fibrous carbonate minerals which displace the clastic grains outwards. The bonding by the carbonate cement is so good that the

Digitised by the Department of Library Services in support of open access to information, University of Pretoria, 2021

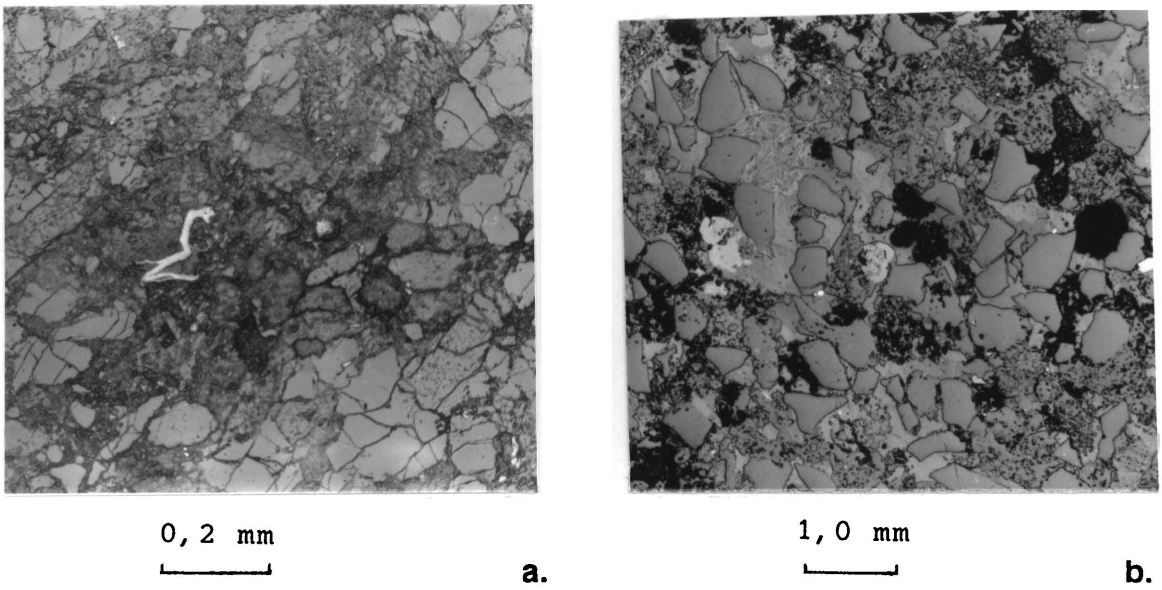

Fig. 5.10. a. Clast-supported fabric of the laminated sandstone-type mineralization with a molybdenite flake (reflected light). **b.** Matrix- supported fabric of the carbonate-cemented type of mineralization (reflected light, oil)

rock is virtually impermeable to water in the weathering environment, with the result that fresh sulphide minerals are preserved only a few millimetres below the buff-black manganese enriched weathering crust. Molybdenite grains in the sandstones usually have a crumpled appearance (Fig 5.11). This is interpreted as due to crystallization of

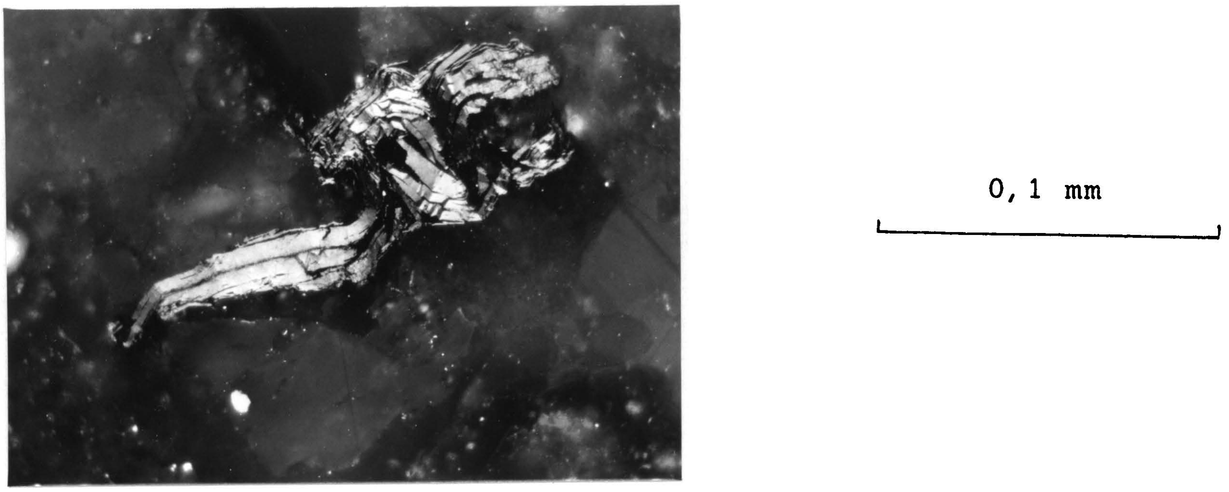

Fig. 5.11. Crumpled molybdenite flake (reflected light, oil immersion)

Digitised by the Department of Library Services in support of open access to information, University of Pretoria, 2021

the molybdenite flakes shortly after deposition of the sandstone body and well before the diagenetic reduction of the pore volume has taken place. The same conclusion is gained from the matrix-supported fabric of the carbonate-cemented sandstones. Here the sand was cemented by the carbonate minerals before the confining pressure due to burial was too high.

Comparison of the radiograph of a polished specimen with the distribution of uranium-bearing minerals indicates that only a small proportion of the uranium is concentrated in discrete minerals and as replacement of phytoclasts (Fig. 5.12). In many instances the uranium is concentrated as a thin coating around sand grains (Fig. 5.13). Comparison of polished specimens with roughly equal concentrations of uranium and molybdenum shows a marked deficiency in molybdenite grains, indicating that the majority of molybdenum is probably finely dispersed through the sandstone, as was observed in the case of uranium.

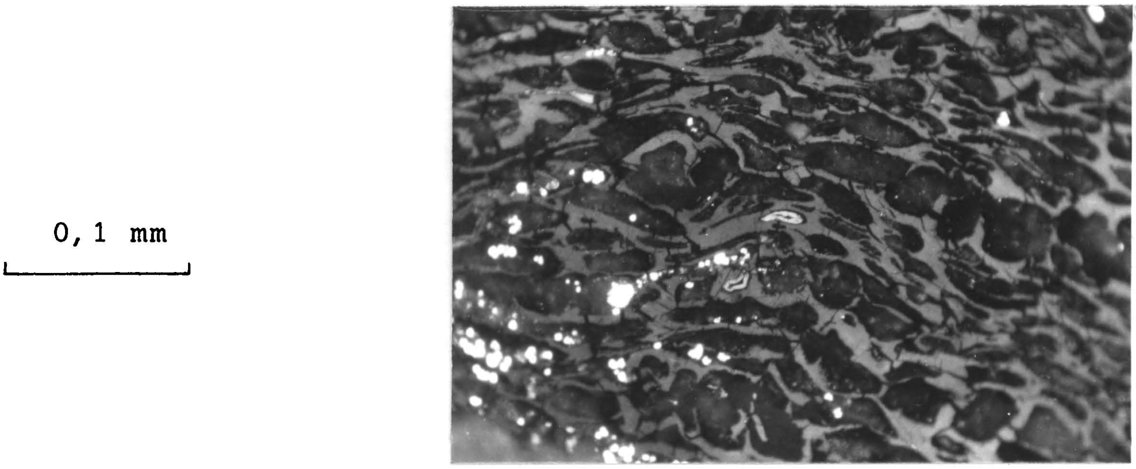

Fig. 5.12. Replacement of a phytoclast by a uranium mineral (reflected light).

Sulphide minerals identified by means of ore-microscopy are pyrite, which is frequently framboidal (Fig 5.14), chalcopyrite, bornite, löllingite, covellite (Fig. 5.15 and 5.16) and arsenopyrite.

UNIVERSITEIT VAN PRETORIA
UNIVERSITY OF PRETORIA
YUNIBESITHI YA PRETORIA

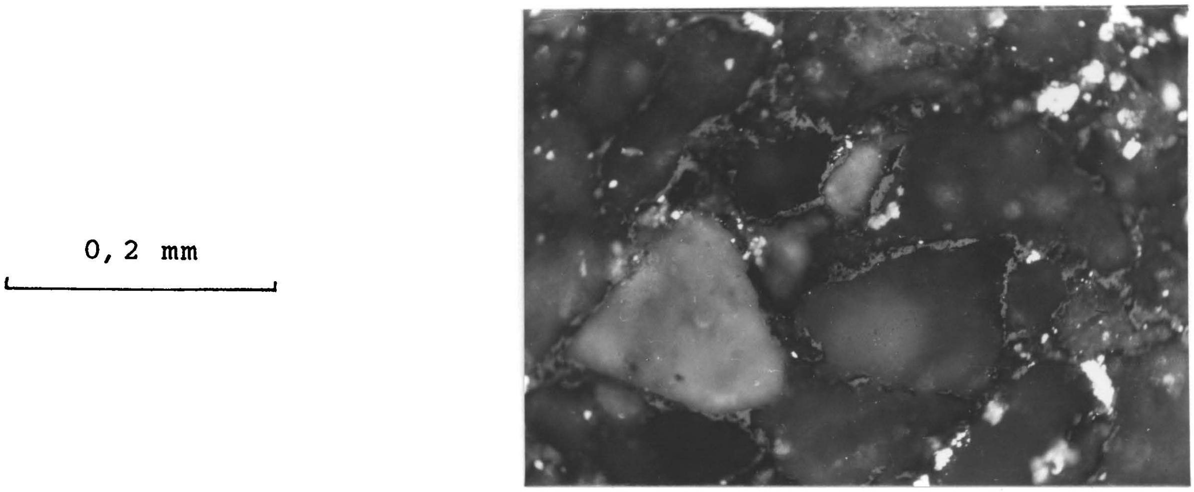

Fig. 5.13. Uranium minerals coating sand grains in a mineralized sandstone (reflected light).

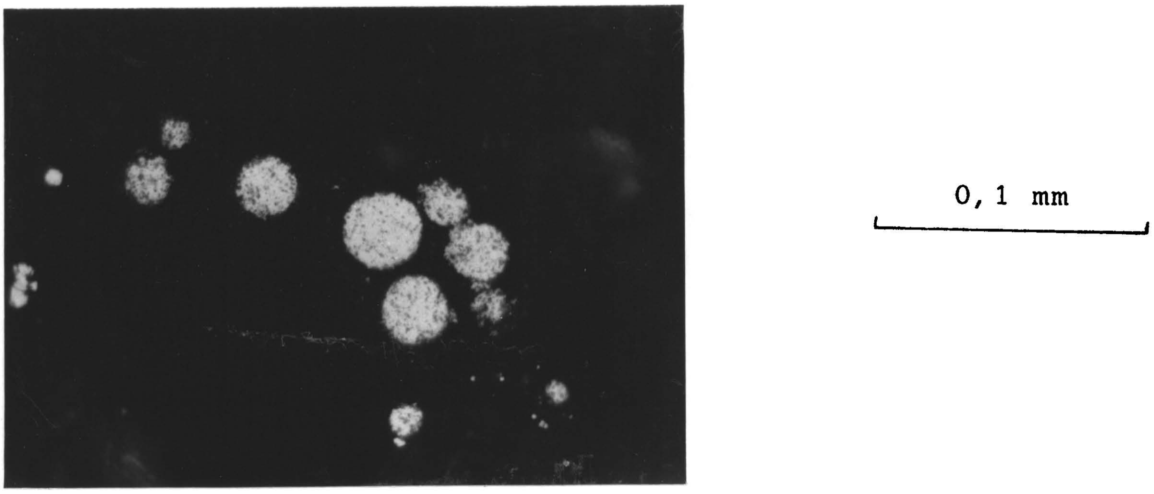

Fig. 5.14. Framboidal pyrite (reflected light).

Digitised by the Department of Library Services in support of open access to information, University of Pretoria, 2021

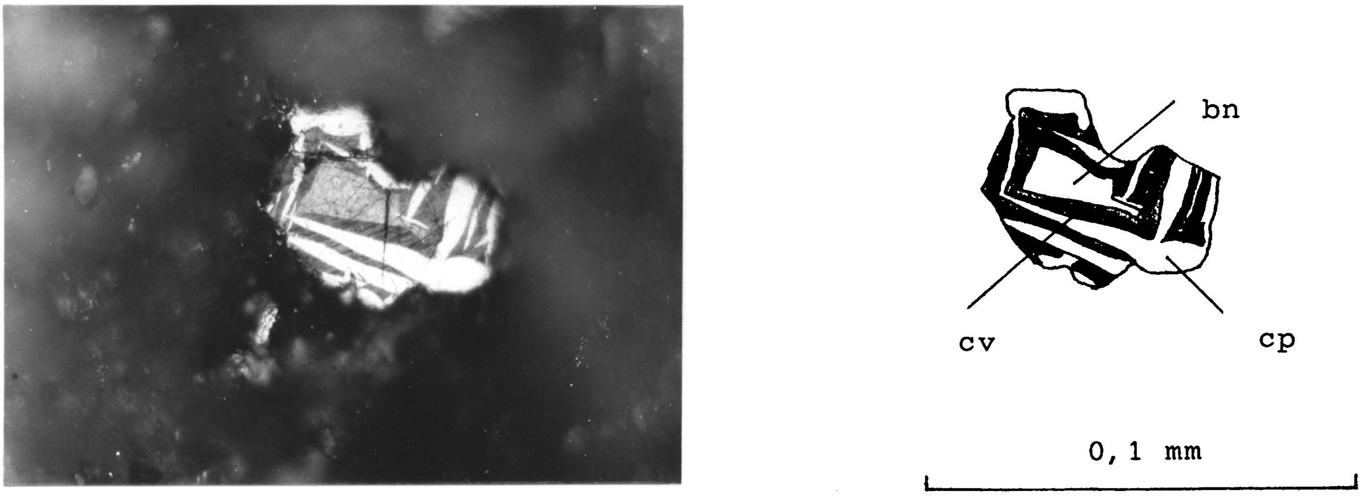

Fig. 5.15. Bornite (bn), covellite (cv) and chalcopyrite (cp) (reflected light).

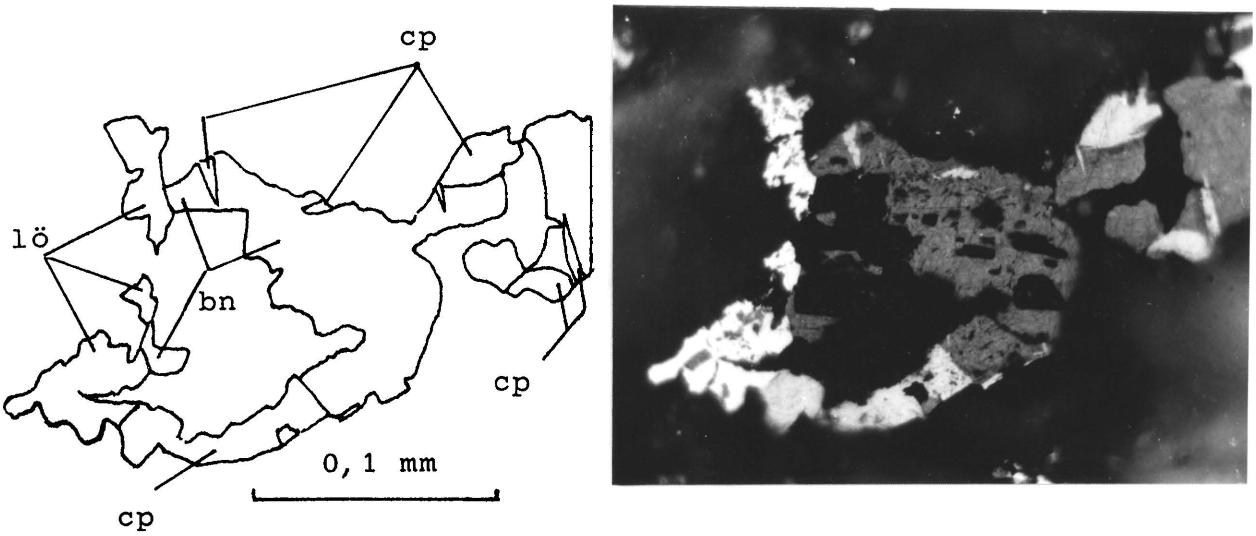

Fig. 5.16. Löllingite (lö), chalcopyrite (cp) and bornite (bn) (reflected light).

Digitised by the Department of Library Services in support of open access to information, University of Pretoria, 2021

6. Results

A detailed description of each of the 49 occurrences investigated falls outside the scope of this thesis. Therefore only a selection of occurrences will be used to illustrate the characteristics of the different types of uranium-molybdenum mineralization.

6.1. Occurrences related to laminated sandstone-type mineralization.

6.1.1. Uranium mineralization on Vogelfontein 436.

The farm Vogelfontein is situated 30 km south of Fraserburg (Fig. 6.1). Despite its low molybdenum potential this example was chosen because of its good three-dimensional exposures and the fact that it was the first one to be investigated and was

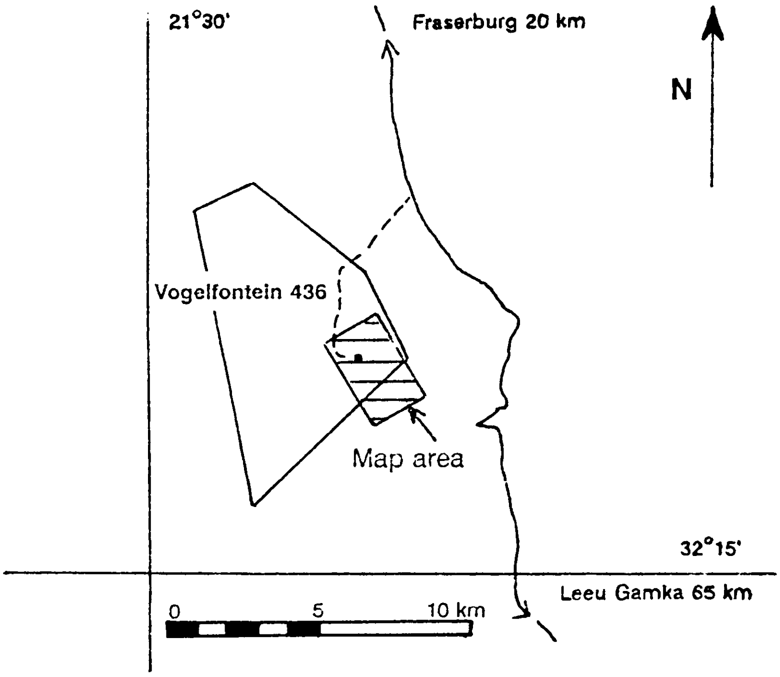

Fig. 6.1. Locality map showing the position of the area investigated on the farm Vogelfontein 436.

therefore studied in great detail. The model for laminated sandstone-type mineralization is largely based on this occurrence, although others have obviously also been taken into account.

The surface distribution of the mineralization and of exploration boreholes are shown in Fig. 6.2. The mineralization generally tends to occur as small and discontinuous pods. The bedding of the sedimentary rocks is for all practical purposes horizontal. The vertical section (Fig. 6.3) shows the position of the main sandstone bed of the Oukloof Sandstone Member in relation to other sandstone beds in the sedimentary column. Portion A - B of the vertical section shows the dominantly mudstone environment below the first sandstone, and the tendency of individual sandstone beds to become thicker with stratigraphic height. The pockets of uranium mineralization are usually concentrated in the thickest sandstone bed.

The cliff faces on Vogelfontein were mapped in detail. The base of the sandstone is undulatory with a vertical variation of a couple of metres. The most prominent undulations are the result of rip-channels cut into the mud-plain during the initial stages of the flood responsible for the deposition of the sandstone body. These channels are about a metre or two deep and of the order of ten metres wide.

Digitised by the Department of Library Services in support of open access to information, University of Pretoria, 2021

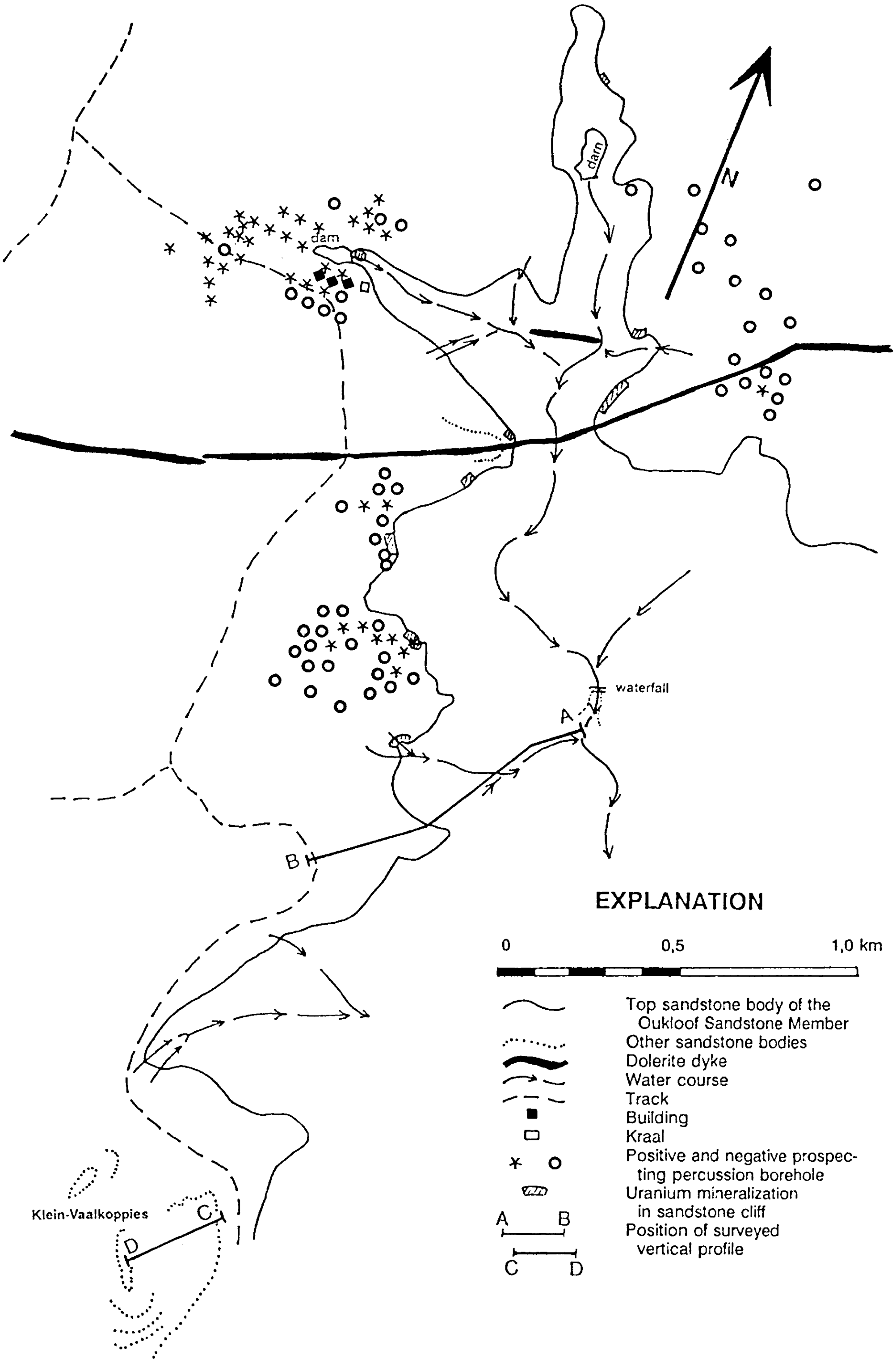

Fig. 6.2. Surface distribution of the uraniferous occurrences on the farm Vogelfontein 436.

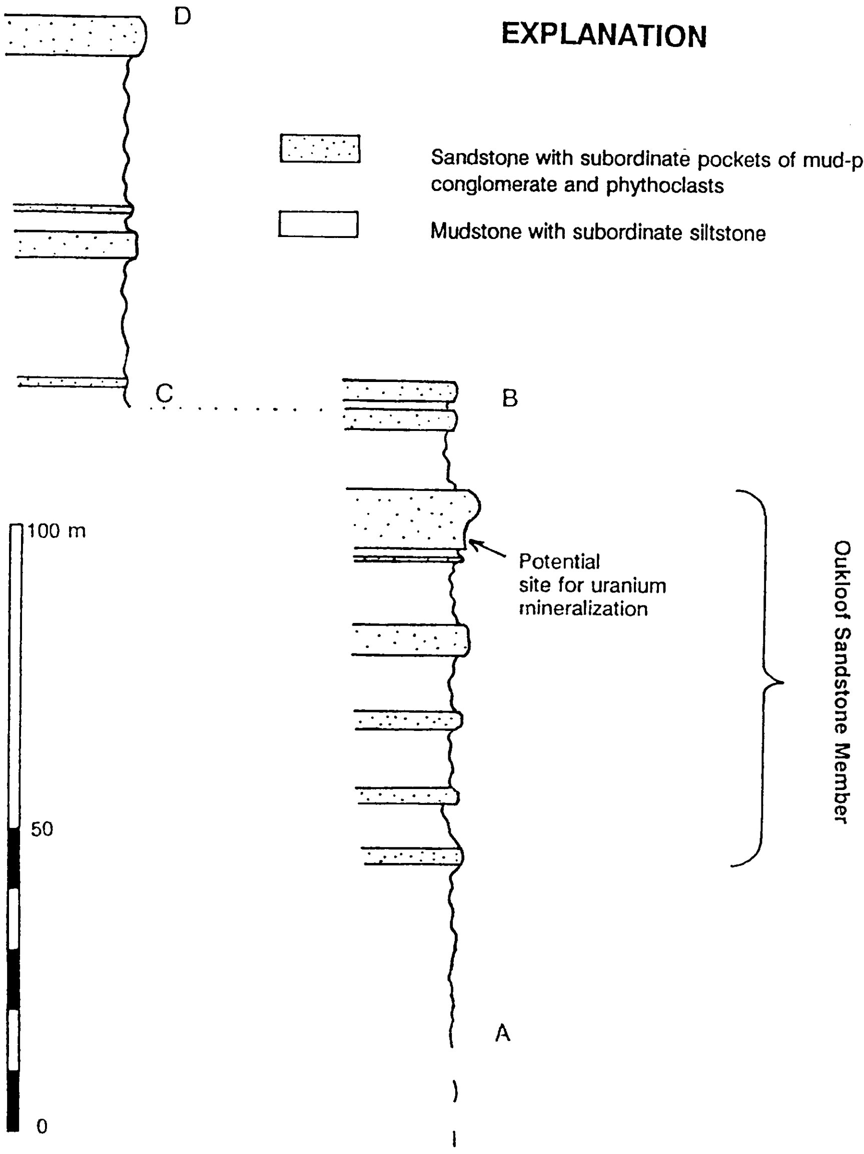

Fig. 6.3. Vertical section (off-set in two profiles AB and CD in Fig. 6.1) showing the position of the main sandstone bed (host to the uraniferous pockets) in relation to other sandstone beds.

Digitised by the Department of Library Services in support of open access to information, University of Pretoria, 2021

6.1.2 Mineralization on Bloemfontein 406

Bloemfontein 406 is situated 37 km east-southeast of Fraserburg (Fig. 6.4). This occurrence in the Poortjie Sandstone Member is selected for its higher molybdenum content and the better borehole control. The following description is based on unpublished diagrams of Dr. D. I. Cole.

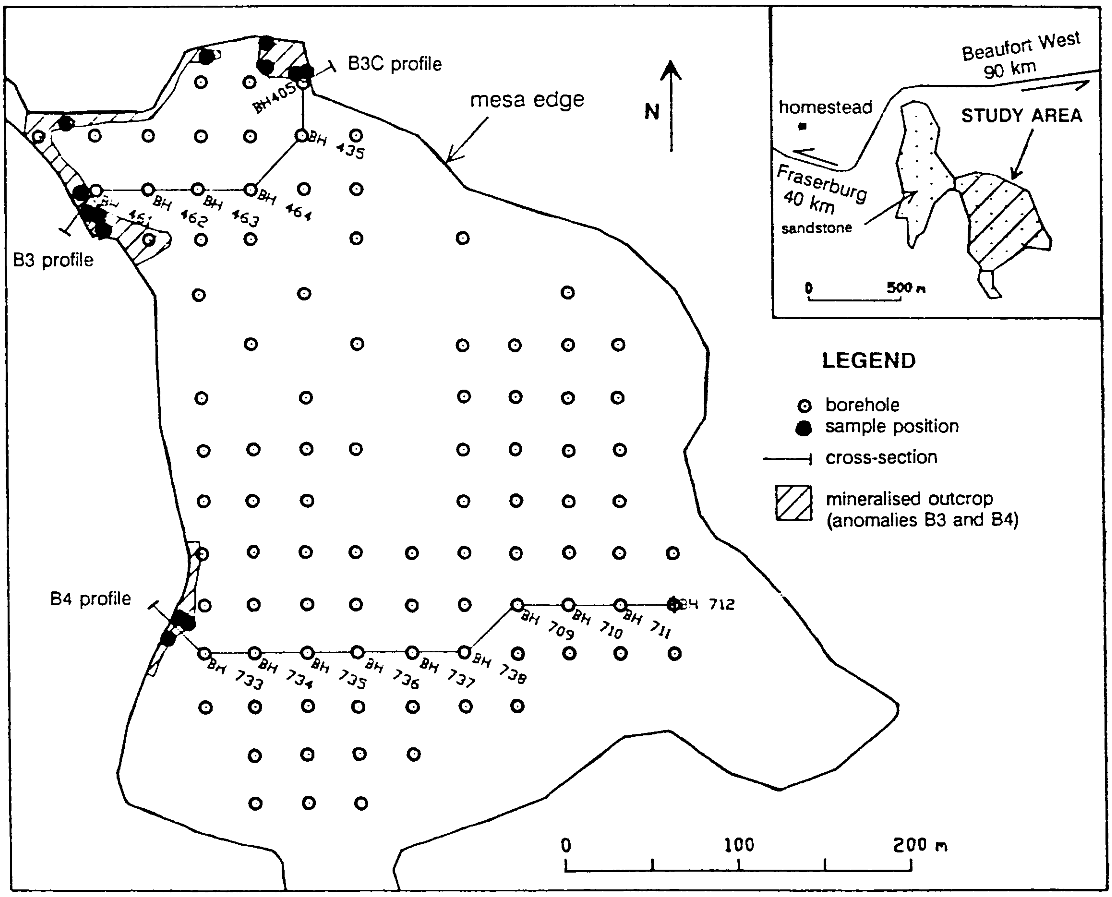

Fig. 6.4. Locality map of the uraniferous occurrences on Bloemfontein 406, showing the mineralized outcrops, the exploration drill-hole grid and the two profiles measured (Cole, pers. comm.).

The mineralization occurs in the sandstone capping of a 25 metre high mesa on mudstone and was explored by means of a 30 metre-square borehole grid (Fig. 6.4).

Digitised by the Department of Library Services in support of open access to information, University of Pretoria, 2021

This sandstone capping forms the southern portion of a multi-storey sandstone sheet with maximum thickness of 33 metres according to borehole inter-sections. According to the description of Kübler (1977) this sheet, distinguished by him as "A", has an average width of 5 km and can be followed for a distance of about 15 km in a north-northeasterly direction. In the portion under investigation a maximum of 10,3 metres of sandstone is preserved, the remainder having been removed by erosion.

The cross-sections (Fig. 6.5 and 6.6) were drawn on the basis of borehole logs and cliff mapping (profiles B3, B3C and B4). From the sections and the contour plan of the base of the sandstone body (Fig. 6.7) it can be seen that the base of the sandstone body is undulatory with a maximum vertical variation of 5 metres. The cross-sections indicate a lower, a middle and possibly a higher ore horizon, but the individual ore-bodies are discontinuous. The thicknesses of the lower and middle horizons, based on borehole intersections (Fig. 6.8 and 6.9 respectively) rarely exceed one metre. It also seems that areas of thicker ore-body development coincide to some extent with areas of lower floor elevation of the sandstone sheet, especially in the case of the lower ore horizon (compare Figures 6.7, 6.8 and 6.9). Figures 6.10 and 6.11 represent uranium value contours for the lower and middle ore-body respectively. The close

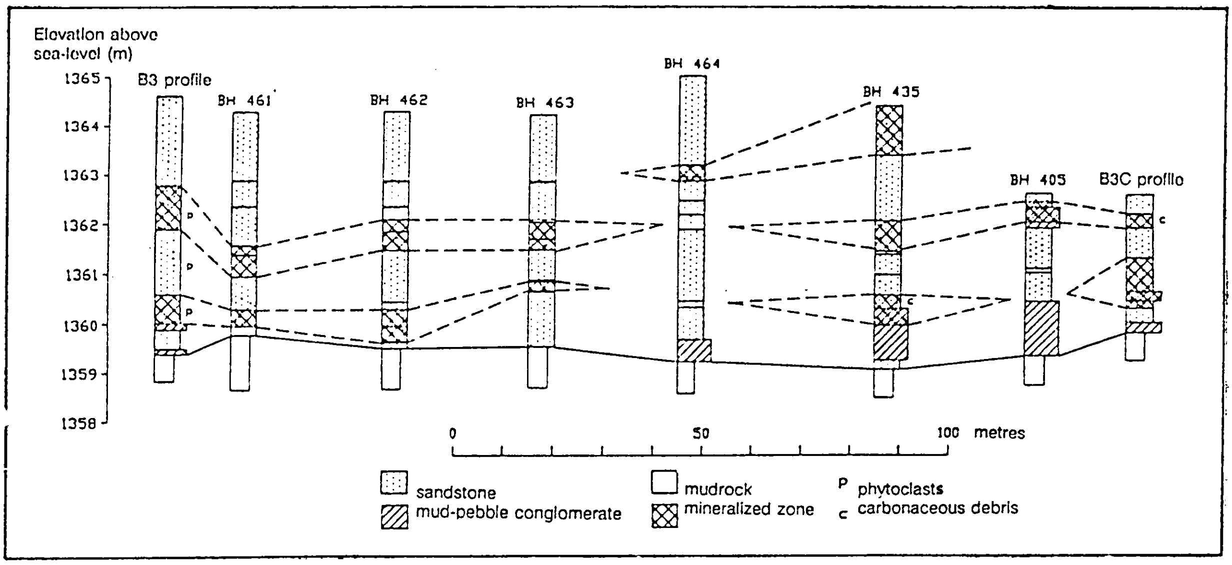

Fig. 6.5. Geological section along B3 - B3C through anomaly B3 on Bloemfontein 406, based on borehole data and measured profiles (Cole, pers. comm.).

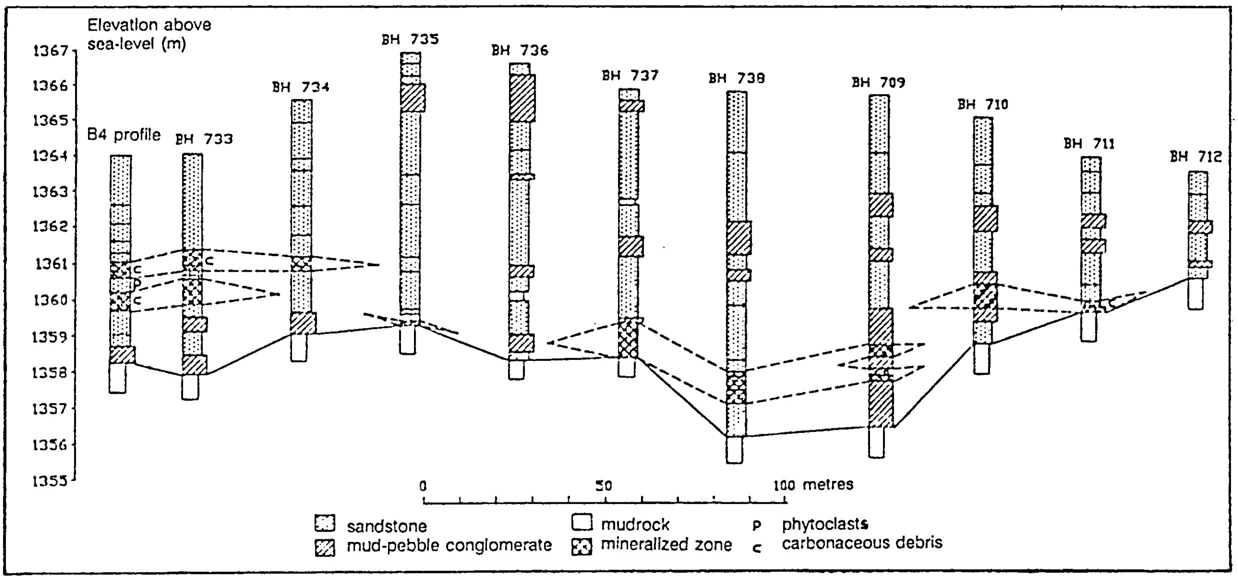

Fig. 6.6. Geological section along line B4 - BH 712 through anomaly B4 on Bloemfontein 406 (Cole, pers. comm.).

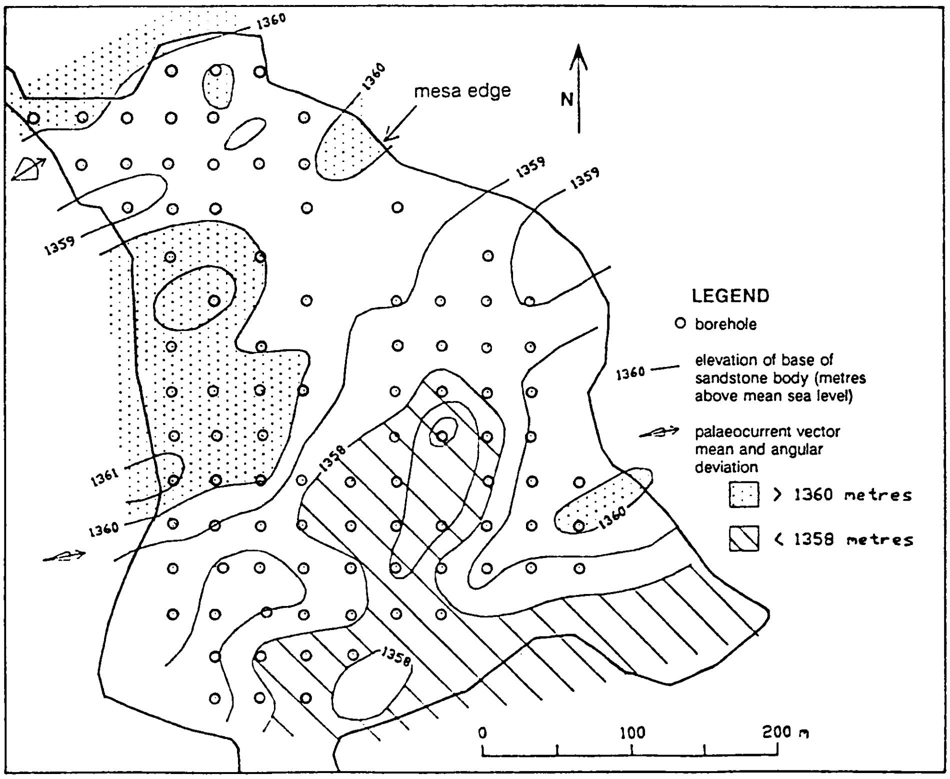

Fig. 6.7. Contour map of base of the sandstone sheet at the uraniferous occurrences on Bloemfontein 406 (Cole, pers. comm.).

Digitised by the Department of Library Services in support of open access to information, University of Pretoria, 2021

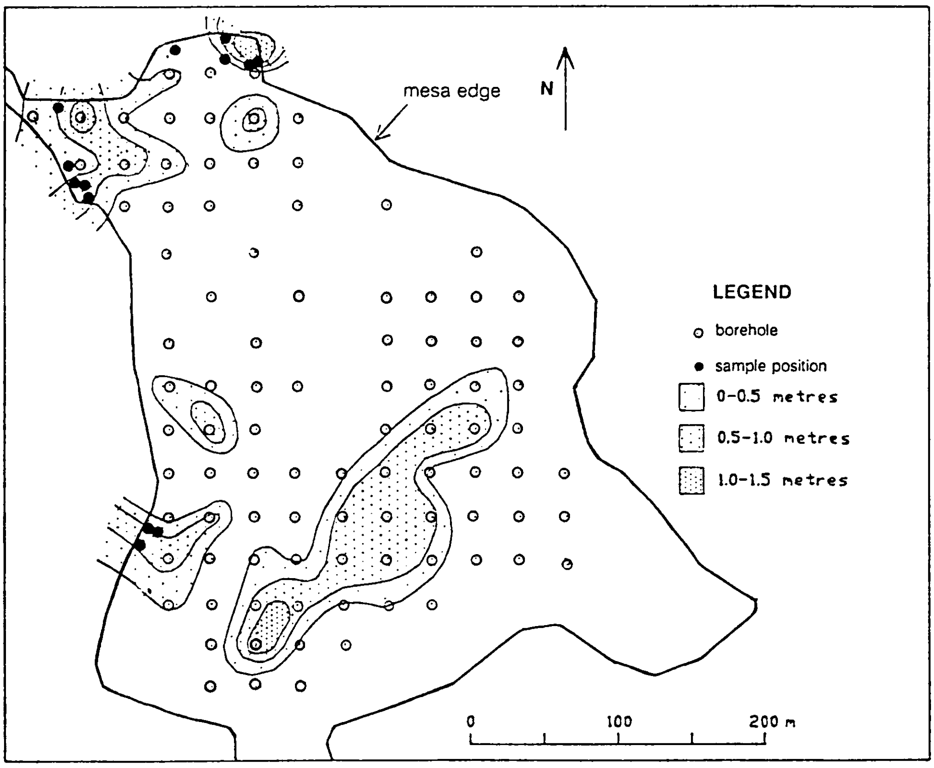

Fig. 6.8. Thickness variation of the lower mineralized zone in the anomalies B3 and B4 on Bloemfontein 406 (Cole, pers. comm.).

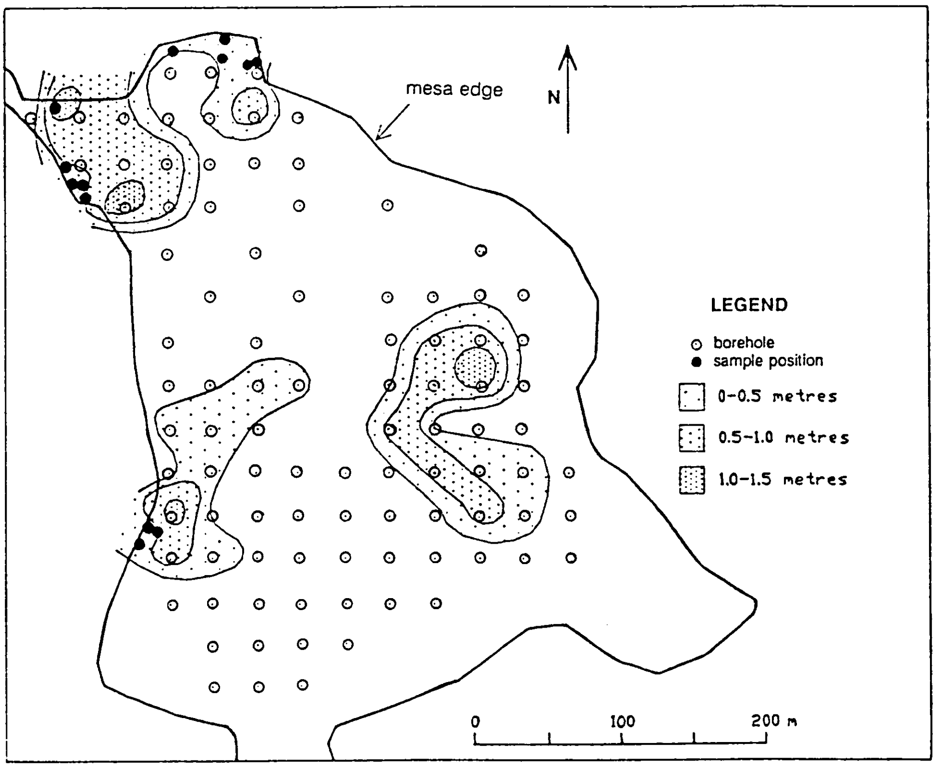

Fig. 6.9. Thickness variation of the middle mineralized zone in the anomalies B3 and B4 on Bloemfontein 406 (Cole, pers. comm.).

Digitised by the Department of Library Services in support of open access to information, University of Pretoria, 2021

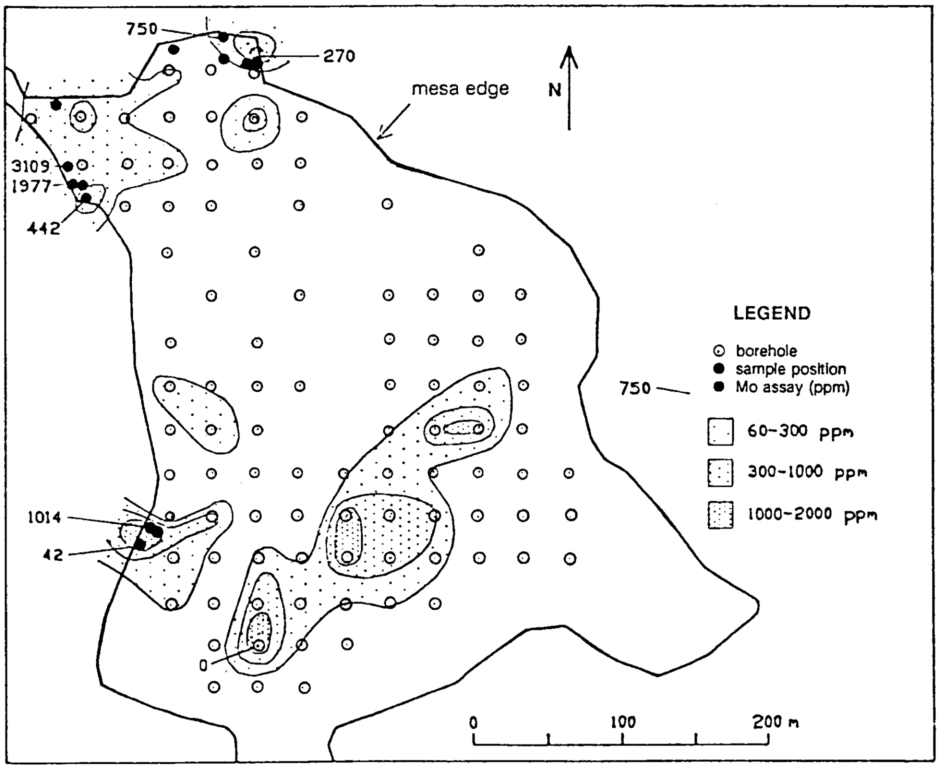

Fig. 6.10. Grade contours of uranium in the lower mineralized zone on Bloemfontein 406 (Cole, pers. comm.). Spot values for molybdenum are also shown.

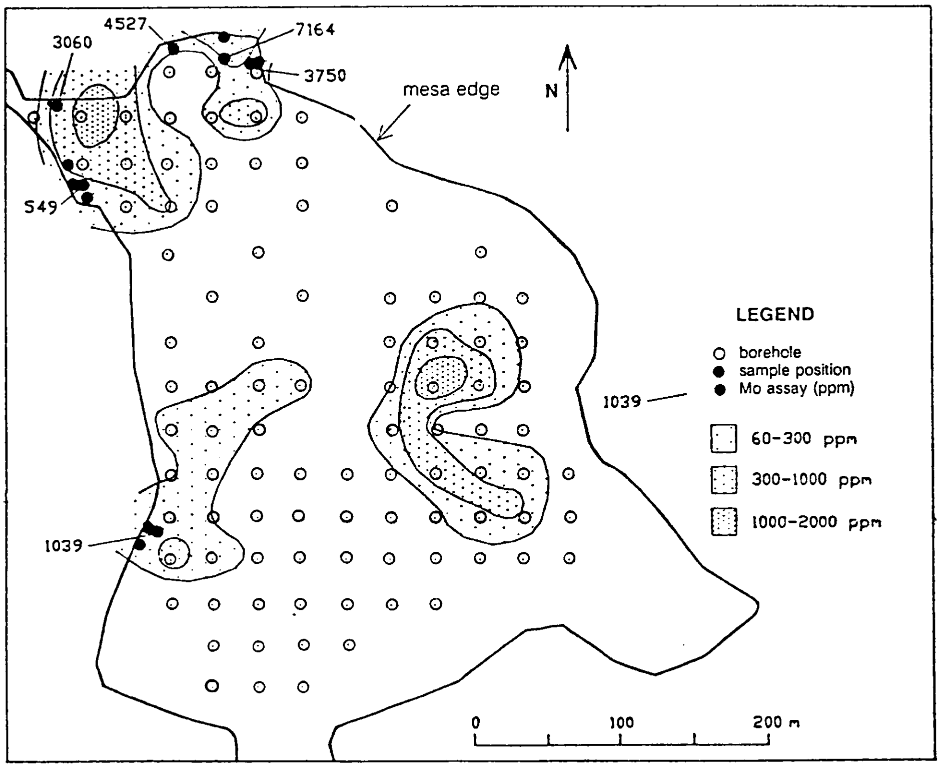

Fig. 6.11. Grade contours of uranium in the middle mineralized zone on Bloemfontein 406 (Cole, pers. comm.). Spot values for molybdenum are also shown.

agreement between the thickness and grade of the mineralized sandstone is indeed remarkable (cf. Figures 6.8 and 6.10 and also 6.9 and 6.11).

Unfortunately no molybdenum values were determined by BEUCAR MINERALS, the exploration company responsible for the drilling. Only molybdenum sample-values obtained during the present study on the surveyed profiles on Figures 6.10 and 6.11 are shown. Other occurrences where the mineralization is associated dominantly with the laminated sandstone-type of ore are the following: Leeuwe Kloof 402, Krugels Claim 459, Damsfontein 397, Blydevooruitzicht 299, Driefontein 464, De Goede Hoop 463, Vinkekuil 144, Klippekraal 145, Banks Gaten 250, Riet Valley 452, Brandewyns Gat 214, Veldmans River 9, Kareepoort 80 and Kraanvogel Valley 120.

6.2. Occurrences related to both laminated and carbonate-cemented sandstone-type mineralization.

The prospect on the farm Riet Kuil 307, some 45 km west of Beaufort West (Fig. 6.12) was selected as it illustrates the three-dimensional relation of the two ore-types, viz the laminated and the carbonate-cemented sandstone type rather well. This is due to test-mining, extensive exploratory drilling and reasonable outcrops in cliffs. The sedimentology of the occurrences in the Moordenaars Sandstone Member in the Riet Kuil area have previously been described by Moon (1974), Kübler (1977), Stear (1980) and Cole (1980).

At Riet Kuil four sandstone bodies are present. Of these the R3 body contains most of the uranium and it can be followed for a distance of 20 km in a north-northeasterly direction. It averages 6 km in width and its maximum thickness measured in a borehole is 36 metres. The mineralized bodies are situated near the southern extremity of this sandstone body.

The diagrams used in the following description are from Dr. D. I. Cole. Fig. 6.12 shows the general geology of the area and the positions of the test mine and the mineralized outcrops (Anomaly A). A section through Anomaly A (Fig. 6.13) indicates

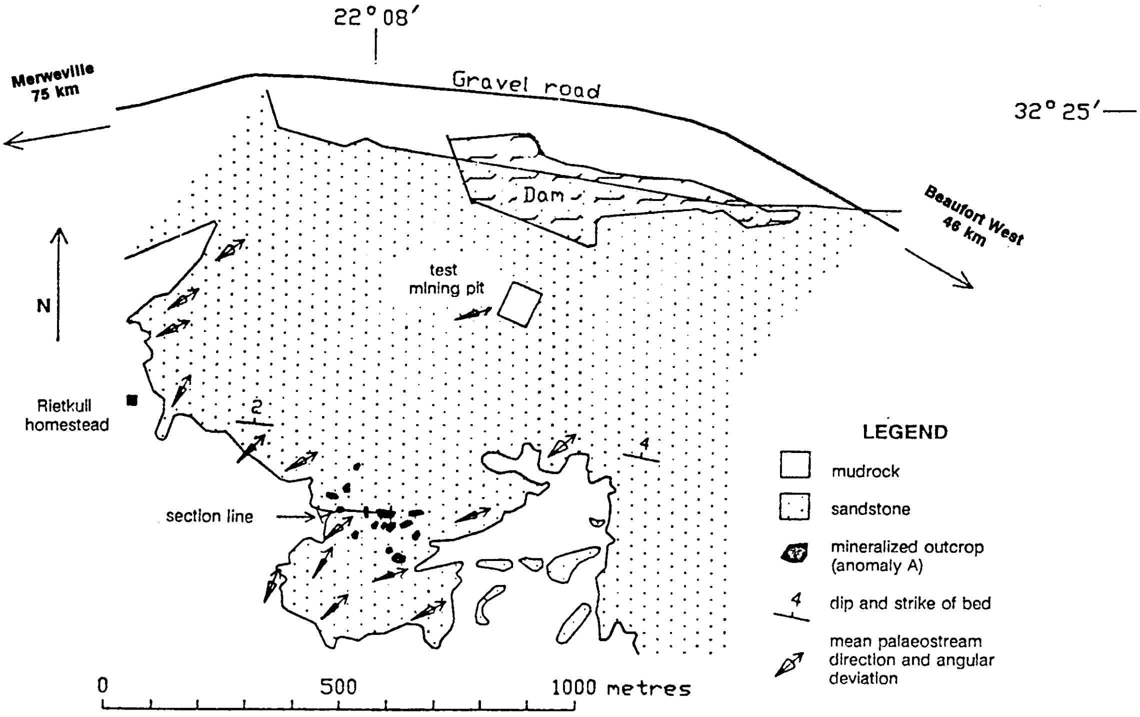

Fig. 6.12. Map showing the geological setting of Anomaly A on the farm Riet Kuil 307 with reference to the test mine (Cole, pers. comm.).

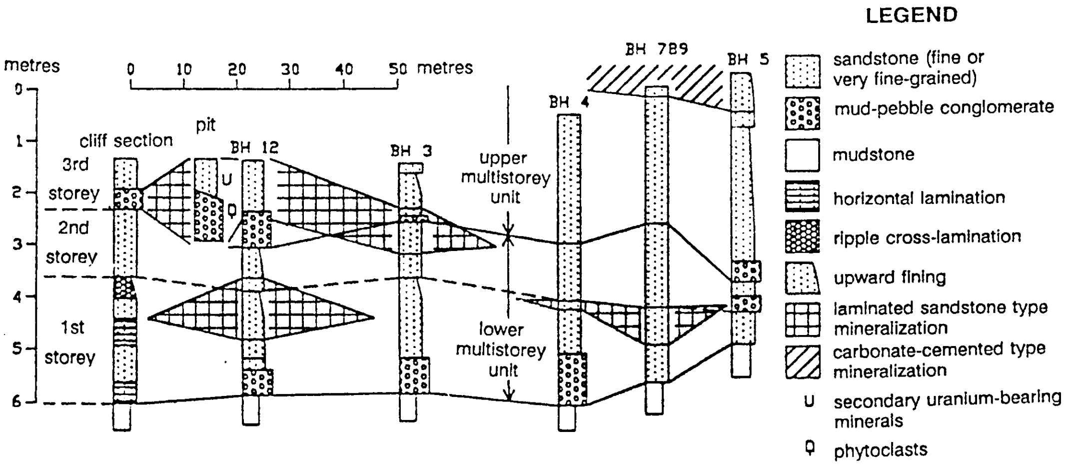

Fig. 6.13. Section through Anomaly A on Riet Kuil 307, showing the relation of the upper carbonate-cemented sandstone type ore-body with relation to the lower ore-bodies (Cole, pers. comm.). (Note vertical exaggeration)

Digitised by the Department of Library Services in support of open access to information, University of Pretoria, 2021

two main mineralized lenses, a bottom one associated with laminated sandstone and a higher one associated with mud-pebble conglomerate. These lenses are once again typically discontinuous and have a maximum thickness of about 1,5 metres. Above these two is a third ore-body of the carbonate-cemented type. The same relationship was found in a drill section east of the test mine. During subsequent investigations of other occurrences it was found that the carbonate-cemented type normally occurs above the laminated sandstone-type ore-bodies.

Other occurrences where the laminated sandstone type is found in close proximity to the carbonate-cemented type are the following: Goede Verwagting 462, Koekemoer 482, Ezelsfontein 433, Matjes Kloof 235, Brakfontein 329, Kaffersfontein 328, Vlekfontein 90, Elandsfontein 128, Hendrikskraal 298, Nmark 119 and Augustus Kraal 129.

6.3. Occurrences related to only carbonate-cemented sandstone-type mineralization.

The occurrence at Karee Poort 80 was selected as an illustration of carbonate-cemented type uranium mineralization. This occurrence is located in a plateau (Fig. 6.14) formed by a multistorey tabular sandstone body, which in this area has a maximum thickness of about 13 metres. The mineralization is hosted by thin (generally less than 0,4 m thick) pods and lenses of carbonate-cemented sandstone at an average elevation of 7,8 metres above the base of the arenite body. The conditions during the formational stages of mineralization were probably not favourable (due to the absence of a continuous laminated sand body near the base of the succession or the absence of enough organic material in the sediment?) to precipitate a lower ore-body as at Riet Kuil.

Immediately below the weathering crust of the mineralized rock secondary yellow uranium minerals may be present and these give rise to high scintillometer readings. Limonitic phytoclasts are common in the uraniferous sandstone.

UNIVERSITEIT VAN PRETORIA
UNIVERSITY OF PRETORIA
YUNIBESITHI YA PRETORIA

Digitised by the Department of Library Services in support of open access to information, University of Pretoria, 2021

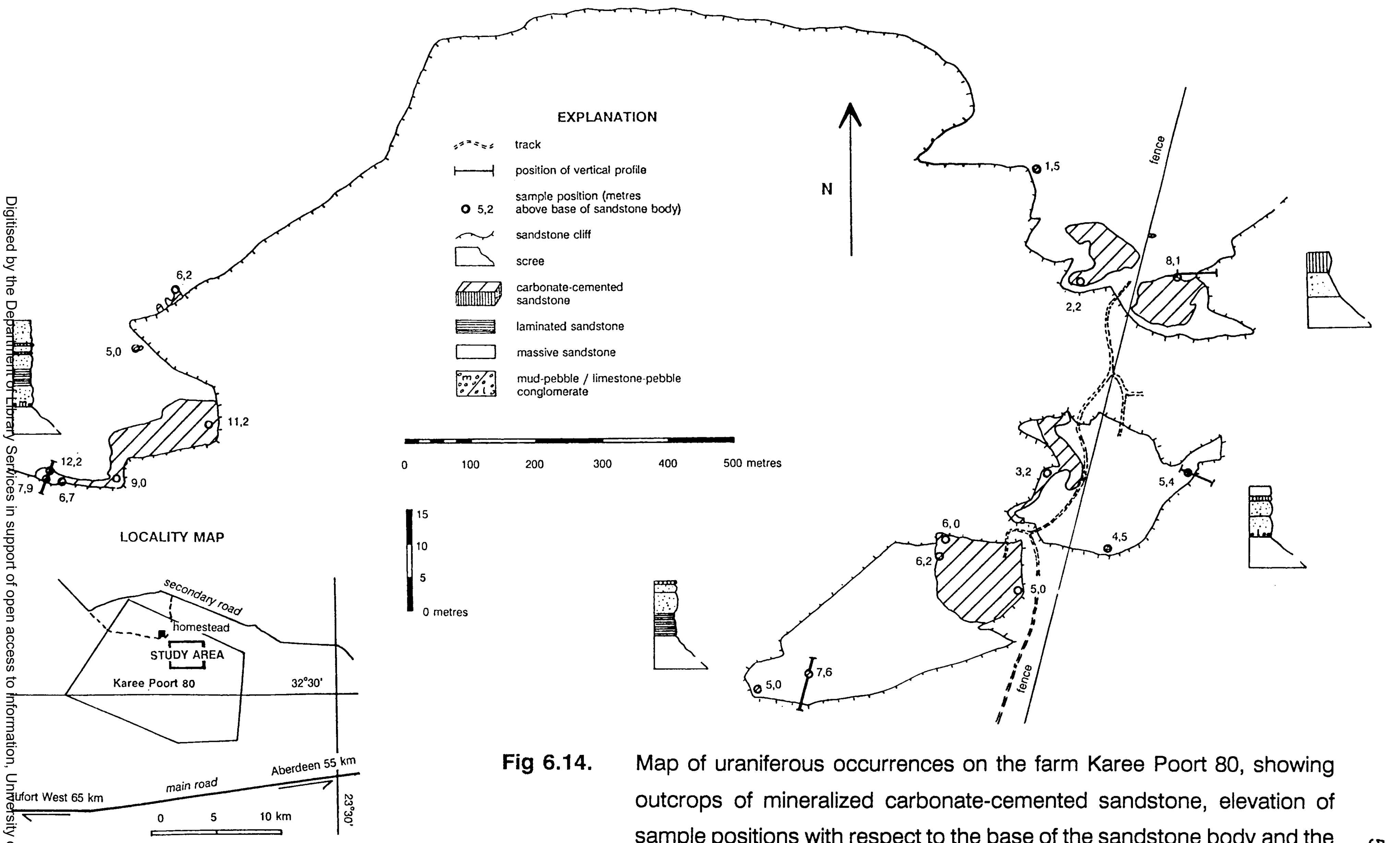

Fig 6.14. Map of uraniferous occurrences on the farm Karee Poort 80, showing outcrops of mineralized carbonate-cemented sandstone, elevation of sample positions with respect to the base of the sandstone body and the positions and profiles of vertical sections measured.

On the extension of the sandstone body towards the west of the homestead similar occurrences have been investigated by a prospecting company. The economic potential of the occurrences on Karee Poort are rated as low due to the low volume and small thickness of the ore-bodies.

Other occurrences where the mineralization is predominantly associated with carbonate-cemented sandstone are: Mealieberg 45, Beerenvalley 150, Elandsfontein 128, Bullekraal 251, Die Bad 286, Vindragersfontein 280, Van Der Byls Kraal 265, Haane Kuil 335, Bushmans Kop 302, Quaggasfontein 357, La-de-da 178, Rystkuil 351, Onbekend 141, Richmond Townlands, Knapdaar 45, Kokers Graafs Vlakte 221, Taai Bosch Fontein 137 and Vischgat 223. Of these carbonate-cemented sandstone deposits only the one on Rystkuil was attractive enough for an exploration company to develop an underground test mine for the production of a bulk sample for metallurgical testing.

Digitised by the Department of Library Services in support of open access to information, University of Pretoria, 2021

UNIVERSITEIT VAN PRETORIA
UNIVERSITY OF PRETORIA
YUNIBESITHI YA PRETORIA

7. Possible indicators of molybdenum mineralization in the Karoo

The field investigation showed that two factors control the molybdenum potential in suitable geological environments in the Karoo, namely rock type and stratigraphy. Consideration was also given to the possible use of stream sediment sampling and metal poisoning of livestock as exploration guides.

7.1. Potential host rocks

In the southern Karoo basin significant U-Mo-bearing bodies are restricted to sandstones of the Beaufort Group. Four potential types of host material within the sandstone beds were identified, namely:

- i. finely laminated sandstone,
- ii. carbonate-cemented sandstone,
- iii. carbonaceous debris (phytoclasts) and
- iv. mud-pebble conglomerate.

Of these the laminated sandstone, the carbonaceous debris and the mud-pebble conglomerate are found near the base of sandstone bodies, i.e. domains that probably remained waterlogged until the sediment was completely lithified .

In the weathering environment the laminated sandstone beds characteristically form hollow cliffs, usually capped by massive sandstone beds (Fig. 7.1.), and they are light in colour, but local iron staining is common due to the ubiquitous presence of pyrite in the fresh rock. The sulphuric acid formed during the oxidation of the pyrite weakens the cementing medium of the rock, resulting in the crumbly nature of the sandstone in outcrop. The U and Mo enrichment is commonly in the form of thin (less than 0,6 m) tabular bodies less than 10 000 m^2 in areal extent.

The phytoclasts and lenses of mud-pebble conglomerate within the sandstone beds are only mentioned for the sake of completeness. Both, especially the former, can contain very high metal concentrations, but the volume of the individual bodies is insignificant as their surface area varies from a fraction of a square metre to a

Digitised by the Department of Library Services in support of open access to information, University of Pretoria, 2021

maximum of tens of square metres (in the case of mud-pebble conglomerate).

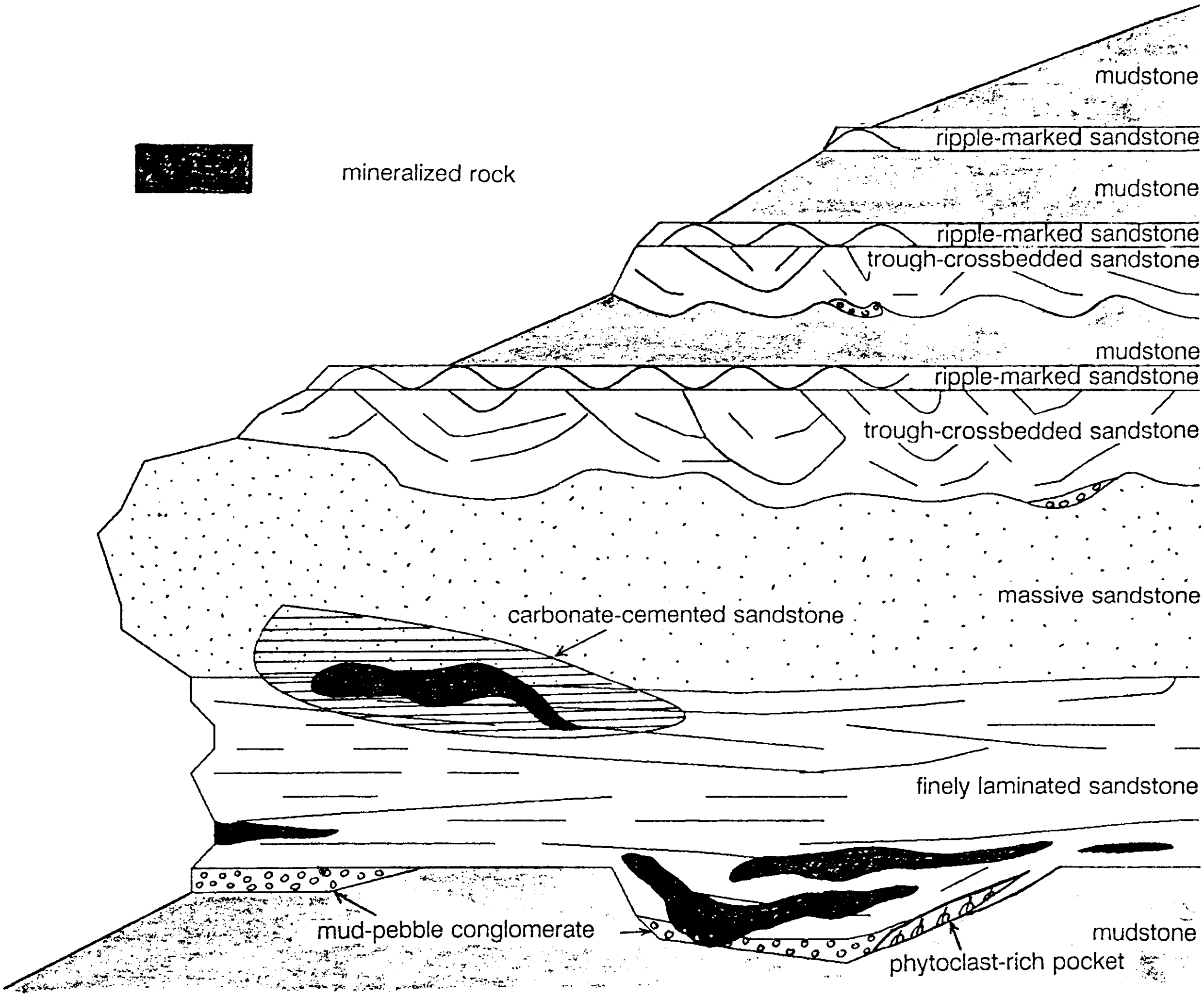

Fig. 7.1. Schematic section through a typical sandstone cliff showing four kinds of mineralization: Finely laminated sandstone, carbonate-cemented sandstone, mud-pebble conglomerate and one of the normally mineralized pockets of phytoclasts.

The carbonate-cemented sandstone, locally referred to as "koffieklip", can be identified in the field by its black-buff manganese-enriched crust between 0.5 and 15 mm thick, formed by weathering. These "koffieklip" occurrences have no evident relation to the stratigraphy of the sandstones. In the field the impression was gained that they may have a relation to the palaeowater-table. These mineralized bodies are tabular, and commonly cut across bedding planes (Fig. 7.1.). Their areal extent is generally less than 1 000 m^2 and on account of their small volume they are of little economic significance.

7.2. Stratigraphical position of the ore bodies

The Poortjie Sandstone Member appears to have the highest economic potential which is reflected by the fairly large number of occurrences (43 %) that warranted investigation, their above average size and their fairly high grade. The initial field analyses obtained from samples of the Oukloof Sandstone Member (though based on an imperfect X-Met 840 calibration) were less encouraging.

7.3. The value of geochemical stream sediment sampling

In 1977 the Geological Survey commenced with a geochemical stream sediment sampling project in the south-western Karoo as its contribution to the uranium exploration in that area. All first order streams were sampled, giving a sample density of about one sample per km^2. The results for the Beaufort West degree square were analyzed statistically by Hückel (1979). He came to the conclusion that this regional geochemical exploration project has succeeded in delineating areas with a relatively high uranium (and molybdenum) potential.

Early in the present project fourteen of these 1:50 000 quarter-degree geochemical maps (Fig. 7.2.) were selected for a detailed investigation as to their value in exploration. Each of these maps contained between one and 34 known uranium occurrences. The total area covered is about 9 000 km^2 and contains 195 known occurrences. The geochemical maps for U, Cu, P, Zn, Co, Mo, and V (based on Geological Survey XRF analyses) as well as those for U (determined by neutron activation analysis) were studied. Anomalous values of copper are associated with dolerite intrusions (see also 7.4.) and in the case of uranium only some values determined by means of the neutron activation method were anomalous.

Digitised by the Department of Library Services in support of open access to information, University of Pretoria, 2021

3221 AA	3221 AB	3221 BA	3221 BB	3222 AA	3222 AB
3221 AC	3221 AD	3221 BC	3221BD	3222 AC	3222 AD
3221 CA	3221 CB				

Fig. 7.2. Locality of the fourteen quarter-degree geochemical stream-sediment maps investigated.

The threshold value (mean plus two standard deviations after definition by Hawkes and Webb (1963)), determined for the neutron activation analyses for uranium on the fourteen geochemical maps lies between 5 and 6 ppm U (Fig. 7.3.). Because the definition of the threshold value is fairly arbitrary (Levinson, 1973) and the range of individual analytical values is rather wide, the lower value (5 ppm U) was chosen for the following discussion.

Inspection of the fourteen quarter-degree geochemical data maps reveals that areas with a higher incidence of uranium occurrences are generally associated with higher uranium values in their immediate surroundings. If an exploration organization followed up each anomalous uranium value on the geochemical data maps by investigating the two rings of square km blocks immediately surrounding it (Fig. 7.4.) in detail, 142 of the 195 uranium occurrences known in the area (73%) would be found. On the other hand 489 anomalous values would return 160 known occurrences, which is 18 higher than the previous number, as in some cases a known occurrence falls in the influence area of more than one anomalous value. The percentage of anomalous values leading to actual mineralization would be about 28. By the elimination of squares falling on mudstone, the area that has to be examined in detail for an occurrence to be

Digitised by the Department of Library Services in support of open access to information, University of Pretoria, 2021

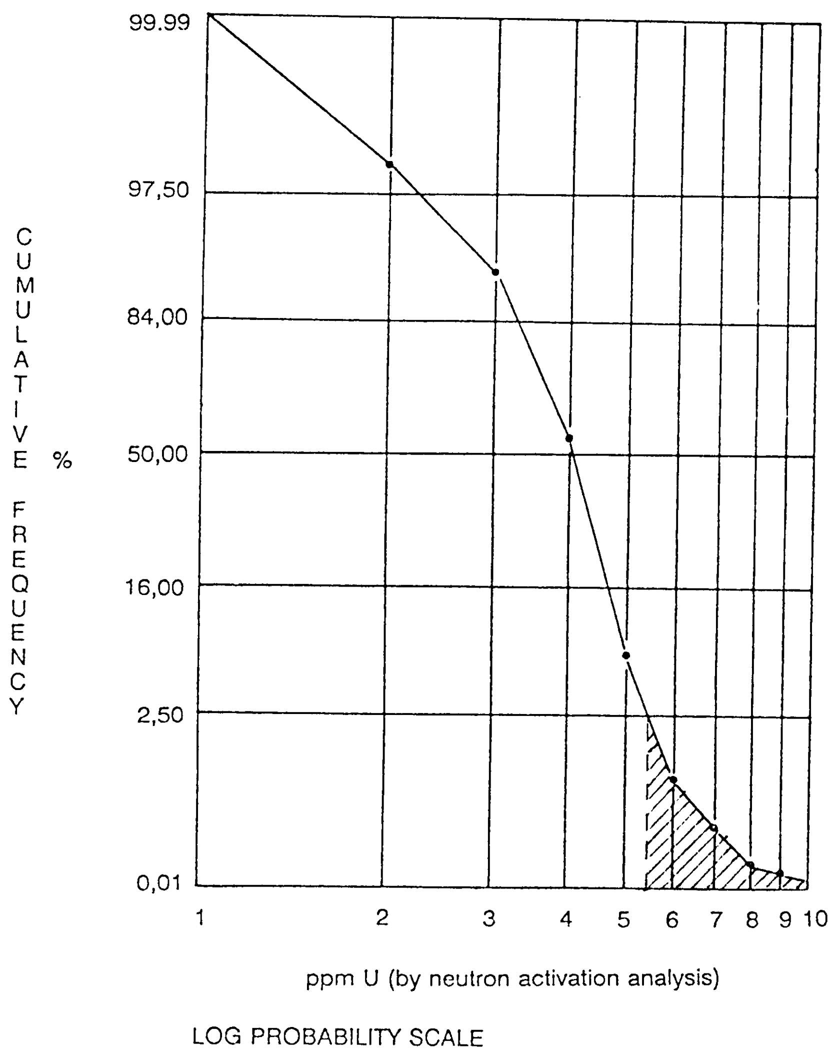

Fig. 7.3. Cumulative frequency distribution for uranium (neutron activation analysis) on the fourteen quarter-degree geochemical stream-sediment maps situated west of Beaufort West. Hatched values are anomalous.

discovered can be reduced further, as potential uranium-molybdenum bodies are restricted to the more prominent sandstone bodies. Thus the area to be covered would be appreciably smaller than the theoretical 12 225 km^2 (489 anomalous values each with an area of influence of 25 km^2, see Fig. 7.4). Thus even on a more detailed scale the maps are useful in closing in on potential targets.

A stream on the farm Leeuwe Kloof 402 (Vredelus), 50 km southeast of Fraserburg, was sampled in detail for a distance of 145 m from a mineralized outcrop with high molybdenum and uranium concentrations (3 500 and 1 000 ppm respectively in

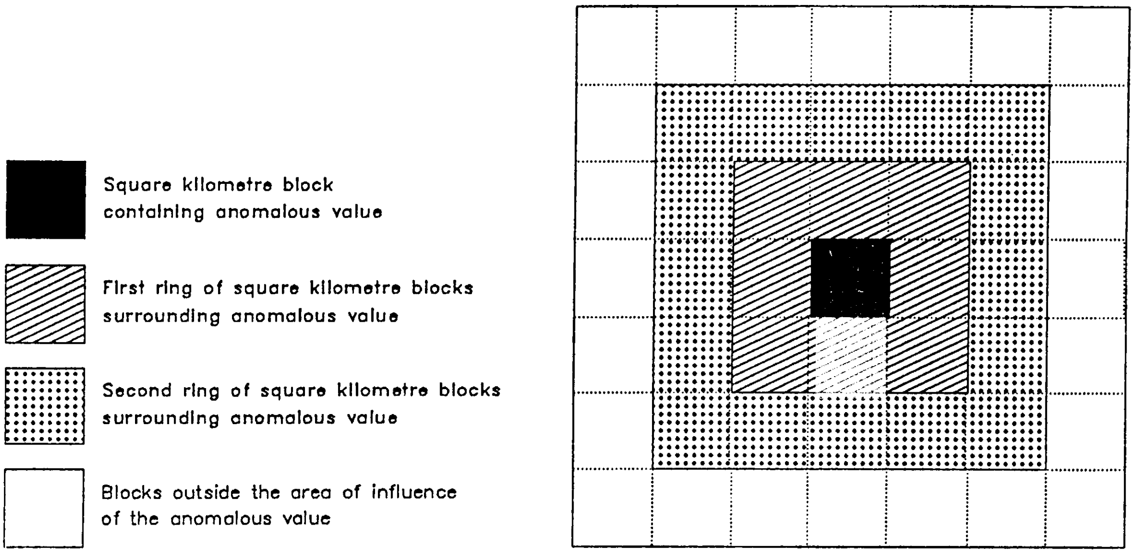

Fig. 7.4. The two significant rings of square kilometre blocks surrounding an anomalous uranium value that have to be investigated if the anomalous value is to be linked to a possible occurrence.

individual samples) to determine whether a molybdenum and uranium dilution pattern could be detected in the stream sediment. The analysis of these samples was done by the standard techniques used for the Geological Survey's stream-sediment sampling programme.

This particular stream, after crossing the sandstone layer, flows over a thick body of mudstone and the samples were collected from this part. There are one high molybdenum value (1 050 ppm at a distance of 60m from outcrop) and two high uranium values (1 110 and 740 ppm at distances of 52 and 80 m respectively) in the set of 18 samples (Fig. 7.5.). The remainder of the samples returned low values (of the order of the detection limit) and no diagnostic down-stream dilution pattern from the outcrop is evident. The three anomalous values are interpreted as a nugget effect, caused by unweathered uranium oxide minerals and molybdenite contained in clasts or as individual grains within the river sediment. To detect this occurrence an impracticably large number of samples would be required.

Digitised by the Department of Library Services in support of open access to information, University of Pretoria, 2021

Although geochemical stream sediment sampling is regarded as one of the best ways of defining exploration targets, the above observation indicates that this is not the case with the Karoo uranium occurrences. The impression gained is that the uranium and molybdenum were solubilized and removed from this environment or that insufficient dispersal took place in the river sediment.

It is concluded that best results in geochemical exploration for uranium will be obtained by stream-sediment analysis by means of neutron activation techniques, as the detection limit of this method is much lower than that of conventional analytical procedures. Targets on the geochemical data maps should then be followed up by field-work, during which favourable sandstone-types are selected visually from outcrops for detail investigation by means of gamma-ray spectrometry and sampling.

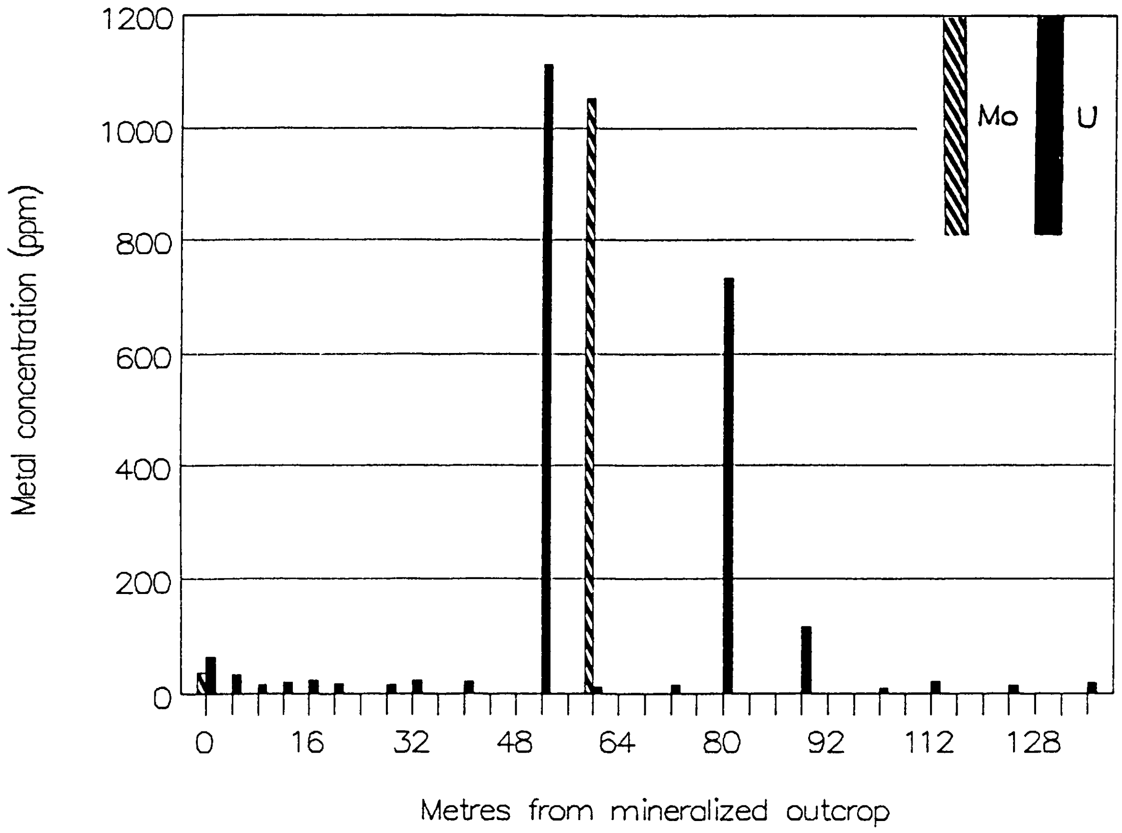

Fig. 7.5. Stream-sediment sampling results of a stream below a mineralized outcrop on the farm Leeuwe Kloof 402.

7.4. Plant toxicity as related to geochemistry as a possible key to molybdenum deposits

The question as to whether metal poisoning in livestock could be utilized as a guide to ore deposits was also addressed, as both molybdenum- and selenium poisoning have been reported from areas close to uranium-molybdenum deposits in Colorado, United States of America. The selenosis reported is probably the result of selenium released from molybdenite, in which it substitutes for sulphur. Initial work by Brown and de Wet (1962) at the Veterinary Research Unit at Onderstepoort indicated that the stock diseases tribulosis (geeldikkop) and enzootic icterus (geelsiekte) represent different stages of selenium poisoning. This information, subsequently proved to be erroneous, was actually utilized by Esso Minerals (Africa) Incorporated in their target selection. Fortuitously the area selected on this basis contains some of the largest uranium occurrences in the Beaufort Group.

During a visit to the Regional Veterinary Laboratory at Middelburg (Cape Province) I was informed by Dr. van Tonder that subsequent work (Louw et al., 1967; van Tonder et al., 1972; and Bath, 1979) proved that these diseases were unrelated to selenium poisoning as was shown on the basis of the selenium content of pastures and of the livers of affected animals. The analytical methods for selenium determination used by Brown and de Wet (1962) were shown to be inaccurate and subsequent analysis of plant material returned less than one ppm Se. In fact, Louw et al. (1967), van Tonder et al. (1972) and Bath (1979) showed that the two diseases are caused by two totally different factors. Tribulosis is the result of feeding on pastures containing the weed Tribulus terrestris (dubbeltjie) which, under certain conditions, is toxic to livestock, but the toxicity is unrelated to heavy metals in the soil. Enzootic icterus has been proved by analyzing grazing and liver specimens of affected animals to be due to chronic copper poisoning. It was also established that high copper concentrations in plant material occur in pastures on dolerite. A remarkable correlation therefore exists between outcrop areas of dolerite and outbreaks of enzootic icterus (Figs. 7.6.(a) and 7.6(b)). The higher incidence of the disease towards the southwest is probably related to the lower rainfall and the more frequent periods of drought in that area. The reason is that animals under stress are more susceptible to metal poisoning, as under these

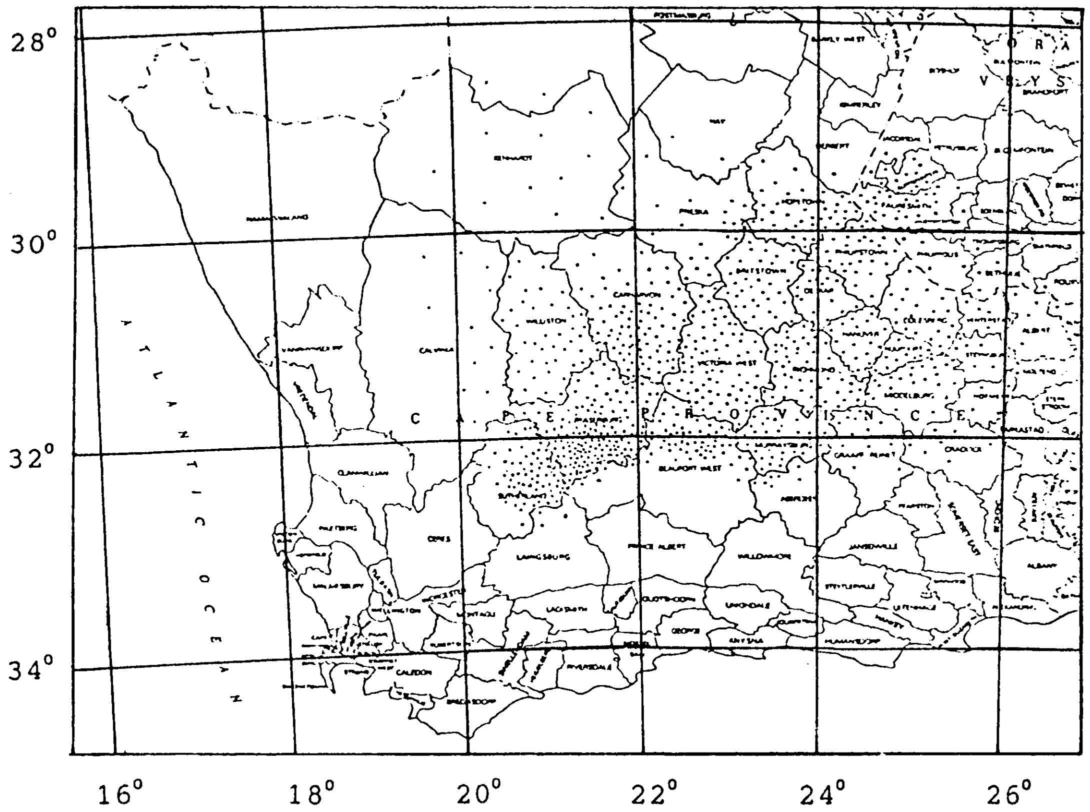

Fig. 7.6.(a). The approximate extent of enzootic icterus (after Bath, 1979).

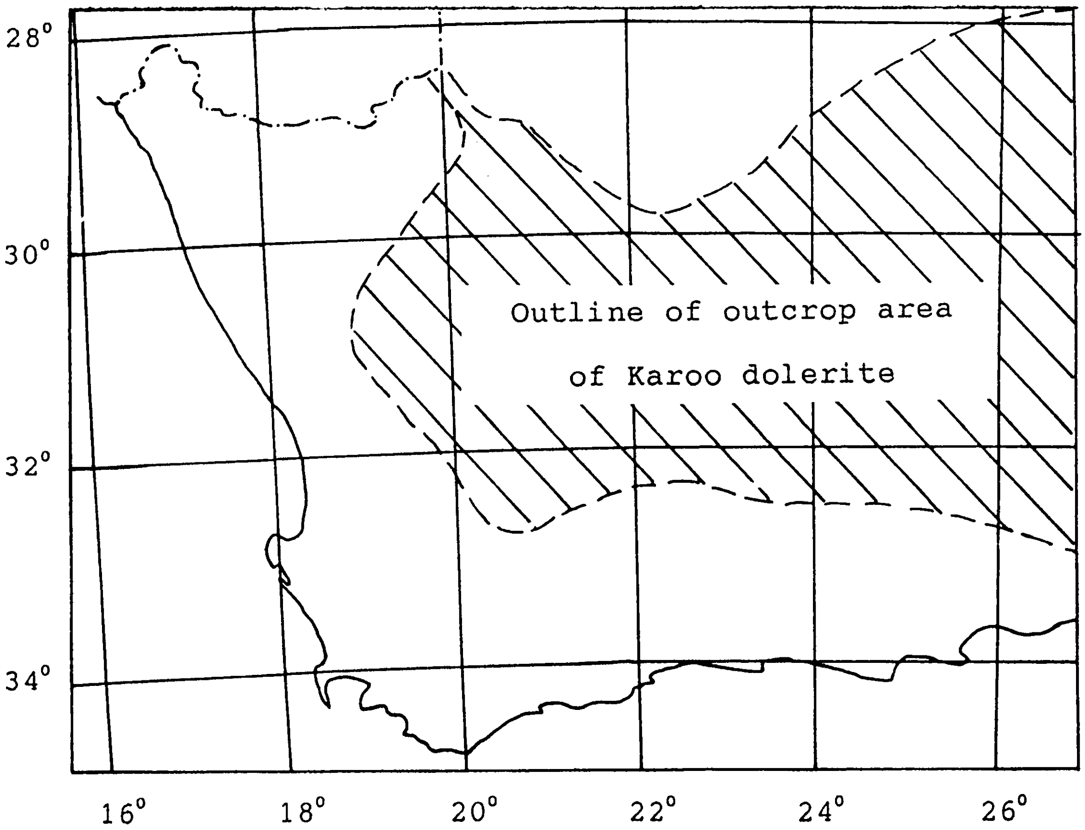

Fig. 7.6.(b). The approximate outline of the outcrop area of the Karoo dolerite (Geological map - 1:1 000 000).

conditions metals are released from the body reserves, where they have been stored metabolically during periods of adequate food supply. Ironically enzootic icterus is cured by dosing the livestock with ammonium- or sodium molybdate!

Moon (1974) analyzed samples from various uranium occurrences for selenium and found values below the analytical detection limit (5 ppm). The indications therefore are that the selenium concentration of the water in rivers that fed the depositional system of the Adelaide Subgroup was low.

Heavy metal poisoning (molybdenosis and selenosis) of livestock therefore does not appear to be a guide to uranium-molybdenum mineralization in the southern Karoo. The remarkable correlation between the incidence of enzootic icterus and the outcrop area of dolerite intrusions, however, indicates that the cause of the disease might have been found earlier had the local geology been taken into account.

Digitised by the Department of Library Services in support of open access to information, University of Pretoria, 2021

8. **Statistical analysis of data**

A data set was prepared containing all the analytical sample values, as well as relevant field observations in digital form. These field observations comprise palaeostream direction, stratigraphy, grain size, sedimentation features, presence of organic material, elevation above base of sandstone body, relative elevation of the sample within the ore-body, presence of secondary uranium minerals and presence of carbonate cement. Use was made of a SAS programme to analyze the data set statistically.

Various methods (for example cluster analysis and tree diagrams) were experimented with. Though some success was achieved, the best results were obtained by dividing the data-set into subsets by means of parameters observed in the field. These subsets were then compared with each other on the basis of population distribution and population means. These means (Table 8.1.) form the basis of the following discussion. The determination of the means was by a method described by Lepeltier (1969) which makes use of cumulative frequency curves plotted on log-probability paper (Fig. 8.1.).

The data set is statistically not representative of rocks of the Adelaide Subgroup, but rather of mineralized zones. There may also be a bias in the set due to the selection of samples after field analysis but before laboratory analysis.

8.1. Palaeostream direction

The palaeostream directions measured during the present project were processed by Cole (1988) and used to modify Theron's (1973) palaeocurrent map and are represented in Fig. 8.2. In the area of interest three stream directions can be distinguished, namely a southwesterly, a south-southeasterly and a west-northwesterly direction. The separation of the data set into these three directions indicates that a sub-division according to palaeostream directions alone is too coarse to be of any significance. A subdivision based on palaeostream direction and the two most important rock types for uranium-molybdenum potential, namely fissile sandstone and

Digitised by the Department of Library Services in support of open access to information, University of Pretoria, 2021

Table 8.1. Mean values for the various statistical parameters applied to the geochemical data set.

	Mo	U	V	Co	Cu	As	P_2O_3	TiO_2	Al_2O_3	Elev. above base of ss.	Pb	Fe_2O_3	Zn
	ppm	ppm	ppm	ppm	ppm	ppm	%	%	%	mm	ppm	%	ppm
ALL LABORATORY ANALYSES	112	391	87	33	13	106	0	0,4	11	1675	57	2,5	69
STRATIGRAPHY													
Moordenaars Sandstone	94	493	82	29	8	90	-	-	-	-	56	2,0	54
Poortjie Sandstone	293	793	93	42	11	126	-	-	-	-	85	2,5	82
Oukloof Sandstone	1	46	76	28	19	121	-	-	-	-	1	2,5	62
Abrahamskraal Sandstone	16	254	80	39	16	28	-	-	-	-	53	1,8	68
Barberskrans Sandstone	160	210	82	19	9	84	-	-	-	-	40	2,5	51
Davidskolk Sandstone	36	422	80	38	8	37	-	-	-	-	65	2,0	94
Loxton Sandstone	38	890	64	11	23	36	-	-	-	-	133	1,5	36
Richmond Sandstone	-	-	-	-	-	-	-	-	-	-	-	-	-
Wortelfontein Sandstone	-	-	-	-	-	-	-	-	-	-	-	-	-
Nuwefontein Sandstone	-	-	-	-	-	-	-	-	-	-	-	-	-
ROCK TYPE													
Fissile sandstone	157	226	88	30	14	106	0	0,4	12,5	1500	45	2,5	63
Carbonate-cemented sandstone	19	78	87	30	19	93	0	0,4	10,0	1800	32	3,5	83
Mud-pebble conglomerate	13	45	91	31	28	52	0	1.0	7	300	4	2,8	83
Siltstone	56	1665	73	42	8	75	0	0	10	2550	104	2,0	71
Mudstone	1	42	92	28	27	4	0	0,8	8	-900	10	4,0	95
Phytoclasts	1824	380	90	51	23	163	0,4	0,5	-	600	185	2,5	15
RELATIVE ELEVATION													
Total profile	155	425	89	38	10	82	-	-	-	-	69	-	68
Present-day erosion surface	360	3973	112	84	10	115	-	-	-	-	237	-	114
Upper 1/3 of profile	154	585	87	33	9	119	-	-	-	-	55	-	76
Middle 1/3 of profile	240	641	85	36	9	142	-	-	-	-	94	-	71
bottom 1/3 of profile	232	816	91	33	10	127	-	-	-	-	74	-	69
ORGANIC MATTER IN SAMPLE													
Present	345	449	-	-	-	-	-	-	-	1700	88	2,5	72
Absent	45	138	-	-	-	-	-	-	-	1550	35	2,5	67
PALAEOSTREAM DIRECTION													
Southwest	89	309	85	31	14	100	-	-	-	-	52	2,5	68
S-Southeast all rock types	152	191	84	20	9	70	-	-	-	-	41	2,5	63
N-Northwest	36	422	80	38	8	37	-	-	-	-	65	2,0	94
Southwest	149	226	-	-	-	-	-	-	-	-	-	-	-
S-Southeast fissile s. stone	196	248	-	-	-	-	-	-	-	-	-	-	-
N-Northwest	27	156	-	-	-	-	-	-	-	-	-	-	-
Southwest	57	1783	-	-	-	-	-	-	-	-	-	-	-
S-Southeast siltstone	13	194	-	-	-	-	-	-	-	-	-	-	-
N-Northwest	48	1508	-	-	-	-	-	-	-	-	-	-	-

Digitised by the Department of Library Services in support of open access to information, University of Pretoria, 2021

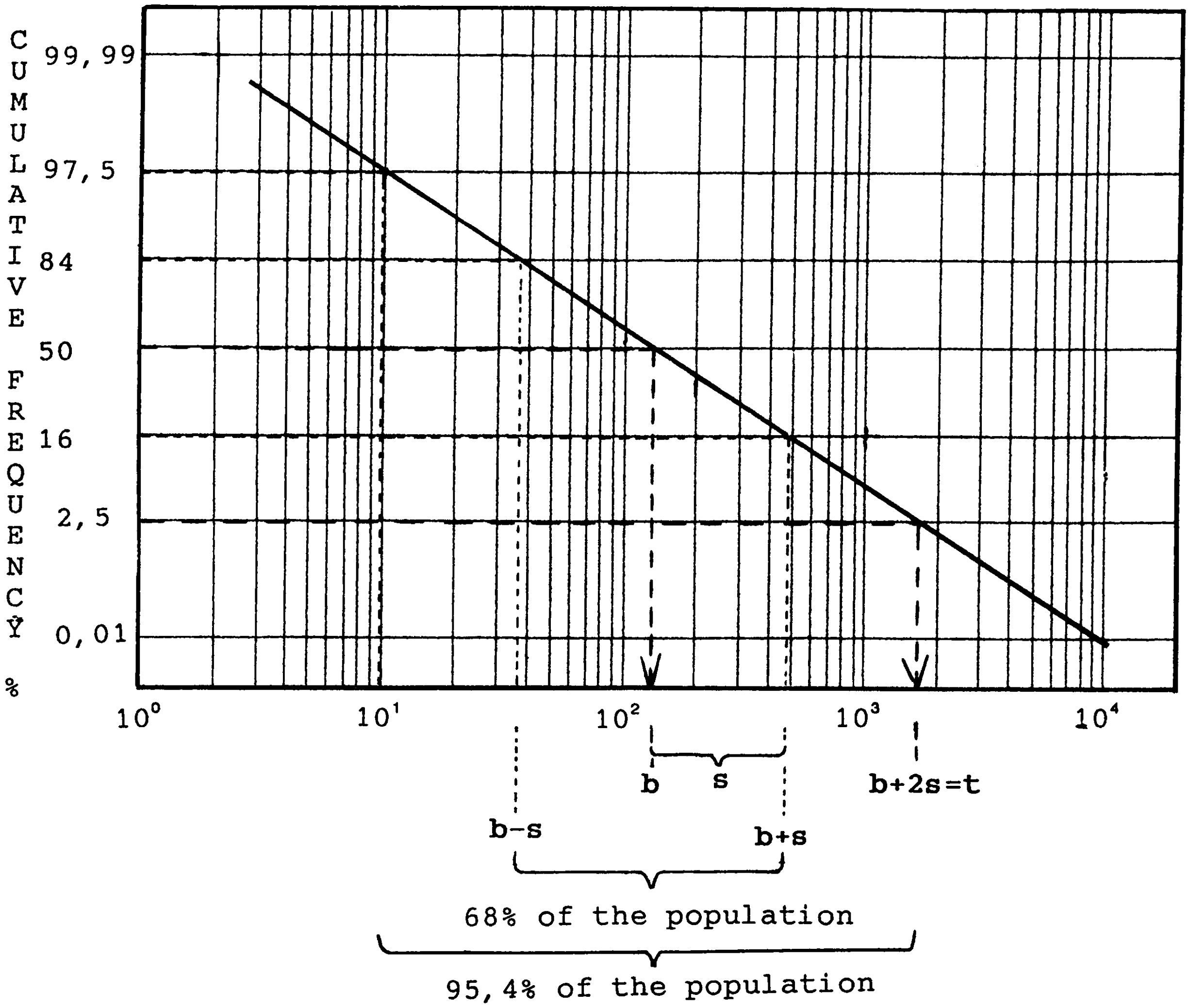

Fig. 8.1. Log-probability plot of a fictitious log-normal population distribution showing the position of the geometric mean (=background), standard deviation and threshold for the population, indicated by **b**, **s** and **t** respectively. (After Lepeltier, 1969)

siltstone (see sub-section 8.3.) was therefore investigated. In this case the molybdenum potential (population mean) declines from SSE (196), SW (149) to WNW (27) (Fig 8.3.). From the stratigraphy (8.2.) it is obvious that the SW direction is negatively biased by the low molybdenum values obtained in the Oukloof Sandstone. Also the low value for the WNW-direction is probably not significant because of the small sample population (12 samples for the WNW direction).

Digitised by the Department of Library Services in support of open access to information, University of Pretoria, 2021

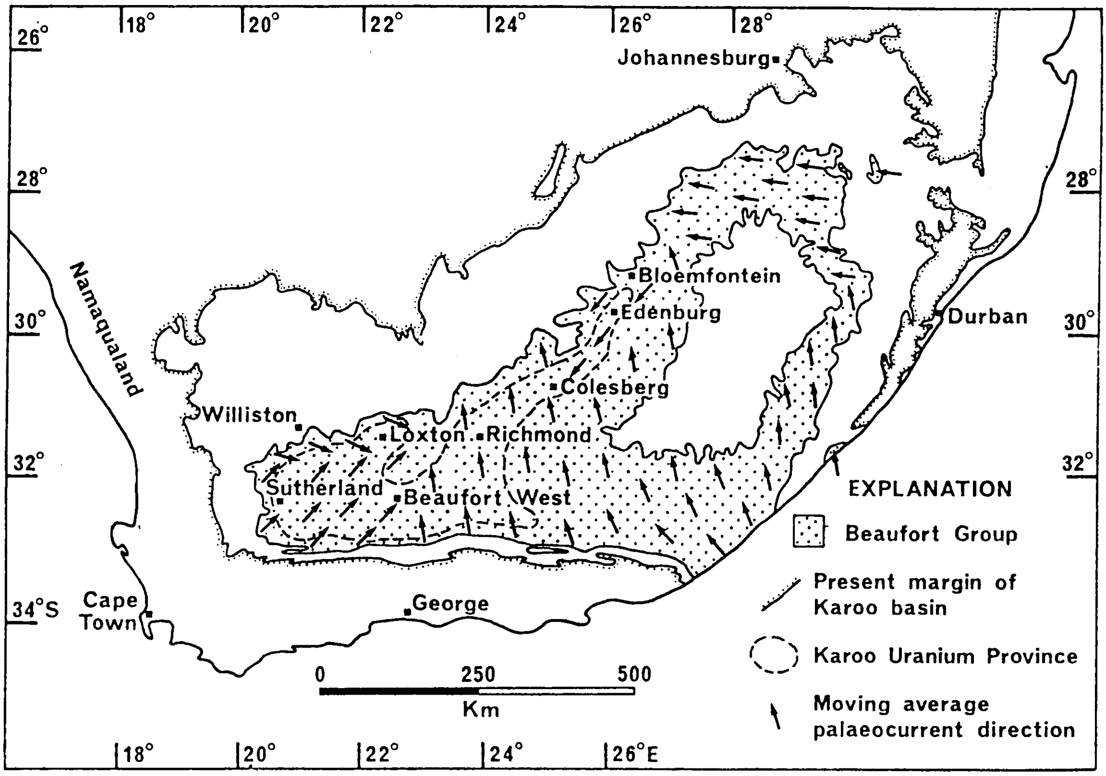

Fig. 8.2. Palaeostream directions in the Beaufort Group (after Cole, 1991).

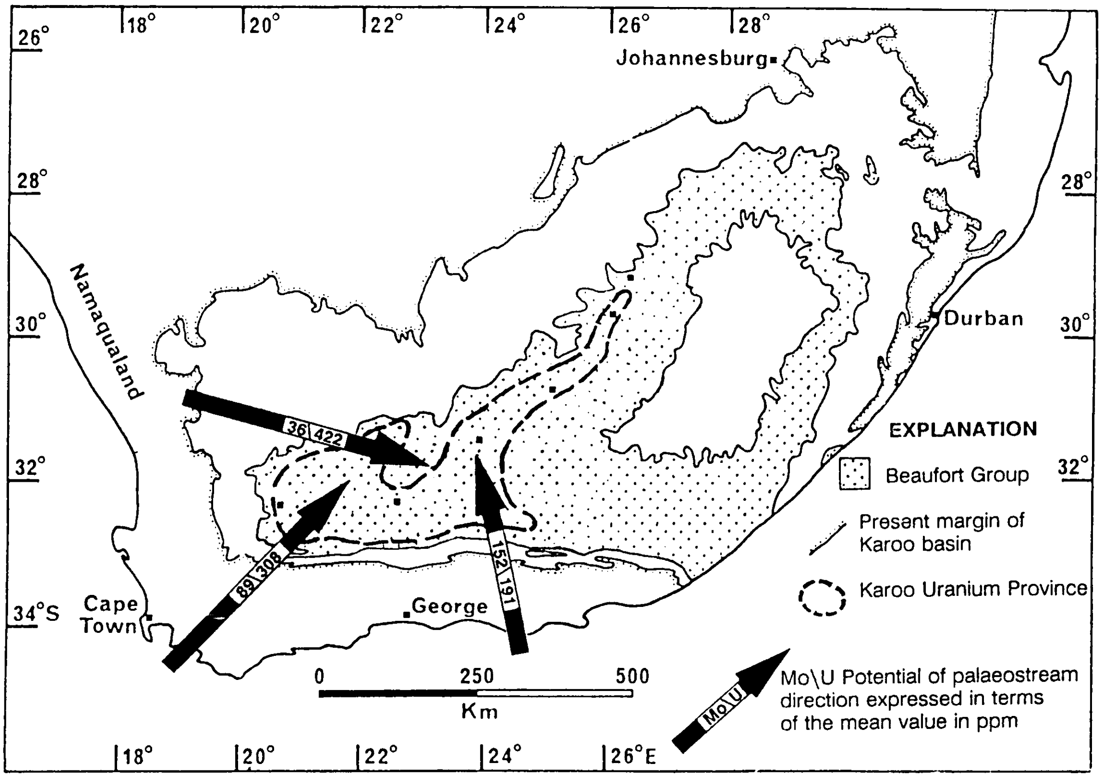

Fig. 8.3. The uranium-molybdenum potential of the three palaeostream directions that fed the Karoo basin during the time the Adelaide Subgroup was deposited.

8.2. Stratigraphy

The sandstone packages investigated during the present study are shown in the stratigraphic correlation diagram (Fig 8.4.). The Koornplaats and Combrinkskraal Sandstone Members have already been eliminated during the rating stage of the investigation. Too few samples were obtained from the Richmond and Wortelfontein Sandstone Members to be statistically significant.

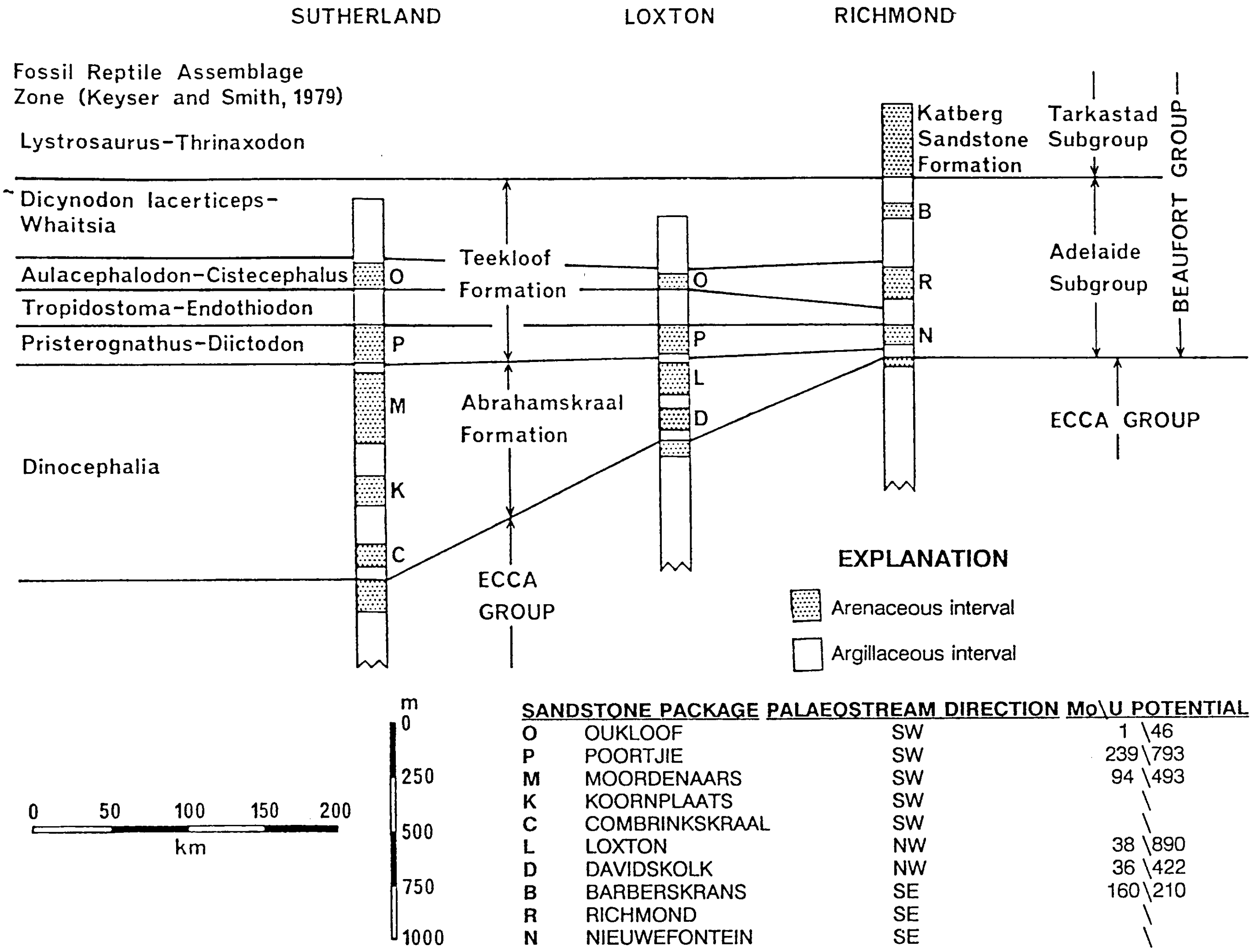

SANDSTONE PACKAGE		PALAEOSTREAM DIRECTION	Mo\U POTENTIAL
O	OUKLOOF	SW	1 \46
P	POORTJIE	SW	239\793
M	MOORDENAARS	SW	94 \493
K	KOORNPLAATS	SW	\
C	COMBRINKSKRAAL	SW	\
L	LOXTON	NW	38 \890
D	DAVIDSKOLK	NW	36 \422
B	BARBERSKRANS	SE	160\210
R	RICHMOND	SE	\
N	NIEUWEFONTEIN	SE	\

Fig. 8.4. Simplified correlation diagram for the Beaufort Group in the southern Karoo Basin giving the uranium-molybdenum potential for the different sandstone packages expressed in terms of the mean metal concentration (ppm).

Digitised by the Department of Library Services in support of open access to information, University of Pretoria, 2021

The Poortjie Sandstone Member represents the best molybdenum target in terms of its mean (293 ppm Mo), nearly three times as high as the mean of the combined sample set (112 ppm Mo). This molybdenum potential is associated with the second highest uranium potential (793 ppm) which is about twice as high as that of the total set (391 ppm U) and is only surpassed by that of the Loxton Sandstone Member (890 ppm U). The Oukloof Sandstone Member has the lowest U-Mo potential. The Barberskrans Sandstone Member has the second highest molybdenum potential (160 ppm) followed by the Moordenaars Sandstone Member (94 ppm). The potential of the other sandstones is negligible. In terms of uranium the Moordenaars (493 ppm) and Davidskolk Sandstone Members (422 ppm) may have some potential, whereas the remaining members are of little consequence.

8.3. Rock type

Under the subdivision according to rock type only the fissile sandstone and plant debris feature prominently with means of 157 and 1 824 ppm Mo respectively. However, as was mentioned in sub-section 7.1. the latter has no potential because of the small volume. The high Mo content does, however, reflect the adsorptive effect of carbonaceous matter on molybdenum.

Siltstone has the highest U potential (1 665 ppm), but virtually no Mo potential (56 ppm). This is probably what Anderson and Fraenkel (1979) observed and interpreted as a spatial separation of molybdenum and uranium. The next highest potential is that of plant debris (380 ppm, lower than expected according to field scintillometer signals) and fissile sandstone (226 ppm). The other rock types have neither a significant molybdenum nor significant uranium potential both in terms of mean metal values and volume (7.1.).

8.4. Organic matter

The data set was divided into two sub-sets based on the macroscopical visibility of organic matter in the sample (Table 8.2.). A positive correlation exists between the presence of organic matter in the sample and the molybdenum and uranium concentration. In the case of molybdenum the metal concentration is seven times higher when macroscopic organic matter is present and in case of uranium the enrichment factor is three. This confirms the strong concentrating influence of carbonaceous matter on these metals (8.3.).

Table 8.2.

Element	Mean element concentration of sub-set: Sub-set with visible organic material	Mean element concentration of sub-set: Sub-set without visible organic material
molybdenum	345	45
uranium	449	138

8.5. Accompanying elements

To establish inter-element correlations the data set was divided for each of the relevant elements (U\Mo, V, Co, Cu, As, Zn and Pb) into two subsets. The one subset contained all data for which the concentration of the accompanying element is higher than the mean of that element and the other those that are lower. For each of the two sub-sets the mean of the Mo and U concentration was determined. From the listing in Tables 8.3. and 8.4. it follows that there is a positive correlation between molybdenum

Table 8.3.

Element and mean value at which subdivision into sub-sets was made	Mean molybdenum concentration of sub-set: Sub-set with values greater than mean	Mean molybdenum concentration of sub-set: Sub-set with values less than mean
U (226 ppm)	441	161
V (88 ppm)	428	44
Co (30 ppm)	242	67
Cu (14 ppm)	54	290
As (106 ppm)	370	62
Zn (63 ppm)	152	176
Pb (45 ppm)	515	36

UNIVERSITEIT VAN PRETORIA
UNIVERSITY OF PRETORIA
YUNIBESITHI YA PRETORIA

Table 8.4.

Element and mean value at which subdivision into sub-sets was made	Mean uranium concentration of sub-set	
	Sub-set with values greater than mean	Sub-set with values less than mean
Mo (157 ppm)	586	112
V (88 ppm)	609	137
Co (30 ppm)	845	138
Cu (14 ppm)	170	390
As (106 ppm)	745	245
Zn (63 ppm)	645	160
Pb (45 ppm)	945	109

and uranium (as was expected). Both elements are also positively related to V, Co, As and Pb. The relation with Zn is positive for uranium but between Zn and molybdenum it is indifferent to negative. The relation between copper on the one hand and uranium and molybdenum on the other is strongly negative. The reason for this behaviour of copper is seen in the much more limited domain of solubility of this metal in the exogene environment (Garrels and Christ, 1965). Thus copper was precipitated from solution before it could reach the domain of Mo and U precipitation.

8.6. Elevation

The influence of elevation above the base the of the relevant sandstone body was examined by dividing the data set into two sub-sets, one with elevations below the mean of the total set and the other with elevations higher. The relevant uranium and molybdenum means for the sub-sets are listed in Table 8.5, from which can be seen that elevation above the base has no influence on the relative distribution pattern of the two metals in question.

To test further whether the relative position within the ore body has any influence on the distribution of the element concentrations the data set was divided into five sub-sets, namely samples where the total profile has been sampled, samples from the erosion surface (usually enriched in secondary minerals), and samples derived respectively from the upper, middle and lower third of the profile. The respective means

Digitised by the Department of Library Services in support of open access to information, University of Pretoria, 2021

Table 8.5.

Element	Mean elevation	Mean element concentration of sub-set	
		Sub-set with elevations higher than mean	Sub-set with elevations lower than mean
molybdenum	1 500 mm	153	143
uranium	1 500 mm.	224	224

are listed in Table 8.1. This table illustrates

i. that the elements Mo, U, V, Co, Pb and Zn are concentrated to varying degrees on the erosion surface

and ii. a slight decrease in mean concentration from the bottom to the top for molybdenum and uranium, but no significant change in the ratio between them.

Digitised by the Department of Library Services in support of open access to information, University of Pretoria, 2021

9. Genetic model for Karoo uranium-molybdenum deposits

The provenance from which the molybdenum and uranium were delivered to the streams that fed the depository of the Adelaide Subgroup was discussed by several researchers. The two main sources put forward are:

i. volcanoclastic material in sedimentary rocks of the Beaufort Group in the southwestern part of the Karoo basin which, on devitrification, could have released uranium and possibly molybdenum (Martini, 1974 and Ho-Tun, 1979).

ii. granitic terranes surrounding the Karoo basin (Gilbert, 1978; Scheepers, 1982 and Rust, 1979).

The volcanoclastic material is supposedly derived from volcanic eruptions south of the present African continent (probably related to the volcanic arc of Patagonia which was at that time situated in such a position). The latter source comprises the granite gneisses of Namaqualand and various granites of the Cape Suite. Although evidence has been produced which supports either of the proposed sources, this issue has not been resolved conclusively. For the present study it is sufficient to accept that uranium and molybdenum were available in the depositional environment resulting in the mineralized ore-bodies.

The environment in which the sediments of the Adelaide Subgroup accumulated, is described by Smith (1981) as a warm to hot, semi-arid, flat, featureless continental flood-plain far removed from its source area. This plain was inundated by periodic ephemeral floods originating on higher ground to the southwest, southeast and northwest of the basin. These torrential floods transported arenaceous clastic material (to be deposited as sandstone along the course of the meandering river systems) and vast volumes of suspended mud (to be deposited as mudstones and shales in the form of overbank deposits) into the basin. These, often catastrophic, floods were also responsible for repeated reworking of previously laid-down sediments, usually by undercutting and collapse of vegetated levees and channel banks. Besides mud-pebbles (to be deposited as mud-pebble conglomerates) two types of organic material

Digitised by the Department of Library Services in support of open access to information, University of Pretoria, 2021

were also introduced into the stream:

i. Fresh organic material which would float and be left as shore line deposits by the receding water. These would normally rot away and would not be preserved.

ii. Humic organic material which would sink, join the bed-load and be deposited as phytoclast-rich pockets at the toe of point bars and in scour pools where it could be preserved due to burial in water-logged conditions.

This style of flooding can be observed today in the drier parts of southern Africa where the following key factor to the proposed Karoo model can be observed: After the main flood event (and the deposition of the sand and mud) a trickle of clear water continues to run on the sand surface of the river bed for extended periods (weeks to months). This, however, is only the surface expression of a much greater volume of water which is permeating downstream through the sand bed. Floods in the big sand rivers of Namibia (Kuiseb, Swakop etc.) usually do not reach the coast on surface on an annual basis. According to Stengel's (1963) research of historic sources for the period 1837-1937 the Kuiseb River reached the coast only about once in ten years. By outlining of the water reserve, flood measurement, systematic monitoring of the water table and the measured water withdrawal from the Kuiseb sand aquifer at Rooi Bank for consumption by the coastal towns of Walvis Bay and Swakopmund he calculated an annual subsurface water recharge of 800 000 m^3 (which is about 50% of the allowed withdrawal rate for the aquifer without over-exploitation). Using this and the known surface of the cross-section of the sand aquifer, he arrived at a subsurface water permeation speed of 280 mm per day. In some instances palaeodrainages are followed by these seepages due to the development of barriers in the form of shifting sand dunes. One example is situated between Gobabeb, where the present river course of the Kuiseb has been diverted northwards, and the fresh-water springs at Sandwich Harbour. Another palaeochannel feeds water over a distance of about 60 km from Koichab Pan to the fresh-water springs at Hottentots Bay and Anichab. In the case of the Fish River, in the vicinity of Mariental, ponds in the river, inter-connected by subsurface seepages, seldom dry up. Even in exceptionally arid years this is the case. The permanent nature of these ponds with their fish population gave rise to the name

Digitised by the Department of Library Services in support of open access to information, University of Pretoria, 2021

of the river.

In northern Namaqualand this model can be taken a step further in the case of the Koa Valley. At Henkries, just before the valley descends towards the Orange River, the Koa River was probably dammed up by sand dunes and consequently a marshy area developed, resulting in the accumulation of large volumes of organic material and diatomaceous earth. The water of the Koa Valley, which drains granite gneiss terrains in Namaqualand, percolated through this accumulation of organic material and uranium was deposited mainly in the form of adsorptions on organic material, with a resulting sub-economic uranium deposit. This deposit, according to the Anglo American Corporation (personal communication) that prospected the deposit in the late seventies, is so young (10 000 - 60 000 years) that the uranium decay chain has not reached equilibrium.

The processes active during the formation of the Karoo uranium-molybdenum deposits are envisaged to have followed much the same lines. Humic organic material, as part of the bedload, is seen as the vehicle by which molybdenum and also part of the uranium have been transported into the depositional environment. In the case of molybdenum the metal content of the organic fraction consists of primary molybdenum deposited metabolically by the living flora in the plant tissue and molybdenum adsorbed on the decaying plant matter. The latter molybdenum was probably derived through a process of oxidation of plant matter, release of molybdenum into solution in ground water and re-adsorption to un-oxidized vegetable matter. The uranium in the phytoclast-rich pockets was probably concentrated only by the second route, as uranium has little function in the metabolism of living plants. Reducing conditions, the result of the anaerobic decay of water-logged plant debris, induced the precipitation of the heavy metals such as uranium and molybdenum from the circulating metal-bearing groundwater. The sedimentary facies played a decisive role in the formation of these deposits. It would appear that the laminated sandstone, besides its position close to the base of a sandstone package, also represented a more permeable medium, with the result that most of the lateral ground water movement took place in this facies.

Digitised by the Department of Library Services in support of open access to information, University of Pretoria, 2021

For the preservation of this metal concentration in the sediment the causative reducing environment has to be maintained until lithification has been completed. The requisite for this is that the mineralized zone remains submerged below the watertable. In places such favourable conditions only prevailed in sand-filled erosion scours ripped into the underlying mud plain by the initial flood, i.e. over-deepened channels protruding below the mean base of the sandstone body.

The carbonate-cemented sandstones are probably not palaeo-valley-fill calcretes in the sense of Carlisle's (1983) description of the Australian and Namibian occurrences. In these uranium is found as carnotite. In the Karoo carbonate-cemented occurrences, however, no sympathetic U - V pattern is evident. A more likely model for the formation of the uraniferous carbonate-cemented occurrences of the Karoo is based on the work of Mount and Cohen (1984) who investigated rhizoliths from the marginal lacustrine deposits of Lake Turkana in Kenya. They distinguish between carbonate precipitation by vertical and horizontal root systems. In the former case calcite is precipitated under well-oxygenated, well-drained vadose conditions. These deposits, which are formed by plant roots tapping a variable watertable, are characterized by the absence of organic matter and manganese enrichment (no U-Mo mineralization is therefore expected). The cements of the horizontal root systems contain abundant clay and plant debris, and usually contain higher manganese concentrations (up to 4,5 cation percent). The horizontal root systems are formed by plants in swampy environments, i.e. water-saturated environments. Here reducing conditions prevail, which are favourable for the precipitation of heavy metals. The absence of significant Mo enrichments is explained by the high Ca^{+2} concentration surrounding this environment, which precipitates molybdenum from solution as powellite outside the domain of carbonate precipitation. The ubiquitous presence of phytoclasts and the manganese-enriched weathering crust of the mineralized carbonate-cemented sandstones indicates that the "koffieklip" is probably the product of horizontal root mats in a marshy environment on the flood-plain.

This mechanism for the formation of mineralization in such an environment implies that the heavy metals are precipitated early in the depositional history, well before the major diagenetic reduction in pore space takes place. This is substantiated by the crumpled

Digitised by the Department of Library Services in support of open access to information, University of Pretoria, 2021

nature of molybdenite flakes and the matrix-supported fabric of carbonate-cemented sandstone. No evidence for any post-diagenetic movement of heavy metals (except on the present erosion surface) was found on any of the deposits investigated. The reason for this is seen in the grain size of the Beaufort Group sandstones, which is too fine to permit any substantial water movement after reduction of the pore space through diagenesis. This idea is supported by le Roux (1990) who postulates that only the sandstones of the Molteno Formation hold any potential for roll front type deposits. He substantiates this by his observation in the Molteno Formation of higher uranium concentrations close to dolerite sills. These concentrations he interprets as the result of ground water brought into circulation by the cooling sill.

Digitised by the Department of Library Services in support of open access to information, University of Pretoria, 2021

10. Summary and conclusions

During the present investigation a portable XRF spectrometer was successfully employed to delineate mineralized rocks in the field.

The uranium deposits in the Karoo with which the molybdenum is associated are thin (generally less than 0,6 m thick) planar (usually horizontal) bodies which have areal extents of less than 10 000 m^2. This implies difficult mining conditions for open-cast operations due to high stripping ratios and for underground operations due to limited stope width, accompanied with labour-intensive extraction of broken ore. Further the total volume of a single body is small, which implies that a number of ore bodies, each of relatively·short life-span, will have to be exploited at the same time, feeding a central processing plant. Economic mining under present conditions of low commodity prices and high labour cost appears unlikely.

Factors controlling the molybdenum distribution in the sediments are stratigraphy, rock type and presence of organic material in the rock.

According to this investigation the Poortjie Sandstone Member has the highest molybdenum potential, both in terms of mean molybdenum concentration (391 ppm) and number of individual deposits. This is associated with the second highest uranium potential (only surpassed by the Loxton Sandstone Member). This molybdenum potential is followed by the Barberskrans and the Moordenaars Sandstone Members with mean concentrations respectively less than half and about one quarter of that of the Poortjie Member. According to the results of this study the potential of the other sandstone packages investigated is negligible.

The fissile sandstone is the rock type with the highest molybdenum potential, whereas siltstone has the highest uranium potential in terms of mean grade and volume. The influence of organic material as concentrating factor for both the metals is indicated by higher mean values in pockets of plant debris and in the sample set of rocks containing macroscopically visible phytoclasts.

Digitised by the Department of Library Services in support of open access to information, University of Pretoria, 2021

The accompanying elements Mo\U, V, Co, As and Pb are interpreted as precipitates that formed under mutually favourable conditions. The poor correlation of Zn and Cu with Mo and U is interpreted by precipitation of these metals outside the domain favourable for uranium-molybdenum precipitation.

The genesis of the ore-bodies is seen as early diagenetic and well before compaction and lithification. The mobilizing and transporting medium for the dissolved ions is seen as oxygenated seepage water following the main ephemeral flood event which deposited the sand bodies. When this water percolates through pockets in which anaerobic conditions prevail as a result of buried decaying organic material, the dissolved metals are precipitated. If these are not flushed out by an excess of oxygenated water or oxidized by a drop in the water-table to below the deposit, these bodies are preserved.

Digitised by the Department of Library Services in support of open access to information, University of Pretoria, 2021

11. References

ANDERSON J. R. and FRAENKEL H. C., 1979. The geology and mineralization of a uranium occurrence at Rietkuil farm, Beaufort West district, South Africa: **Abstracts Geocongres '79, Geol. Soc. S. Afr. Beaufort West**, pp. 41-44.

BAAS BECKING, L. G. M., KAPLAN, I. R. and MOORE, D., 1960. Limits of the natural environment in terms of pH and oxidation-reduction potentials: **The Journal of Geology**, vol. 68, No. 3. pp. 243-284.

BASHAM, I. R. and EASTERBROOK, G. D., 1977. Alpha particle autoradiography of geological specimens by use of cellulose nitrate detectors: **Trans. Inst. Mining Metall. Section B**, vol. **86**, pp. 96-98.

BASHAM, I. R., 1981. Some applications of autoradiographs in textural analysis of uranium-bearing samples - a discussion: **Economic Geology**, Vol. 76. pp. 974-982.

BATH, G. F., 1979. Enzootic icterus - a form of chronic copper poisoning: **Journal of the South African Veterinary association**. 50(1). pp. 3-14.

BLOSSOM, J. W.,. Molybdenum, in: KNOERR, A. W. (Editor). **Mineral facts and problems**, 1985 Edition; Bureau of Mines Bulletin 675, United States Department of the Interior, U. S. Govt. Print. Off., pp. 521-530.

BROWN, J. M. M. and DE WET, P. J., 1962. A preliminary report on the occurrence of selenosis in South Africa and its possible role in the aetiology of tribulosis (geeldikkop), enzootic icterus and some other disease conditions encountered in the Karoo areas: **Onderstepoort Journal of Veterinary Research**. 29. pp. 111-135.

BRUET, E., 1952. **Minéraux radioactifs et terres rares**: Bibliotheque Scientifique, Payot, Paris. pp. 116.

Digitised by the Department of Library Services in support of open access to information, University of Pretoria, 2021

BRYNARD, H. J., 1983. Fission-track studies of uranium distribution in geological samples: **Spec. Publ. geol. Soc. S. Afr.**, 7(1983), pp 413-417.

CARLISLE, D., 1983. Concentration of uranium and vanadium in calcretes and gypcretes. In: WILSON, R. C. L., (editor). **Residual deposits: Surface related weathering processes and materials.** Special publication No. 11, The Geological Society of London, Blackwell scientific Publications Ltd., Oxford. pp. 185-195.

COLE, D. I., 1980. The sedimentology of the uranium-bearing sandstones on the farm Riet Kuil 307, Beaufort West area: **Geological Survey of South Africa**, Report No. 1980-0252, p. 89.

COLE, D. I., LABUSCHAGNE, L. S. and SöHNGE, A. P. G. (1991). Aeroradiometric survey for uranium and ground follow-up in the main Karoo basin: **Geological Survey of South Africa**, Memoir **76**.

COLE, D. I. and WIPPLINGER, P. E., 1991. Uranium and molybdenum occurrences in the Beaufort Group of the main Karoo basin, South Africa. In: ULBRICH, H. and ROCHA CAMPOS, A. C. (Editors) **Gondwana Seven Proceedings**, Instituto de Geociências, Universidade de Saõ Paulo, Brazil.

CROCKER, I., WALRAVEN, F. and HAMMERBECK, E., 1977. Report on the molybdenite mineralization of Varschwater 23JS, Nebo district: **Geological Survey of South Africa**, Report no. **1977-0049**, p. 7.

FYFE, W.S., PRICE, N. J. AND THOMPSON, A. B., 1978. **Fluids in the Earth's crust**. Elsevier Scientific Publishing Company, Amsterdam. p. 383.

GARRELS, R. M. and CHRIST, C. L., 1965. **Solutions, minerals, and equilibria**. Harper and Row, New York. p. 450.

GEVORKYAN, R. G., 1968. Effects of alkalinity and temperature on the distribution of molybdenum and tin in the crystallization of a basalt magma. **Geochemistry Internat.**,

5., pp. 1221-1225.

GILBERT, C. E., 1978. Ground investigation of some aerial radiometric anomalies at Pella, Namaqualand District, and Namies, Kenhardt District: **Rep. Geol. Surv. S. Afr. 1978-0285.**

GLEESON, S., 1972. **Ultraviolet guide to minerals**: Charles E. Tuttle Company, Inc. of Rutland, Vermont, U.S.A. and Tokyo, Japan. pp. 169-170.

GOLDSCHMIDT, V. M., 1954. **Geochemistry**: Ed. Muir, A., Oxford Clarendon Press, pp. 730.

GOLDSCHMIDT, V. M. and STORCK, L. W., 1939. Zur Geochemie des Selens II. - Nachr. Gesell. Wiss. Göttingen, Math.-phys. Kl., IV, N.F. 1, 11 (1935). pp. 132-142.

HAMILTON, W. B., 1989. Crustal geologic processes of the United States. In: **Geological Society of America, Memoir 172**, pp. 743-781.

HAWKES, H. E. and WEBB, J. S., 1962. **Geochemistry in mineral exploration**: Harper and Row, London, p. 415.

HERZBERG, W., 1970. Geochemical prospecting for molybdenum on Hartebeestfontein 62KS, Pietersburg district: **Geological Survey of South Africa**, Report no. **1970-0052**, p. 11.

HO-TUN, E. 1979. Volcaniclastic material in lower Beaufort Group, Karoo rocks. **18th Congr. geol. Soc. S. Afr.., Port Elizabeth, Abstr. Part 1**. pp. 197-199.

HÜCKEL, U., 1979. Concentration of total uranium in stream sediments of degree square 3222 (Beaufort West): **Geological Survey of South Africa**, Report no. **1979-0063**, p. 8.

JAKOB, W-R. O., 1987. The geochemistry and radiochemistry of the uranium occurrence on the farm Kaffirsfontein 328, Beaufort West District: D. Sc. thesis (unpublished), **University of Pretoria**, Pretoria, South Africa, p. 152.

KEYSER, A. W., and SMITH, R. M. H., 1979. Vertebrate biozonation of the Beaufort Group with special reference to the western Karoo Basin: **South African Geological Survey Annals**, Vol. 12. p. 1-35.

KING, R. U., 1973. Rhenium. In: BROBST, D. A. and PRATT, W. P. (Editors). **United States mineral resources**, Geological Survey Professional Paper 820, United States Printing Office, Washington. pp. 557-559.

KING, R. U., SHAWE, D. R. and MacKEVETT, E. M., 1973. Molybdenum. In: BROBST, D. A. and PRATT, W. P. (Editors). **United States mineral resources**, Geological Survey Professional Paper 820, United States Printing Office, Washington. pp. 425-435.

KüBLER, M., 1977. The sedimentology and uranium mineralization of the Beaufort Group in the Beaufort West - Fraserburg - Merweville area, Cape Province. M. Sc. Thesis (unpubl.) **University of the Witwatersrand**, Johannesburg. p. 106.

KUZNETSOVA, V. V. and SAUKOV, A. A., 1961. Possible forms of occurrence of molybdenum and rhenium in the coals of middle Asia. **Geochemistry**. pp. 822-829.

LARSEN, G. and CHILINGAR, G. V., 1979. Introduction - diagenesis of sediments and rocks, In: LARSEN, G. and CHILINGAR, G. V. (editors). **Diagenesis in sediments and sedimentary rocks**, Elsevier Scientific Publishing Company, Amsterdam. p. 579.

LEPELTIER, C., 1969. A simplified statistical treatment of geochemical data by graphical representation: **Econ. Geol.** Vol. 64, pp. 538-550.

LE ROUX, J. P., 1985. Palaeochannels and uranium mineralization in the main Karoo Basin of South Africa. Ph. D. Thesis (unpublished) **University of Port Elizabeth**, Port

Digitised by the Department of Library Services in support of open access to information, University of Pretoria, 2021

Elizabeth. p. 250.

LE ROUX, J. P. and TOENS, P. D., 1986. A review of the uranium occurrences in the Karoo Sequence, South Africa. In: ANHAEUSSER, C. R. and MASKE, S. (Eds.). **Mineral deposits of southern Africa, Vols. I & II.** Geol. Soc. S. Afr., Johannesburg, pp. 2119-2134.

LE ROUX, J. P., 1990. Uranium mineralization in the Molteno and Elliot Formations: **S. Afr. J. Geol.**, 1990, 93 (5/6), pp. 738-743.

LEVINSON, A. A., 1973. **Introduction to exploration geochemistry** (Second edition): Applied Publishing Ltd., Wilmette, Illinois, U. S. A., p. 924.

LOUW, G. N., STEENKAMP, C. W. P. and STEENKAMP E. L., 1967. Some aspects of the aetiology of enzootic icterus ("geelsiekte") and tribulosis ovis ("geeldikkop"): **South African Journal of Agricultural Science**. 10. pp. 215-228.

LOVERING, F., 1972. In: Fairbridge, R. W. (Ed.)., **The encyclopedia of geochemistry and environmental sciences**: Van Nostrand Reinhold Company, New York. p. 1321.

MARTINI, J., 1974. On the presence of ash beds and volcanic fragments in the greywackes of the Karoo System in the southern Cape Province (South Africa): **Trans. geol. Soc. S. Afr. 77**, pp. 113-116.

MARTINI, J., 1980. On some molybdenum occurrences associated with emerald deposits in the Gravelotte area, eastern Transvaal: **Geological Survey of South Africa**, Report no. **1980-0125**, p.11.

MASON R., in press. Felsic magmatism and hydrothermal gold deposits - a tectonic perspective. In: **Proceedings of the 8th International Basement Tectonics Conference - Butte Montana.**

Digitised by the Department of Library Services in support of open access to information, University of Pretoria, 2021

MAYNARD, J. B., 1983. **Geochemistry of sedimentary ore deposits**: Springer Verlag New York Inc. p. 305.

Minerals Bureau, 1991. **MB BULLETIN**, Vol. 4/2 1991: Minerals Bureau, Johannesburg. pp. 22.

MOON, C. J., 1974. The geology and geochemistry of some uraniferous occurrences in the Beaufort West area - Cape Province: **Geological Survey of South Africa**, Report no. 1974-0092, p. 73.

MOUNT, J. F. and COHEN, A. S., 1984. Petrology and geochemistry of rhizoliths from Plio-Pleistocene fluvial and marginal lacustrine deposits, East Lake Turkana, Kenya: **Journal of sedimentary Petrology**, Vol. 54, No. 1, March 1984, pp. 0263-0275.

PETERSEN, R. G., HAMILTON, J. C. and MYERS, A. T., 1959. An occurrence of rhenium associated with uraninite in Coconino Country, Arizona: **Economic Geology,** Vol. 54, pp. 254-267.

PRETORIUS, L. E., 1977. Aspects of uranium mineralization in the Beaufort West Karoo: M. Sc. Thesis (unpublished), **University of Stellenbosch**. p. 116.

PRETORIUS, L. E., 1985. Stable isotope, sedimentological and chemical aspects of the lower Beaufort Group Uranium Province in the southwestern Karoo Basin, South Africa. Ph. D. Thesis (unpublished) **University of Queensland**, Australia. p. 233.

RHODES, J. and RAUTALA, P., 1983. Application of a microprocessor-based portable XRF analyzer in minerals analysis: **Int. J. Appl. Radiat. Isot.** Vol. **34**. No.1. pp. 333-343

RUST, I. C. (Ed.), 1979. Excursion guide book Pt. 1-4: Geocongres 79. **Geol. Soc. S. Afr.**, E. H. Walton and Co. Ltd., Port Elizabeth. p. 180.

Digitised by the Department of Library Services in support of open access to information, University of Pretoria, 2021

SAAGER, R., 1984. **Metallische Rohstoffe von Antimon bis Zirkonium**, Bank Vontobel, Zürich, p. 176.

SCHEEPERS, R., 1982. Die uraan-, thorium- en molibdeen-verspreiding in geselekteerde leukograniete van die Kaap-Graniet-Suite: M. Sc. thesis (unpubl.) **Stellenbosch University.**

SMITH, R. M. H., 1981. Sedimentology and taphonomy of the lower Beaufort strata near Beaufort West, Cape Province: M. Sc. thesis (unpubl.) **University of Witwatersrand**, p. 126.

STEAR, W..M., 1980. The sedimentary environment of the Beaufort Group Uranium Province in the vicinity of Beaufort West, South Africa. Ph. D. thesis (unpubl.) **University of Port Elizabeth**, Port Elizabeth p. 188.

STENGEL, H. W., 1963. **Wasserwirtschaft - Waterwese - Water Affairs in S. W. A.**, Afrika-Verlag der Kreis, Windhoek. p. 467.

STEPHAN, L. A., 1977. Molybdenum deposits in South Africa: **Geological Survey of South Africa**, Report no. **1977-0025**, p. 72.

STEPHAN, L. A., 1976. Review of the strata-bound W-(Mo)-(Bi)-(Cu) mineralization in the Namaqualand copper district: **Geological Survey of South Africa**, Report no. **1976-0136**, p. 29.

THERON, J. C., 1973, Sedimentological evidence for the extension of the African continent southwards during the late Permian - early Triassic times. In: CAMPBELL, K. S. W., ed., **Gondwana geology: Gondwana Symposium, 3rd, Canberra, Australia.** Australian National University Press, pp. 61-71.

TISCHENDORF, G., LIMPACK, W. and UNGETHüM, H., 1968. Beitrag zur Geochemie des Rheniums - Fortschritte und neue Ergebnisse: **Geologie**, 17. pp. 1208-1218.

Digitised by the Department of Library Services in support of open access to information, University of Pretoria, 2021

TOENS, P., VAN DER MERWE, P. and CAMISANI CALZOLARI, F., 1980. Report on the viability of uranium and molybdenum production in the southern Karoo area as at January 1981: **Nuclear Development Corporation of South Africa, Pretoria. PIN-552 (CV)**

Uzkut, I., 1974. Zur Geochemie des Molybdäns: **Clausthaler Hefte zur Lagerstättenkunde und Geochemie der mineralischen Rohstoffe, Heft 12**. Borntraeger, Berlin. p. 226.

VAN DER VYVER, G.P., 1991. Rhenium - an exotic element. **MB Bulletin**, Vol.4/2 1991, Minerals Bureau, Johannesburg. pp. 12-13.

VAN TONDER, E. M., BASSON, P. A. and VAN RENSBURG I. B. G., 1972. "Geeldikkop" experimentally induced by feeding tribulus terrestris L. (Zygophyllaceae): **Journal of the South African Veterinary Medical Association**. 43. pp. 363-375

WINKLER, H. G. F., 1976. **Petrogenesis of metamorphic rocks**, 4 th ed. Springer-Verlag, Berlin. p. 334.

Geological map (1:1 000 000) of the Republics of South Africa, Transkei, Bophuthatswana, Venda and Ciskei and the kingdoms of Lesotho and Swaziland, 1984, compiled by VISSER, D. J. L., Department of Mineral and Energy Affairs, Government Printers, Pretoria.

Digitised by the Department of Library Services in support of open access to information, University of Pretoria, 2021